ISM Dynamics and Star Formation

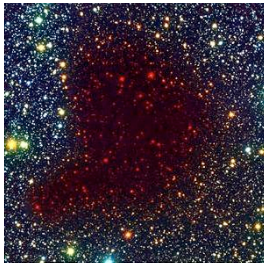

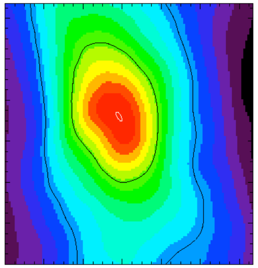

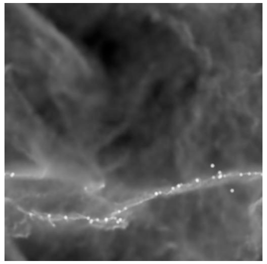

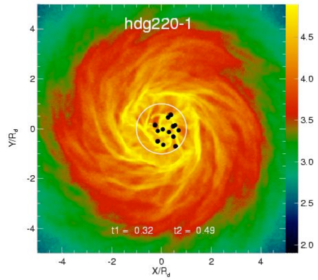

Ralf Klessen

Zentrum für Astronomie der Universität Heidelberg
Institut für Theoretische Astrophysik

thanks to ...

- many thanks to the members of the *star formation group* at the *Institute for Theoretical Astrophysics* at the *Center for Astronomy* of *Heidelberg University*

  - Robi Banerjee
  - Paul Clark
  - Christoph Federrath
  - Simon Glover
  - Thomas Greif
  - Susanne Horn
  - Stefan Schmeja
  - Thomas Peters
  - Dominik Schleicher
  - and many guests

agenda

- phenomenology
- theoretical approach
- formation of molecular clouds
  - on galactic scales
  - locally, in convergent flows
- fragmentation of molecular clouds
  - interplay between gravity and turbulence
- star formation: now and then
  - initial mass function at present days (models & caveats)
  - speculations about Pop III and transition to Pop II

observations

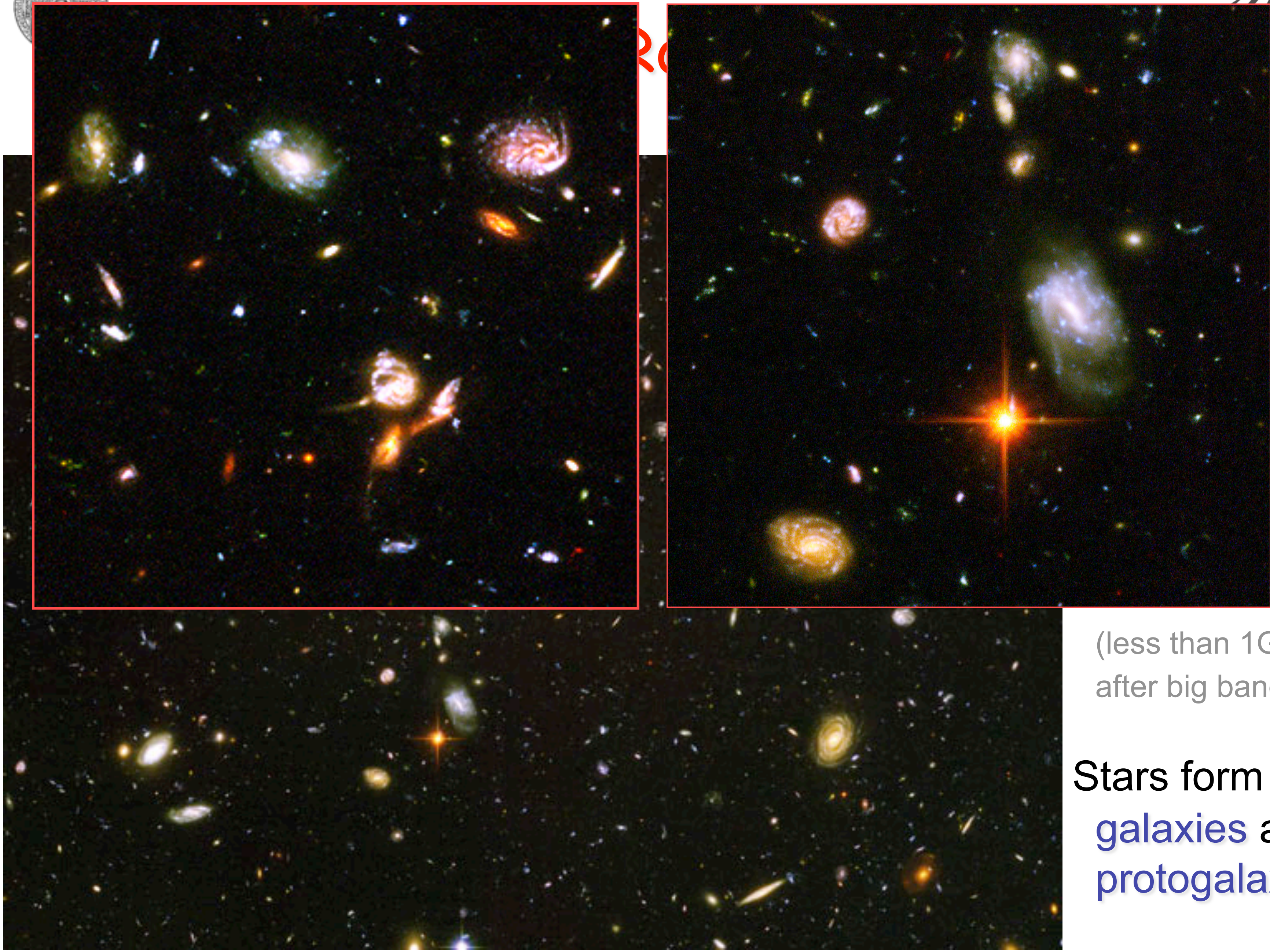

tion

rly

(less than 1Gyr
after big bangl)

Stars form in
galaxies and
protogalaxies

(Hubble Ultra-Deep Field, from HST Web site)

Star formation in interacting galaxies:

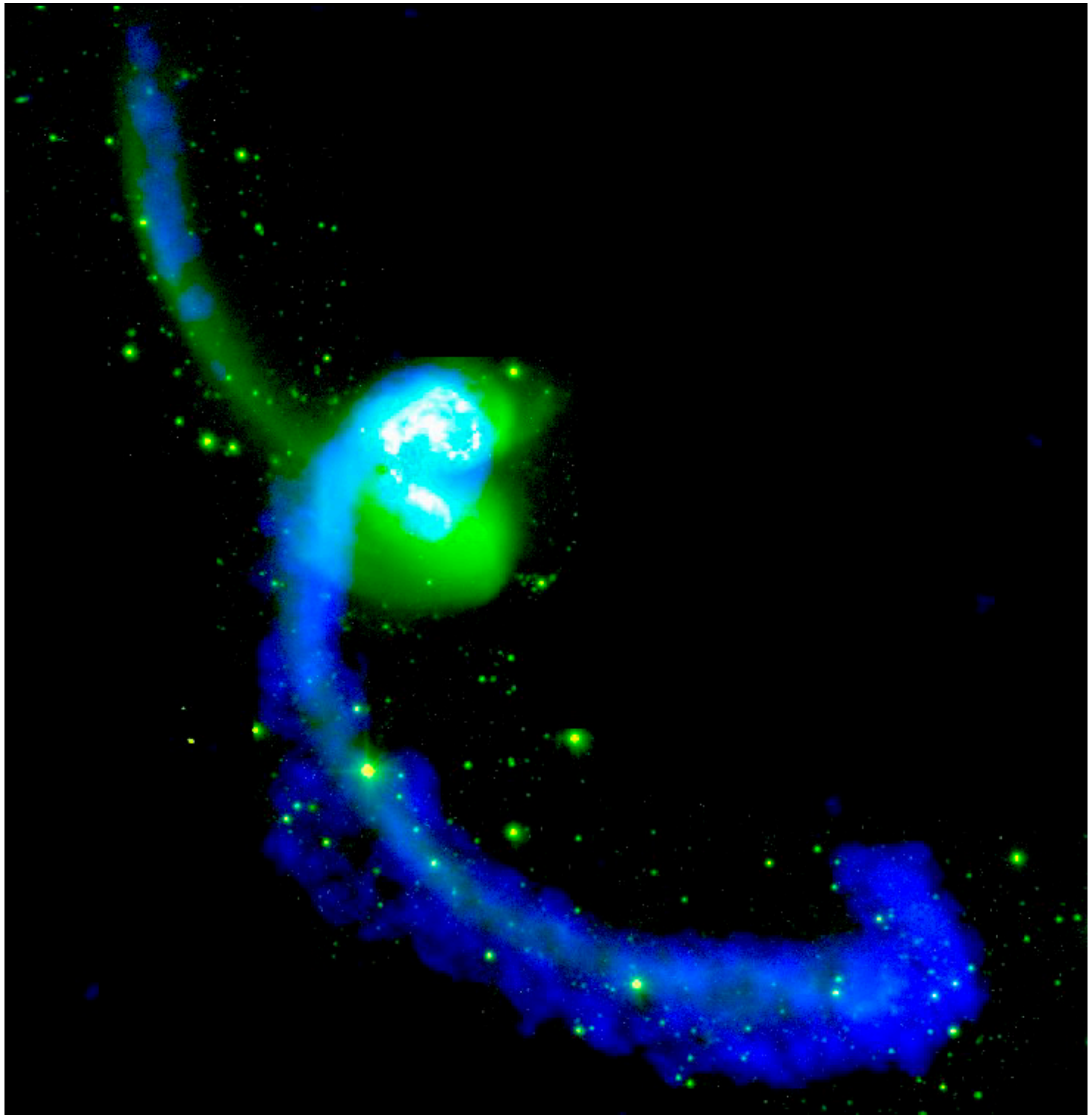

(from the Chandra Webpage)

Antennae galaxy

- *NGC4038/39*
- *distance: 19.2Mpc*
- *vis. Magn: 11.2*
- *optical: white, green*
- *radio: blue*

Star formation in interacting galaxies:

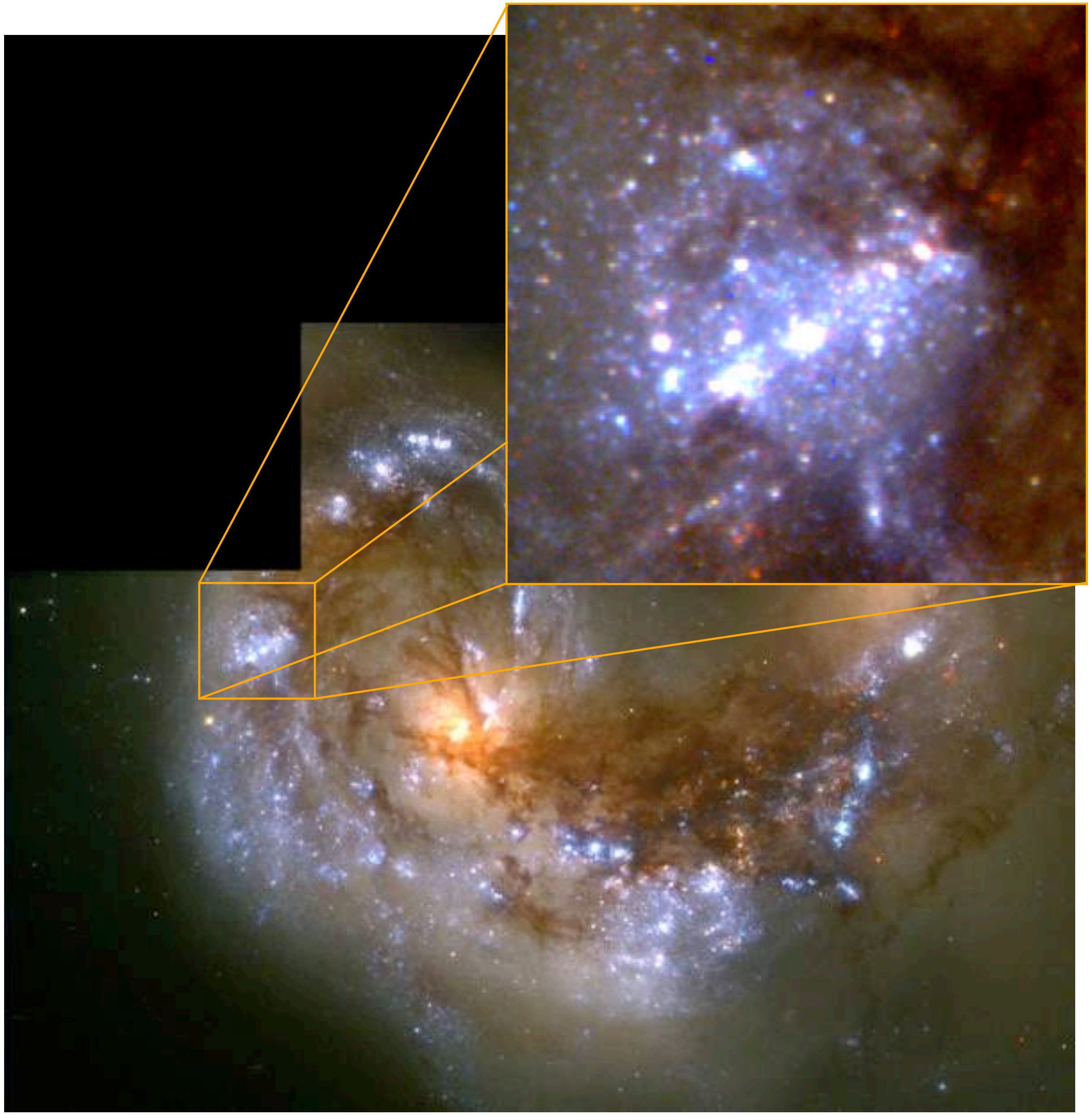

(HST: Whitmore & Schweizer 1997)

Antennae galaxy

- Star formation burst in interacting (merging) galaxies
- Strong perturbation SF in tidal “tales”
- Large-scale gravitational motion determines SF
- Stars form in “knobs” (i.e. superclusters)

young stars in spiral galaxies

(NGC 4622 from the Hubble Heritage Team)

- Star formation *always* is associated with *clouds of gas and dust*.
- Star formation is essentially a *local phenomenon* (on ~pc scale)
- HOW is star formation is *influenced* by *global* properties of the galaxy?

young stars in the Milky Way

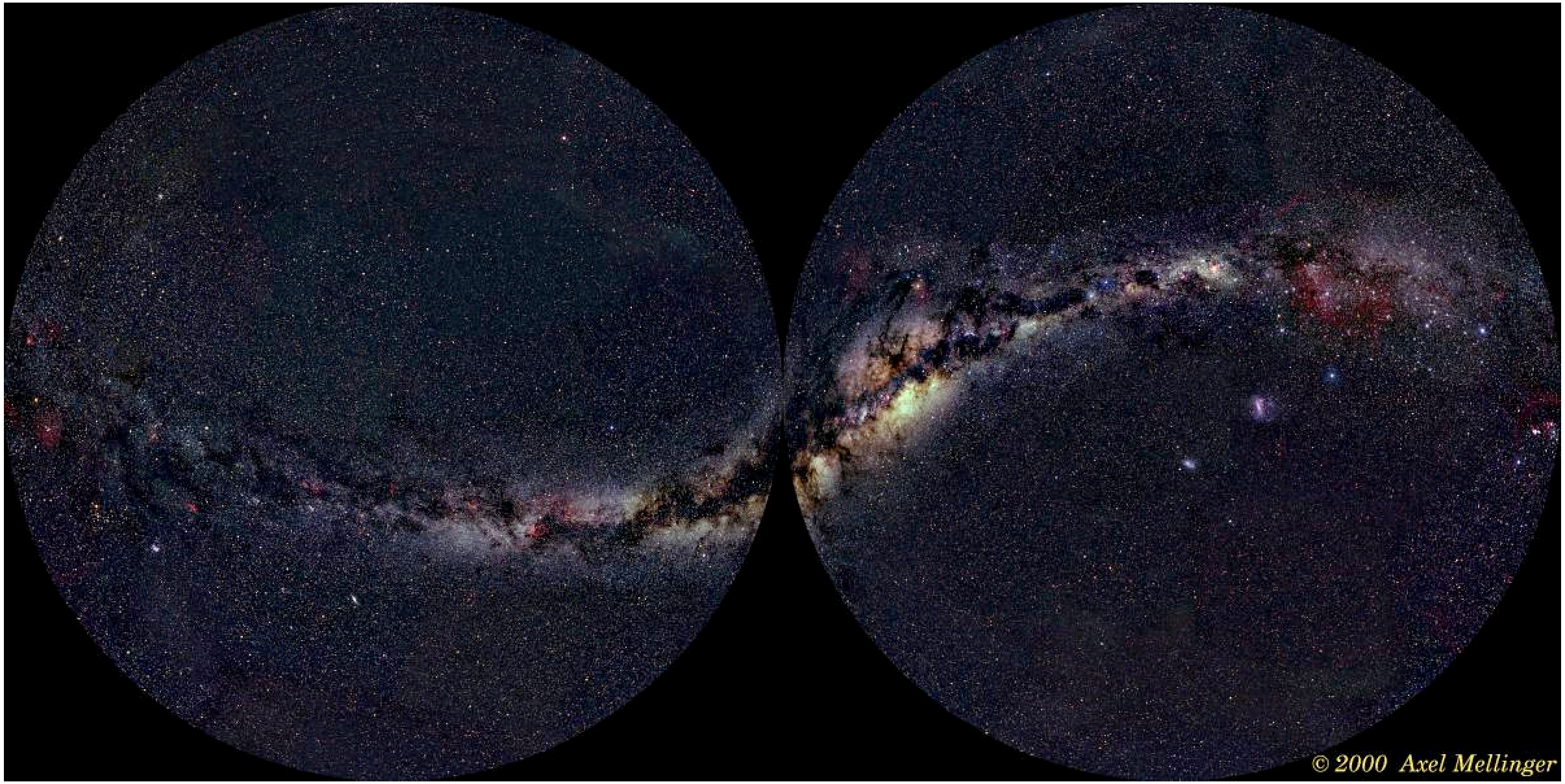

On the night sky, you see ***stars*** and ***dark clouds***:
The brightest stars are massive and therefore young.
→ Star formation is important for understanding the structure of our Galaxy

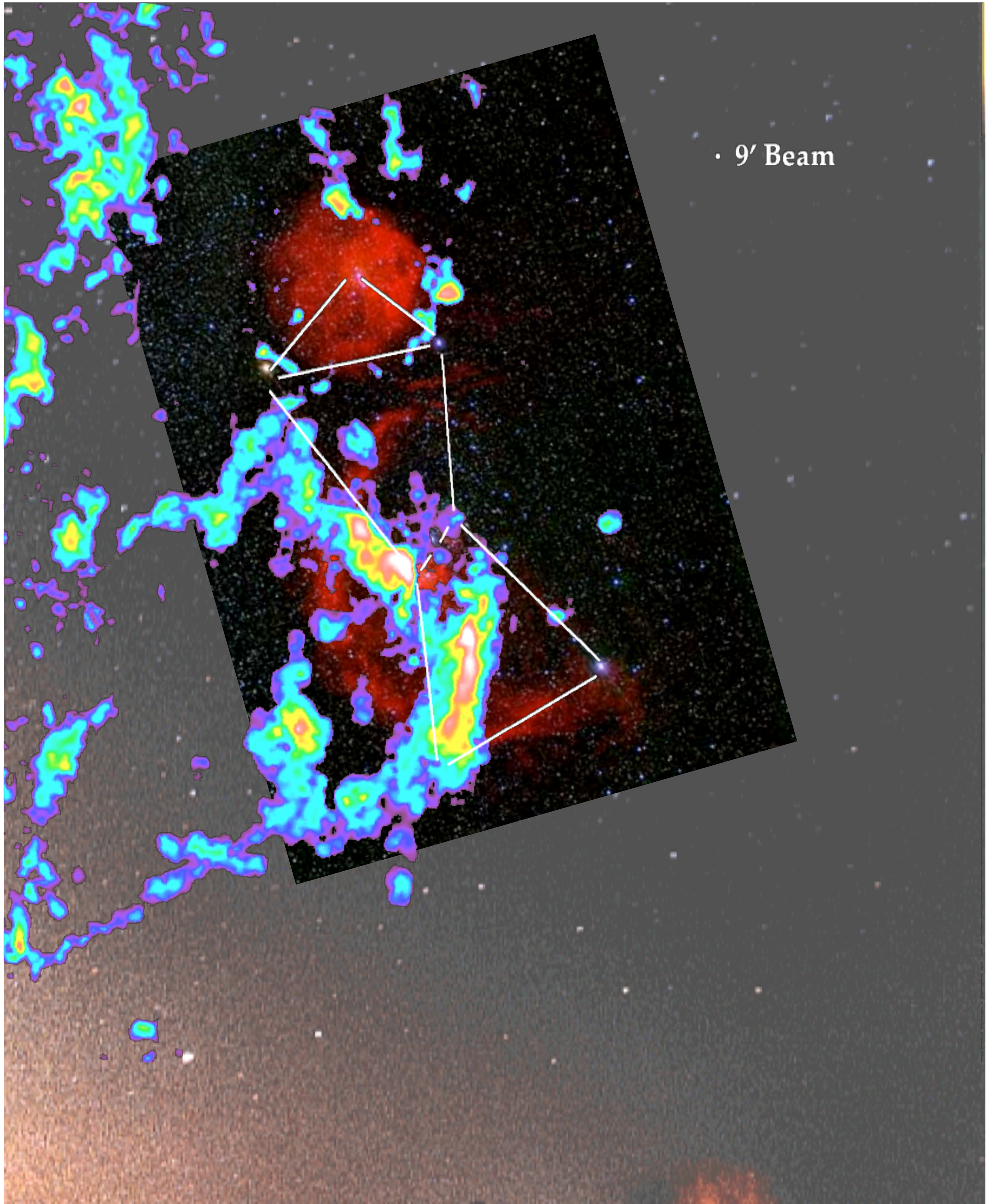

Star formation in Orion

We see

- *Stars* (in visible light)
- Atomic hydrogen (in Hα -- red)
- Molecular hydrogen H_2 (radio emission -- color coded)

Local star forming region: The Trapezium Cluster in Orion

The Orion molecular cloud is the birth- place of several young embedded star clusters.

The Trapezium cluster is only visible in the IR and contains about 2000 newly born stars.

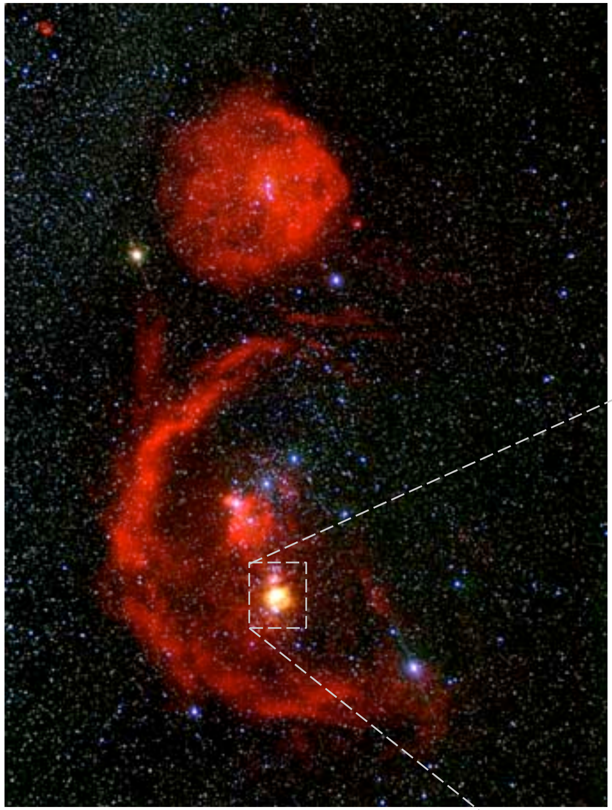

Orion molecular cloud

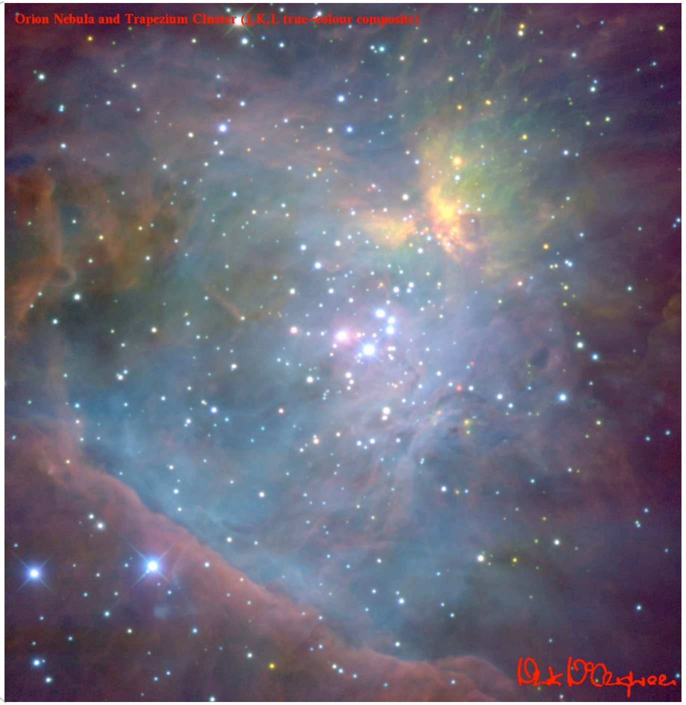

Trapezium cluster

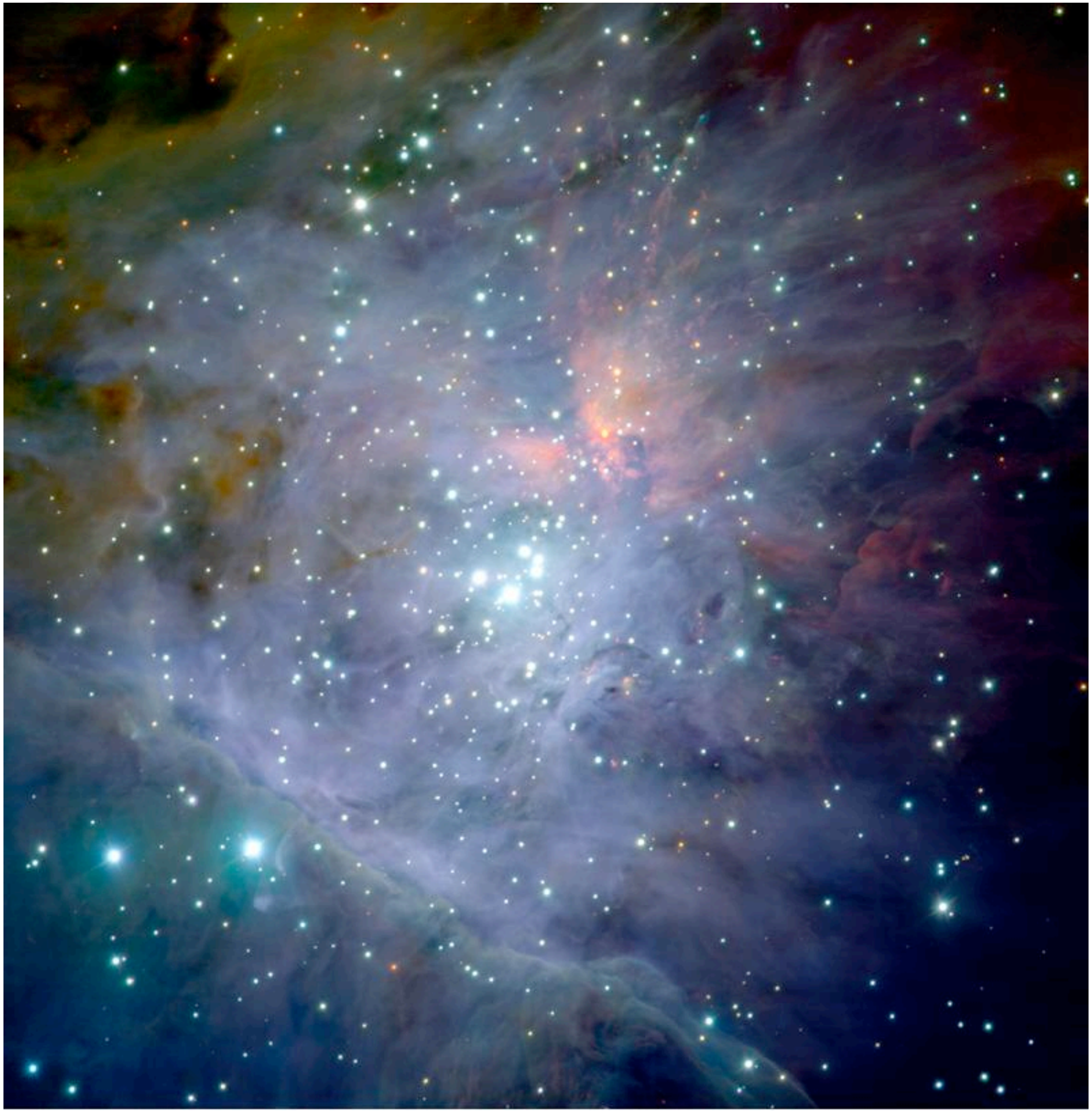

Trapezium Cluster

(detail)

- stars form in clusters
- stars form in molecular clouds
- (proto)stellar feedback is important

(color composite J,H,K by M. McCaughrean, VLT, Paranal, Chile)

Trapezium Cluster: Central Region

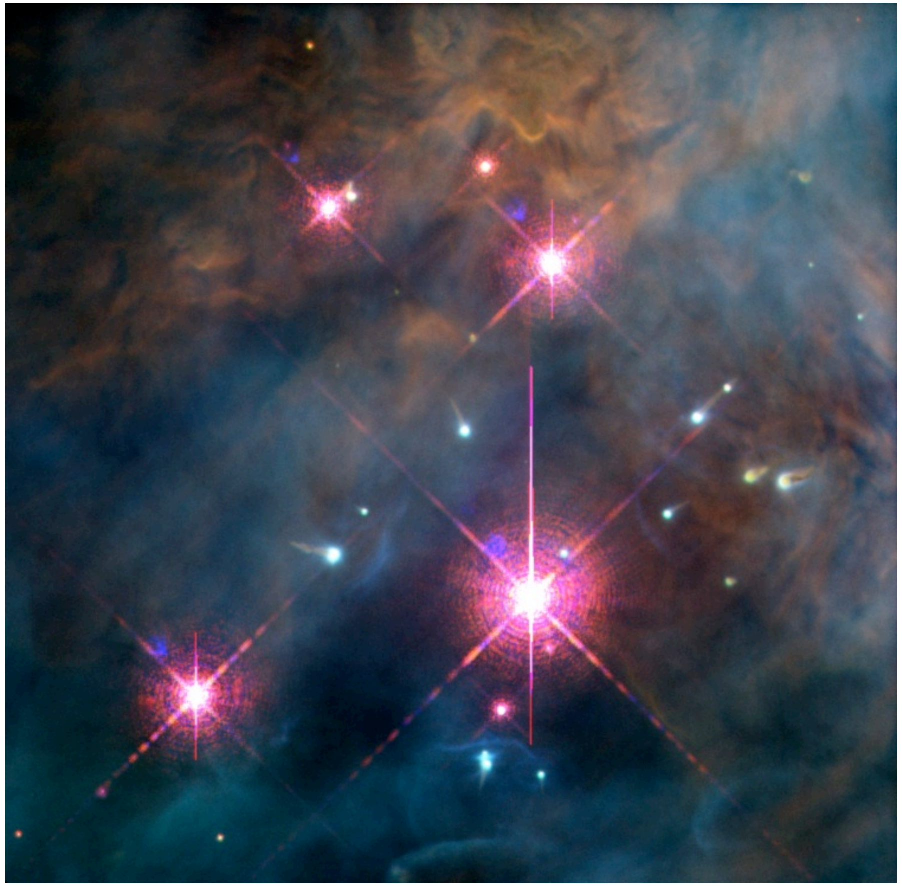

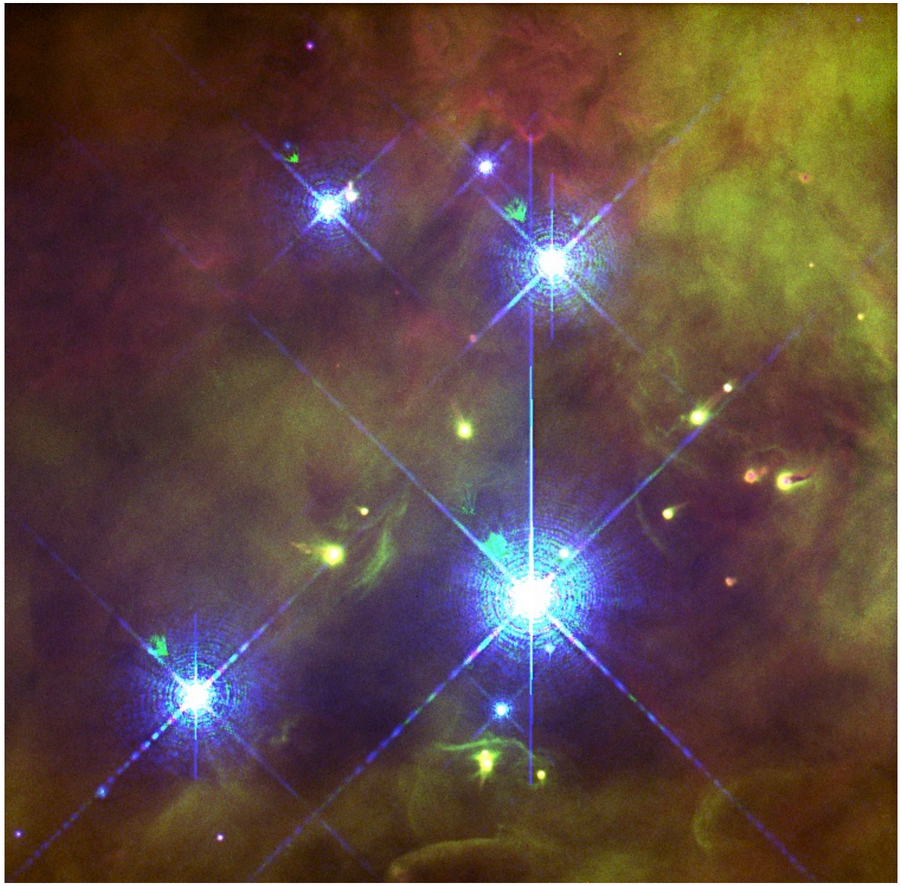

Ionizing radiation from central star
Θ1C Orionis

Proplyds: Evaporating ``protoplanetary´´ disks around young low-mass protostars

(images: Doug Johnstone et al.)

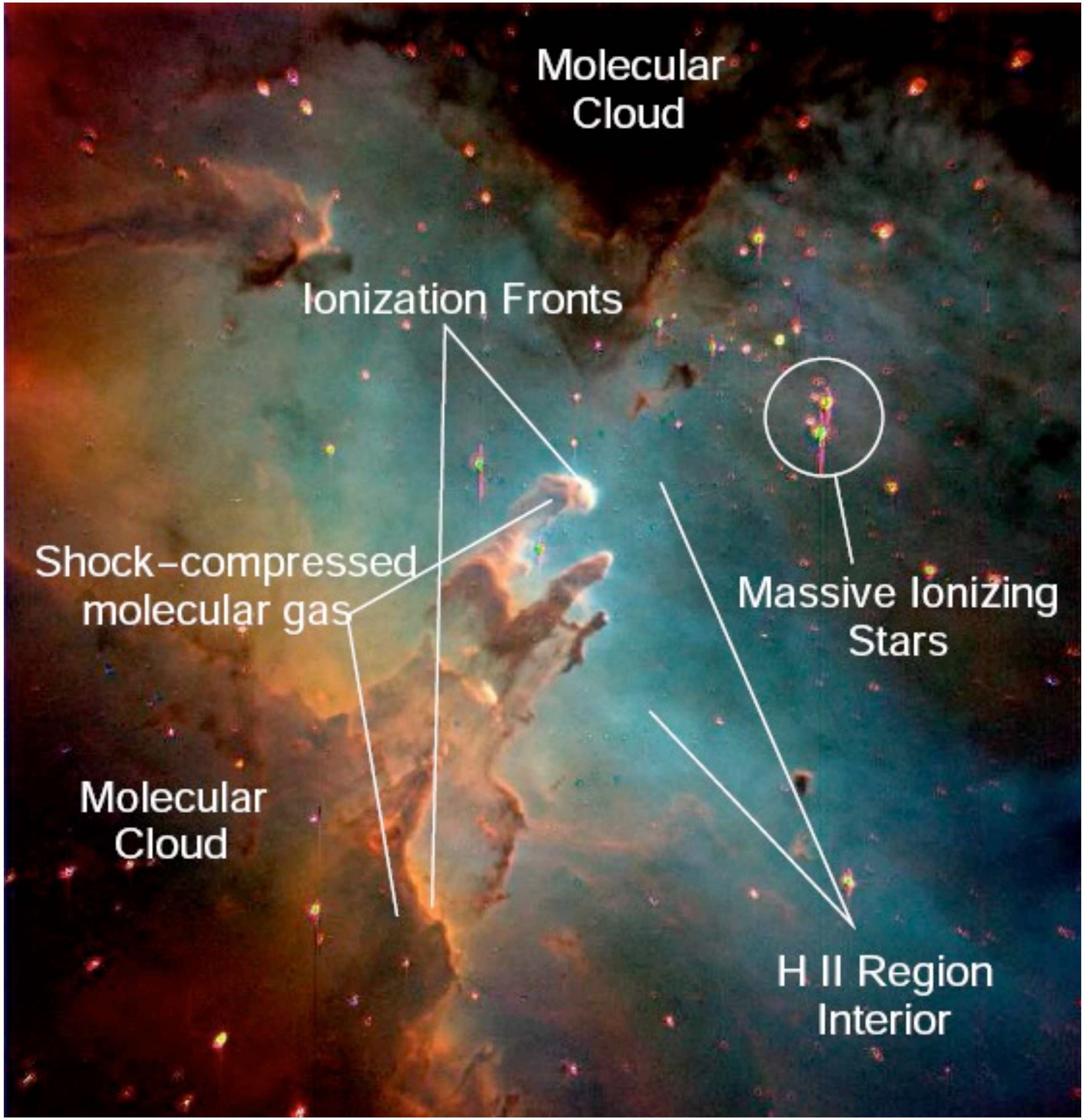

alles in einem Bild

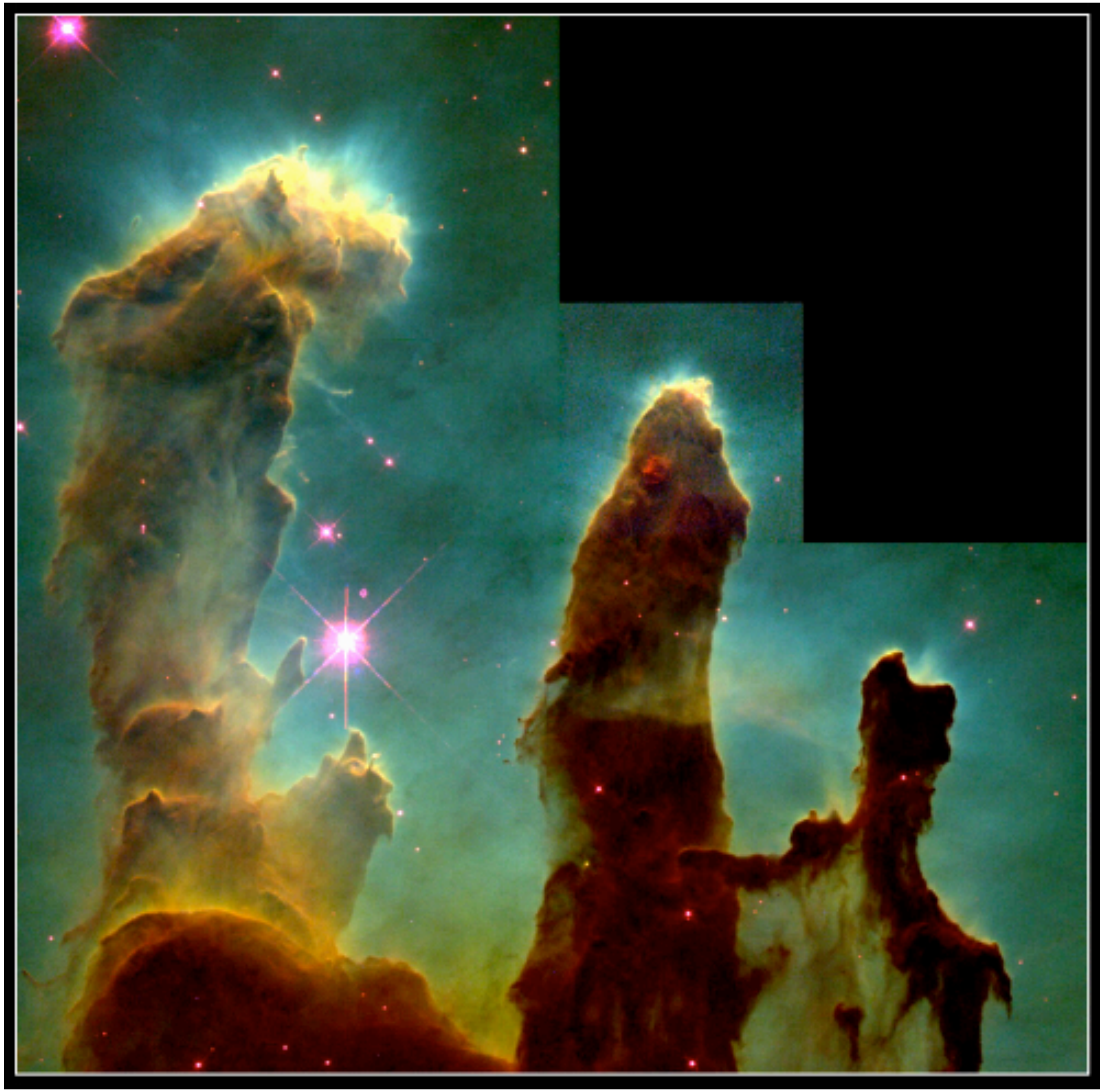

HST Aufnahme

Pillars of God (in Eagle Nebula): Formation of small groups of young stars in the tips of the columns of gas and dust ….

Infrared observation

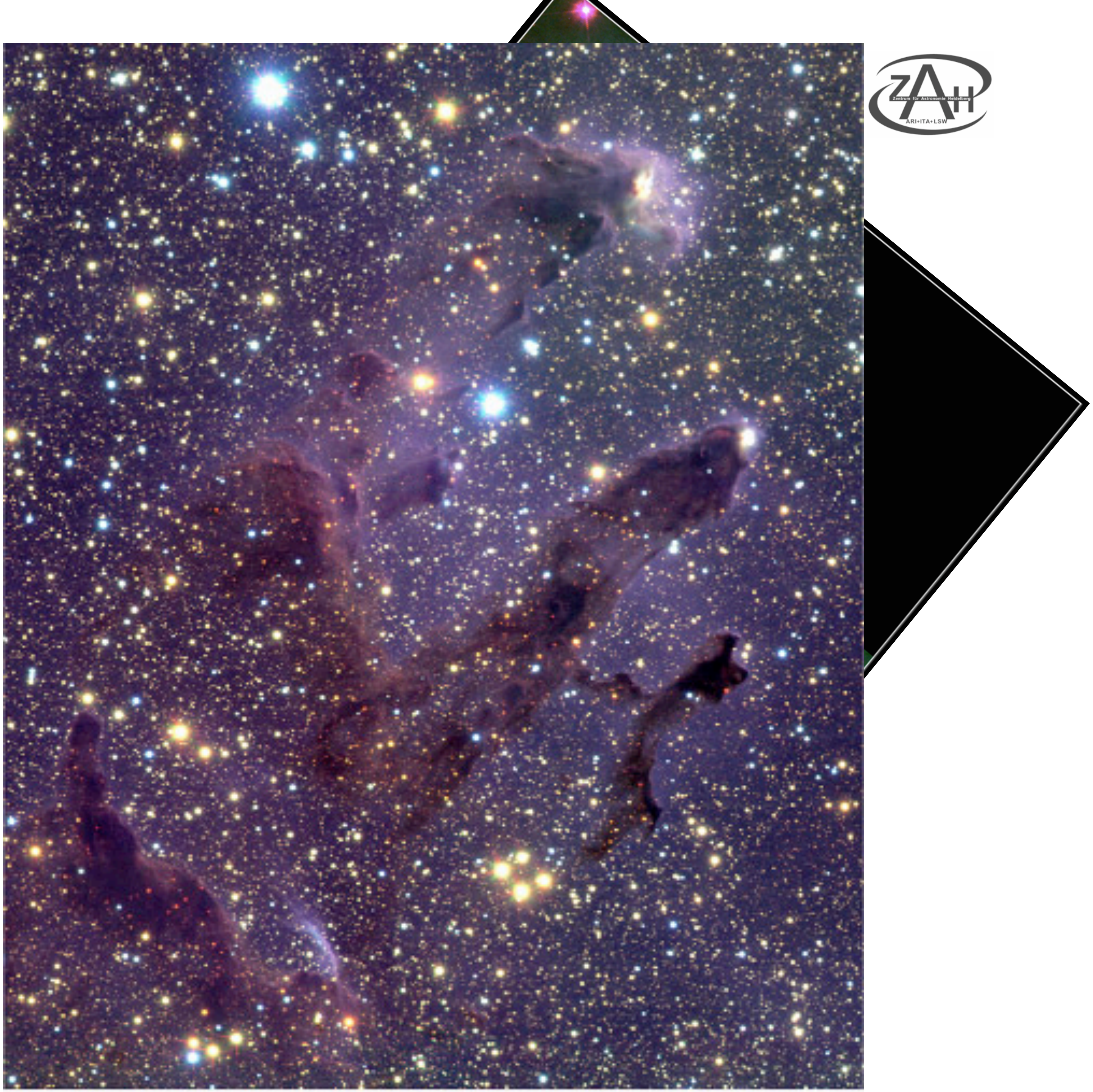

IR observation with ESO-VLT

Pillars of God (in Eagle Nebula): Formation of small groups of young stars in the tips of the columns of gas and dust ….

IR observation with ESO-VLT

Pillars of God (in Eagle Nebula): Formation of small groups of young stars in the tips of the columns of gas and dust ….

theory

Early dynamical theory

- *Jeans (1902):* Interplay between self-gravity and thermal pressure
  - stability of homogeneous spherical density enhancements against gravitational collapse
  - dispersion relation:

$$\boxed{\omega^2 = c_s^2 k^2 - 4\pi G \rho_0}$$

  - instability when $\omega^2 < 0$
  - minimal mass: $\boxed{M_J = \frac{1}{6}\pi^{-5/2} G^{-3/2} \rho_0^{-1/2} c_s^3 \propto \rho_0^{-1/2} T^{-3/2}}$

Sir James Jeans, 1877 - 1946

(full detail in Mac Low & Klessen, 2004, Rev. Mod. Phys., 76, 125-194)

First approach to turbulence

- *von Weizsäcker (1943, 1951)* and *Chandrasekhar (1951):* concept of **MICROTURBULENCE**
  - BASIC ASSUMPTION: separation of scales between dynamics and turbulence

    $\ell_{turb} \ll \ell_{dyn}$
  - then turbulent velocity dispersion contributes to effective soundspeed:

    $$\boxed{c_c^2 \mapsto c_c^2 + \sigma_{rms}^2}$$
  - → Larger effective Jeans masses → more stability
  - BUT: *(1) turbulence depends on k:* $\sigma_{rms}^2(k)$

    (2) supersonic turbulence → *usually* $\sigma_{rms}^2(k) >> c_s^2$

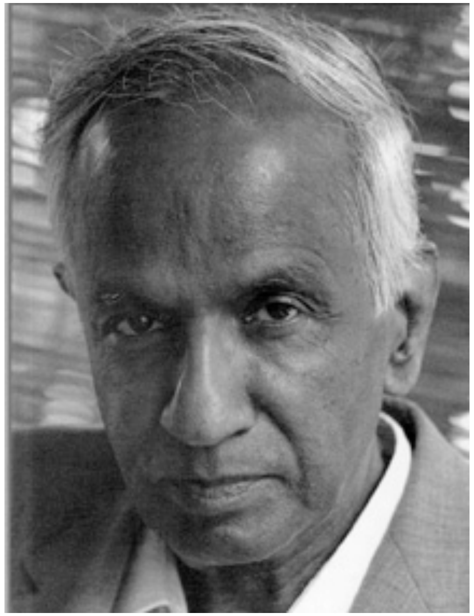

S. Chandrasekhar, 1910 - 1995

(full detail in Mac Low & Klessen, 2004, Rev. Mod. Phys., 76, 125-194)

Problems of early dynamical theory

- Molecular clouds are *highly Jeans-unstable*
  Yet, they do *NOT* form stars at high rate
  and with high efficiency.
  (the observed global SFE in molecular clouds is *~5%*)
  → *something prevents large-scale collapse.*
- All throughout the early 1990's, molecular clouds had been thought to be long-lived quasi-equilitrium entities.
- Molecular clouds are *magnetized.*

(full detail in Mac Low & Klessen, 2004, Rev. Mod. Phys., 76, 125-194)

Magnetic star formation

- *Mestel & Spitzer (1956):* Magnetic fields can prevent collapse***!!!***
  - Critical mass for gravitational collapse in presence of B-field

$$M_{cr} = \frac{5^{3/2}}{48\pi^2} \frac{B^3}{G^{3/2}\rho^2}$$

  - Critical mass-to-flux ratio (Mouschovias & Spitzer 1976)

$$\left[\frac{M}{\Phi}\right]_{cr} = \frac{\zeta}{3\pi}\left[\frac{5}{G}\right]^{1/2}$$

  - Ambipolar diffusion can initiate collapse

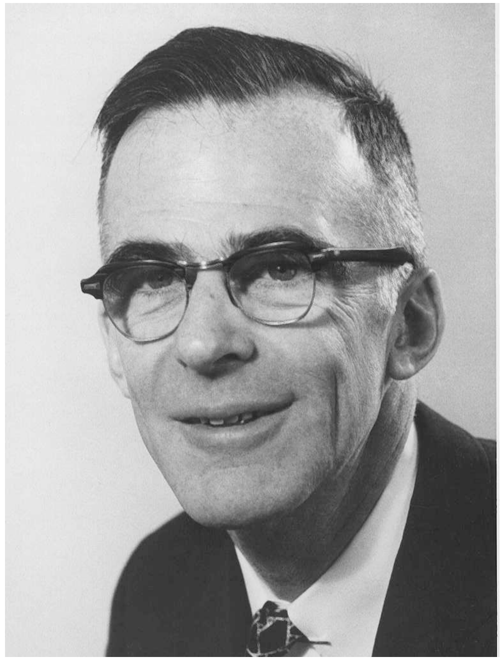

Lyman Spitzer, Jr., 1914 - 1997

(full detail in Mac Low & Klessen, 2004, Rev. Mod. Phys., 76, 125-194)

The "standard theory" of star formation:

- BASIC ASSUMPTION: Stars form from magnetically highly subcritical cores
- Ambipolar diffusion slowly increases (M/Φ): $\tau_{AD} \approx 10\tau_{ff}$
- Once $(M/\Phi) > (M/\Phi)_{crit}$: dynamical collapse of SIS
  - Shu (1977) collapse solution
  - $dM/dt = 0.975\ c_s^3/G = \text{const.}$
- Was (in principle) only intended for isolated, low-mass stars

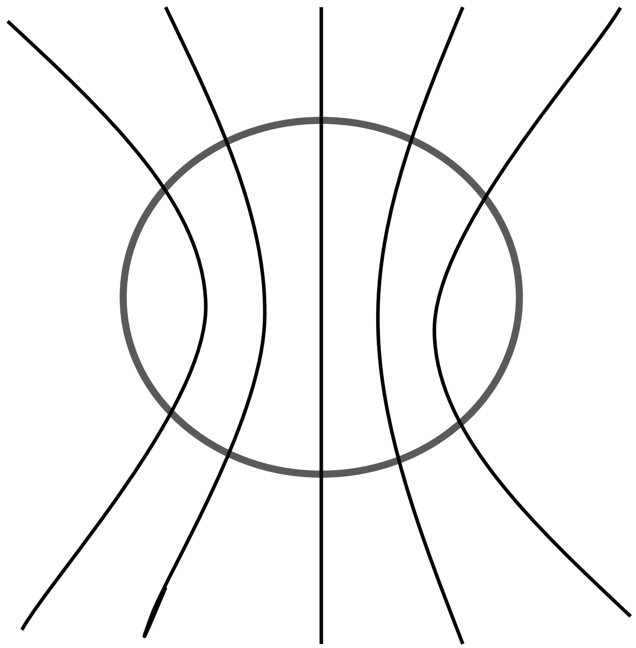

Problems of magnetic SF

- Observed B-fields are weak, at most marginally critical (Crutcher 1999, Bourke et al. 2001)
- Magnetic fields cannot prevent decay of turbulence
  (Mac Low et al. 1998, Stone et al. 1998, Padoan & Nordlund 1999)
- Structure of prestellar cores
  (Bacman et al. 2000, e.g. Barnard 68 from Alves et al. 2001)
- Strongly time varying dM/dt
  (e.g. Hendriksen et al. 1997, André et al. 2000)
- More extended infall motions than predicted by the standard model
  (Williams & Myers 2000, Myers et al. 2000)

Observed B-fields are weak

B versus $N(H_2)$ from *Zeeman measurements*.

(from Bourke et al. 2001)

→ cloud cores are magnetically supercritical!!!

$(\Phi/M)_n > 1$ **no collapse**

$(\Phi/M)_n < 1$ **collapse**

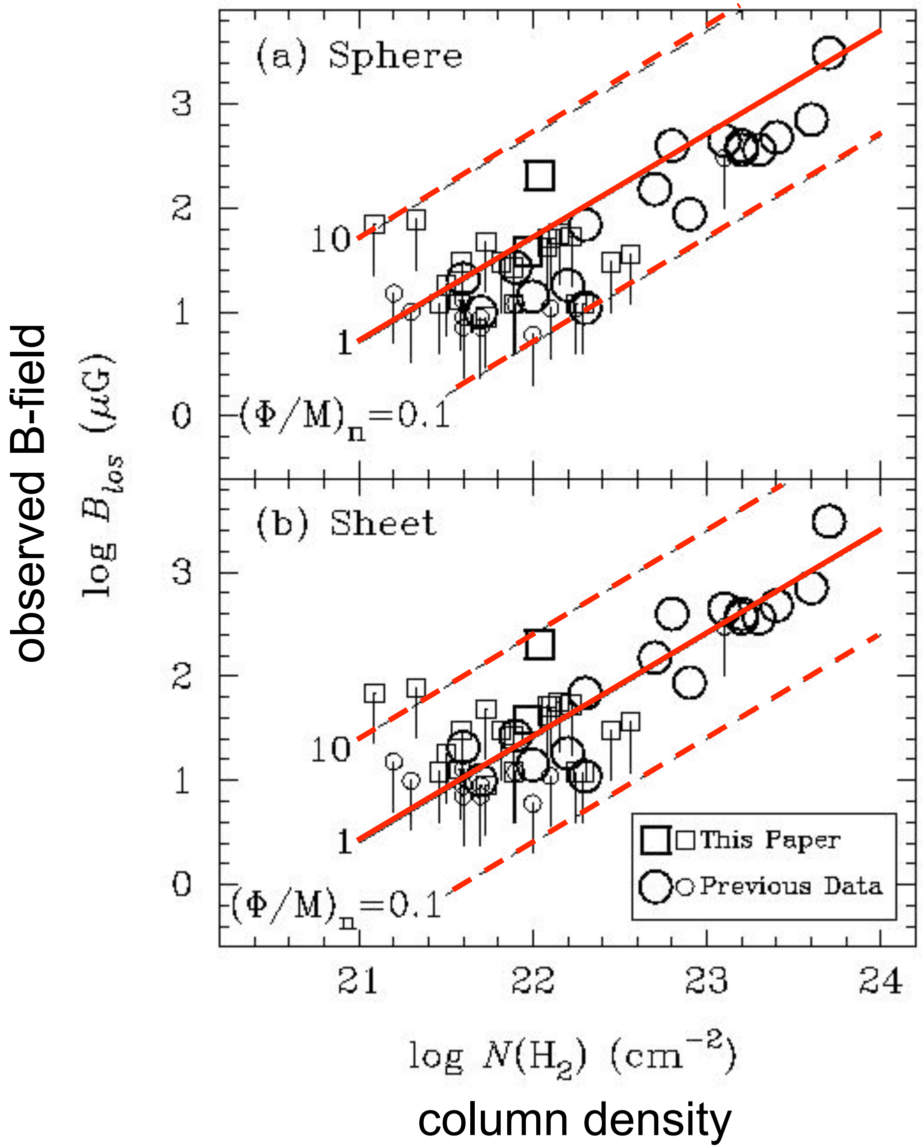

Problems of magnetic SF

- Observed B-fields are weak, at most marginally critical (Crutcher 1999, Bourke et al. 2001)
- Magnetic fields cannot prevent decay of turbulence
  (Mac Low et al. 1998, Stone et al. 1998, Padoan & Nordlund 1999)
- Structure of prestellar cores
  (Bacman et al. 2000, e.g. Barnard 68 from Alves et al. 2001)
- Strongly time varying dM/dt
  (e.g. Hendriksen et al. 1997, André et al. 2000)
- More extended infall motions than predicted by the standard model
  (Williams & Myers 2000, Myers et al. 2000)

Molecular cloud dynamics

- **Timescale problem:** Turbulence *decays* on timescales *comparable to the free-fall time* τ_{ff} ($E \propto t^{-\eta}$ with $\eta \approx 1$).

  (Mac Low et al. 1998,
  Stone et al. 1998,
  Padoan & Nordlund 1999)

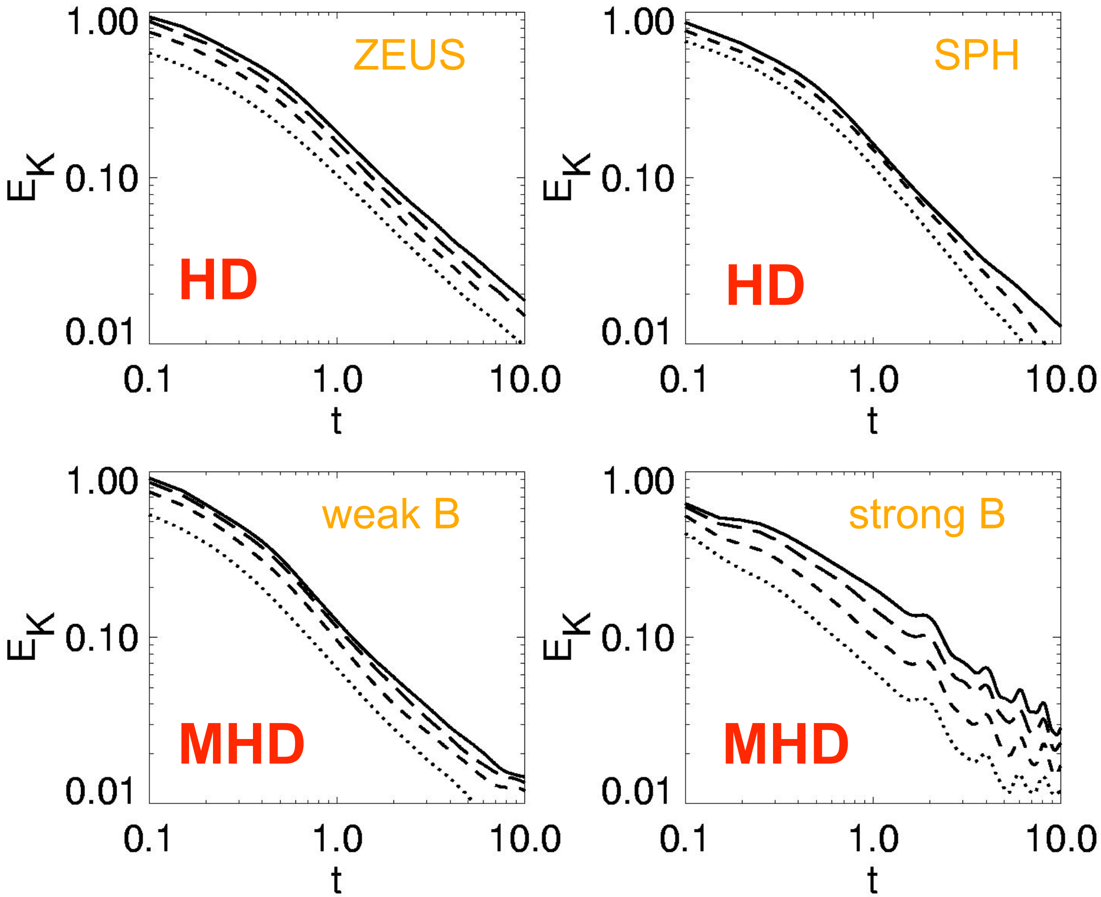

- Magnetic fields (static or wave-like) *cannot* prevent loss of energy.

(Mac Low, Klessen, Burkert, & Smith, 1998, PRL)

Problems of magnetic SF

- As many prestellar cores as protostellar cores in SF regions (e.g. André et al 2002)
- Molecular cloud clumps seem to be chemically young
  (Bergin & Langer 1997, Pratap et al 1997, Aikawa et al 2001)
- Stellar age distribution small ($\tau_{ff} << \tau_{AD}$)
  (Ballesteros-Paredes et al. 1999, Elmegreen 2000, Hartmann 2001)
- Strong theoretical criticism of the SIS as starting condition for gravitational collapse
  (e.g. Whitworth et al 1996, Nakano 1998, as summarized in Klessen & Mac Low 2004)
- Most stars form as binaries

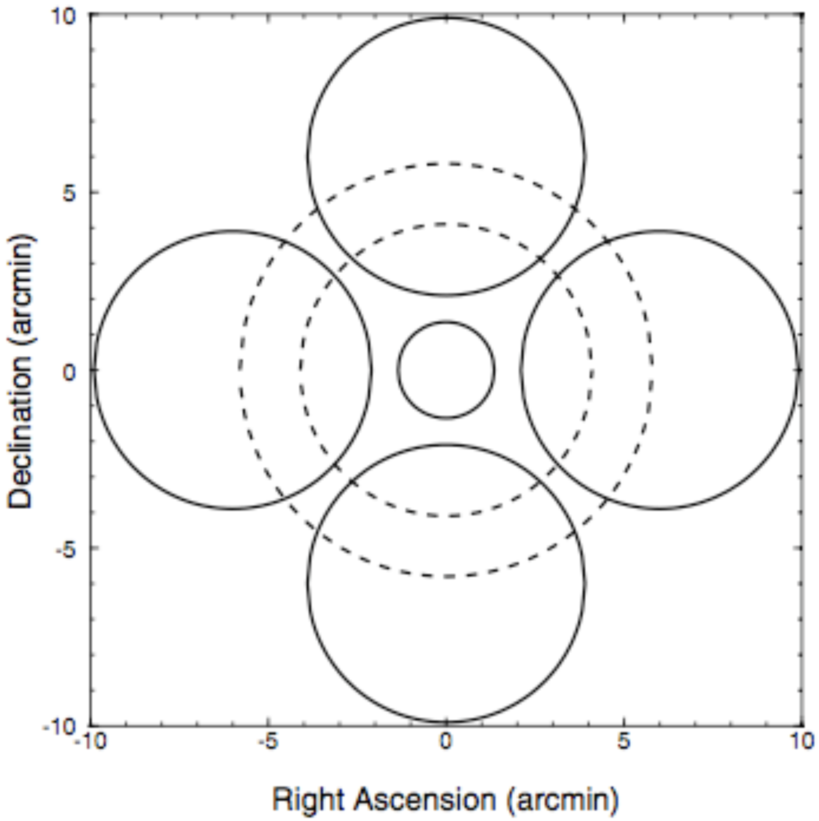

Fig. 1.— The Arecibo telescope primary beam (small circle centered at 0,0) and the four GBT telescope primary beams (large circles centered 6′ north, south, east, and west of 0,0. The dotted circles show the first sidelobe of the Arecibo telescope beam. All circles are at the half-power points.

Crutcher et al. (2008)

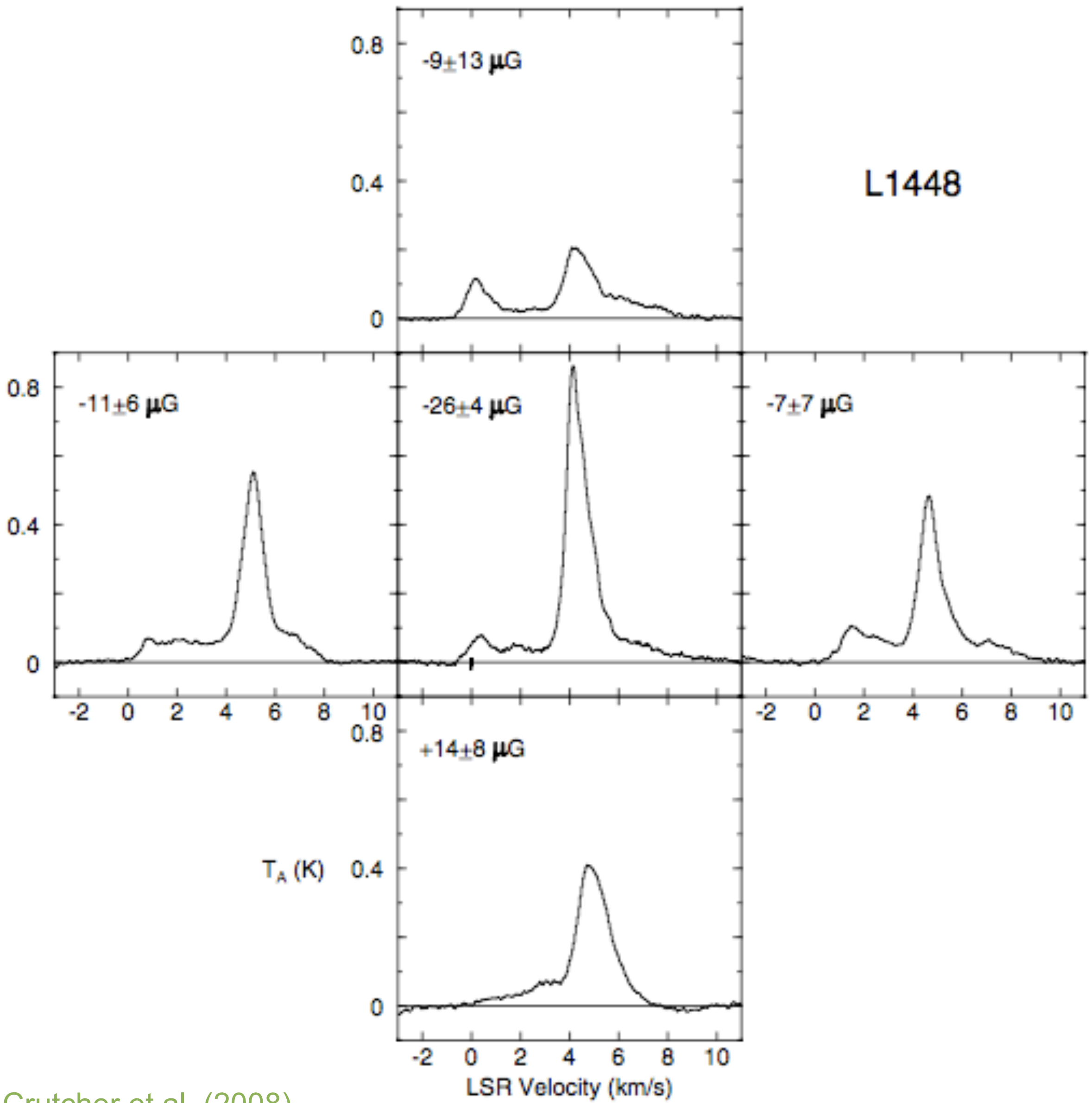

Crutcher et al. (2008)

Fig. 2.— OH 1667 MHz spectra toward the core of L1448CO obtained with the Arecibo telescope (center panel) and toward each of the envelope positions 6′ north, south, east, and west of the core, obtained with the GBT. In the upper left of each panel is the inferred B_{LOS} and its 1σ uncertainty at that position. A negative B_{LOS} means the magnetic field points toward the observer, and vice versa for a positive B_{LOS}.

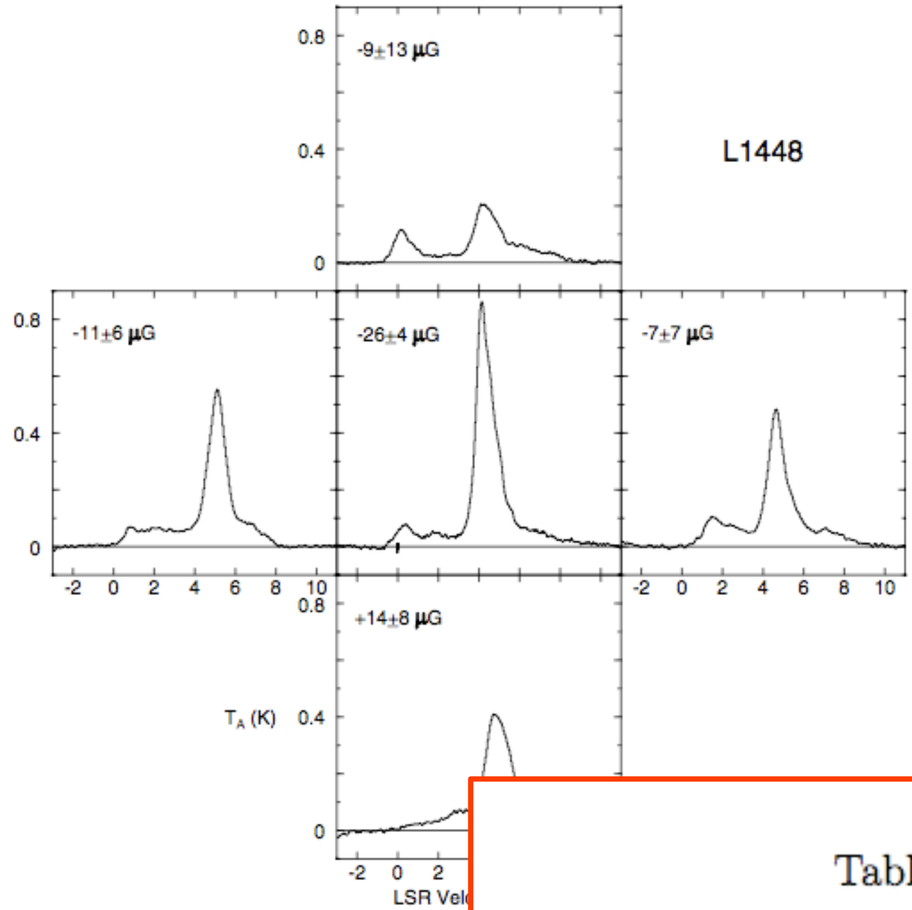

Fig. 2.— OH 1667 MHz spectra toward the
telescope (center panel) and toward each of the
west of the core, obtained with the GBT. In th
and its 1σ uncertainty at that position. A ne
toward the observer, and vice versa for a posit

example: L1448

Table 2. Relative Mass/Flux

Cloud	$\mathcal{R}$	$\mathcal{R}'$	Probability $\mathcal{R}$ or $\mathcal{R}' > 1$
L1448CO	0.02 ± 0.36	0.07 ± 0.34	0.005
B217-2	0.15 ± 0.43	0.19 ± 0.41	0.05
L1544	0.42 ± 0.46	0.46 ± 0.43	0.11
B1	0.41 ± 0.20	0.44 ± 0.19	0.010

Crutcher et al. (2008)

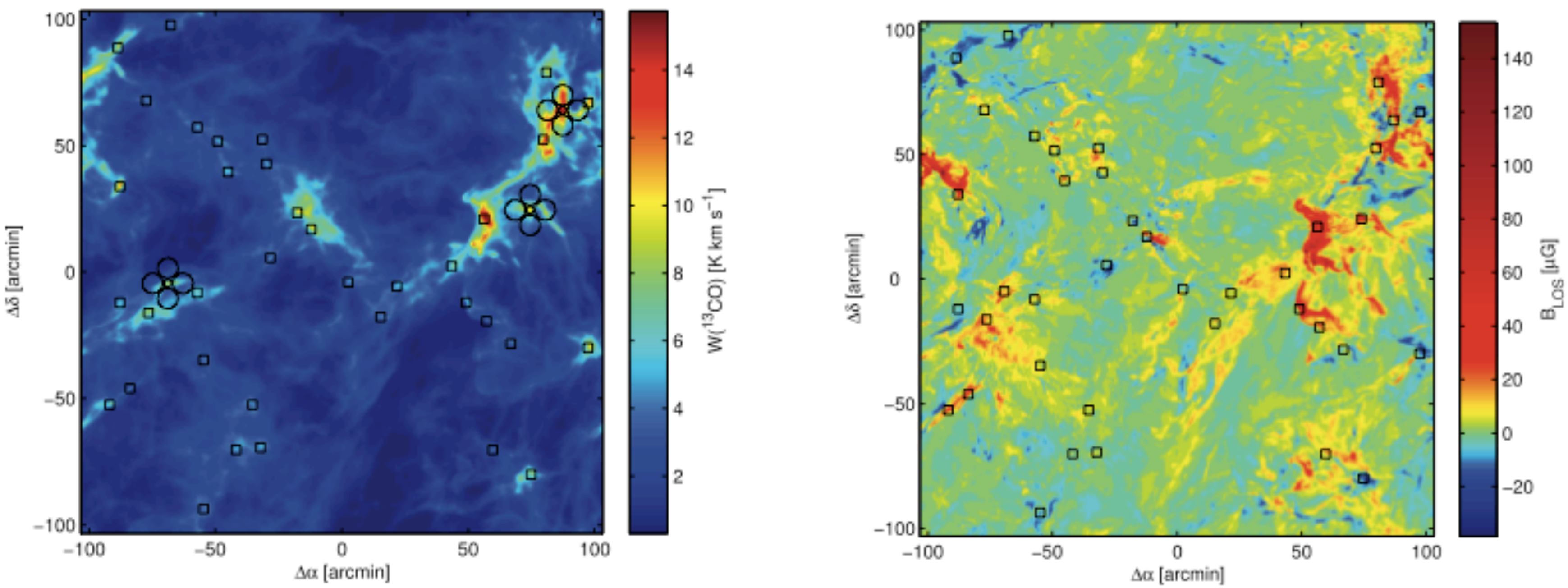

FIG. 1.—*Left*: Simulated ^{13}CO (1–0) map of the model in the *z*-axis direction. The locations of the cloud cores are shown with squares. The circles indicate the locations of telescope beams used in the synthetic observations of three cores. *Right*: Line-of-sight magnetic field strength as calculated from Zeeman splitting.

Lunttila et al. (2008)

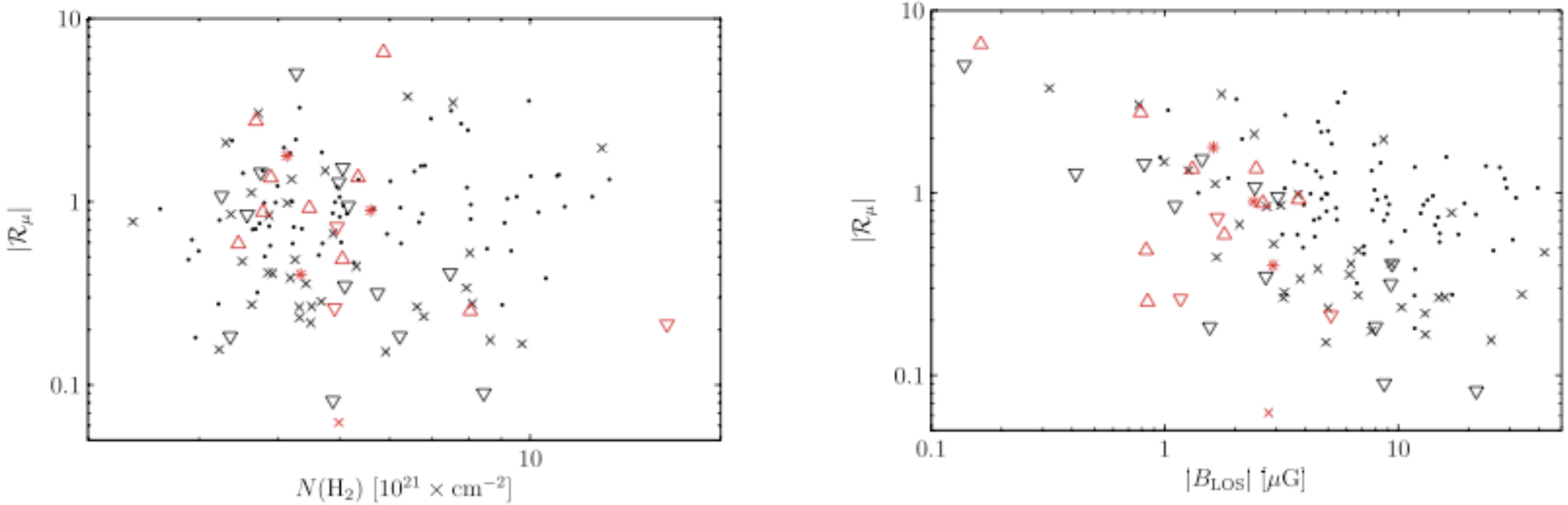

FIG. 3.—*Left*: Relative mass-to-flux ratio for the selected cores as a function of column density. Red symbols indicate the cores with $\mathcal{R}_\mu < 0$. Dots, crosses, triangles pointing down, triangles pointing up, and asterisks denote zero, one, two, three, or four field reversals in the envelopes relative to the core center. *Right*: Relative mass-to-flux ratio as a function of inferred magnetic field strength in the central beam. The symbols have the same meaning as in the left panel.

Lunttila et al. (2008)

current view

gravoturbulent star formation

- idea:

Star formation is controlled by interplay between gravity and supersonic turbulence!

- dual role of turbulence:
  - *stability on large scales*
  - *initiating collapse on small scales*

(e.g., Larson, 2003, Rep. Prog. Phys, 66, 1651;
or Mac Low & Klessen, 2004, Rev. Mod. Phys., 76, 125)

gravoturbulent star formation

- idea:

Star formation is controlled by interplay between gravity and supersonic turbulence!

- validity:

This hold on *all* scales and applies to build-up of stars and star clusters within molecular clouds as well as to the formation of molecular clouds in galactic disk.

(e.g., Larson, 2003, Rep. Prog. Phys, 66, 1651;
or Mac Low & Klessen, 2004, Rev. Mod. Phys., 76, 125)

gravoturbulent star formation

- interstellar gas is highly *inhomogeneous*
  - *gravitational instability*
  - *thermal instability*
  - *turbulent compression* (in shocks $\delta\rho/\rho \propto \mathcal{M}^2$; in atomic gas: $\mathcal{M} \approx 1...3$)

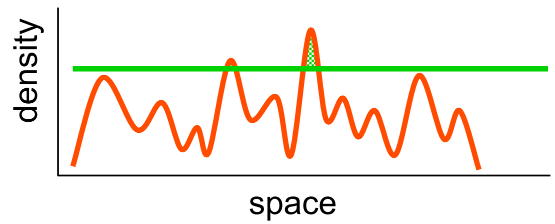

- cold *molecular clouds* can form rapidly in high-density regions at *stagnation points* of *convergent large-scale flows*
  - chemical *phase transition*: atomic → molecular
  - process is *modulated* by large-scale *dynamics* in the galaxy
- inside *cold clouds:* turbulence is highly supersonic ($\mathcal{M} \approx 1...20$)
  → *turbulence* creates large density contrast,
  gravity selects for collapse

  ⟶ $\boxed{\textbf{\textit{GRAVOTUBULENT FRAGMENTATION}}}$

- *turbulent cascade:* local compression *within* a cloud provokes collapse
  → formation of individual *stars* and *star clusters*

(e.g. Mac Low & Klessen, 2004, Rev. Mod. Phys., 76, 125-194) predictions

predictions

- *star formation on galactic scales*
  - global correlations: Schmidt-law
  - efficiencies, rates, timescales, and long-term evolution: starburst vs. low surface density gal.
  - triggers of star formation on global scales
  - formation of dense cold molecular clouds properties of these clouds (structure, turbulence, etc.)
- *star cluster formation within clouds*
  - SF efficiency and timescale
  - properties of young star clusters (structure, kinematics)
  - stellar mass function – IMF
  - multiplicity
  - effects of stellar feedback (jets, outflows, radiation, winds, ...)

agenda

- formation of molecular clouds
  - on galactic scales
  - locally, in convergent flows
  - do molecular clouds loose memory of initial conditions?
- fragmentation of molecular clouds
  - interplay between gravity and turbulence
- star formation
  - initial mass function (models & caveats)
  - some examples
- what‘s next?

galactic scales

molecular cloud formation

- star formation on galactic scales
  → missing link so far:
  formation of molecular clouds
- questions
  - where and when do molecular clouds form?
  - what are their properties?
  - how does that correlation to star formation?
  - global correlations? → Schmidt law

molecular cloud formation

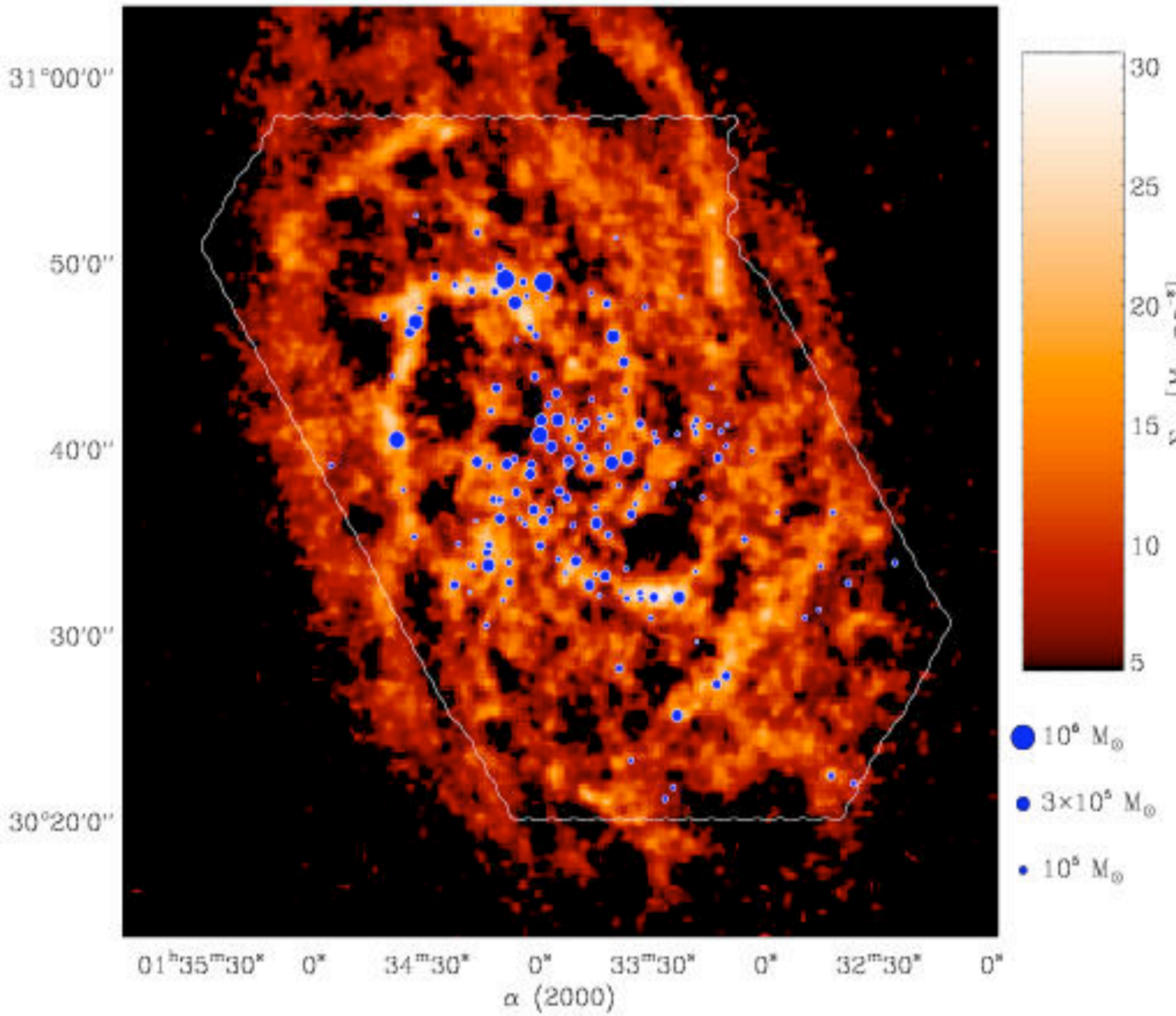

Thesis:

Molecular clouds form at *stagnation points* of large-scale convergent flows, mostly triggered by global (or external) perturbations.

(Deul & van der Hulst 1987, Blitz et al. 2004)

correlation with large-scale perturbations

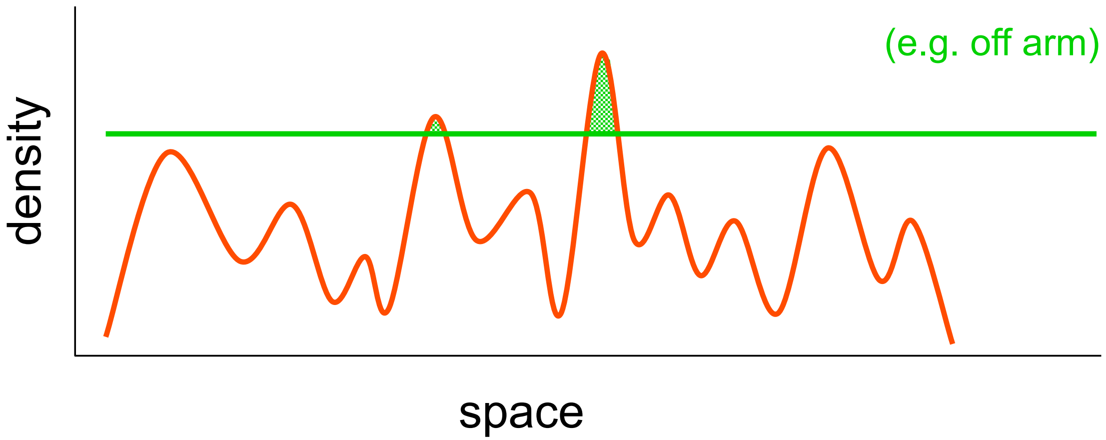

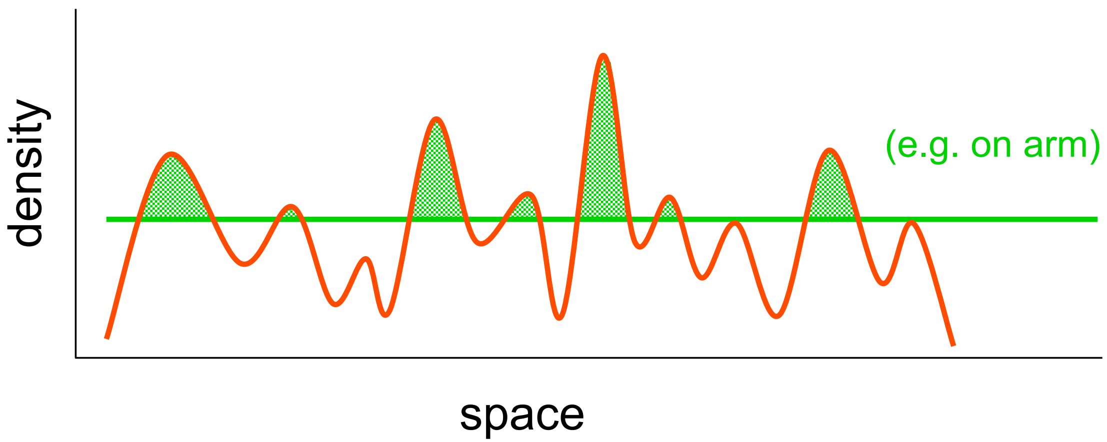

density/temperature fluctuations in warm atomar ISM are caused by *thermal/gravitational instability* and/or *supersonic turbulence*

some fluctuations are *dense* enough to *form H_2* within "*reasonable time*"

→ *molecular cloud*

(Glover & Mac Low 2007a,b)

external perturbuations (i.e. potential changes) *increase* likelihood

(e.g. talk by Clare Dobbs)

star formation on *global* scales

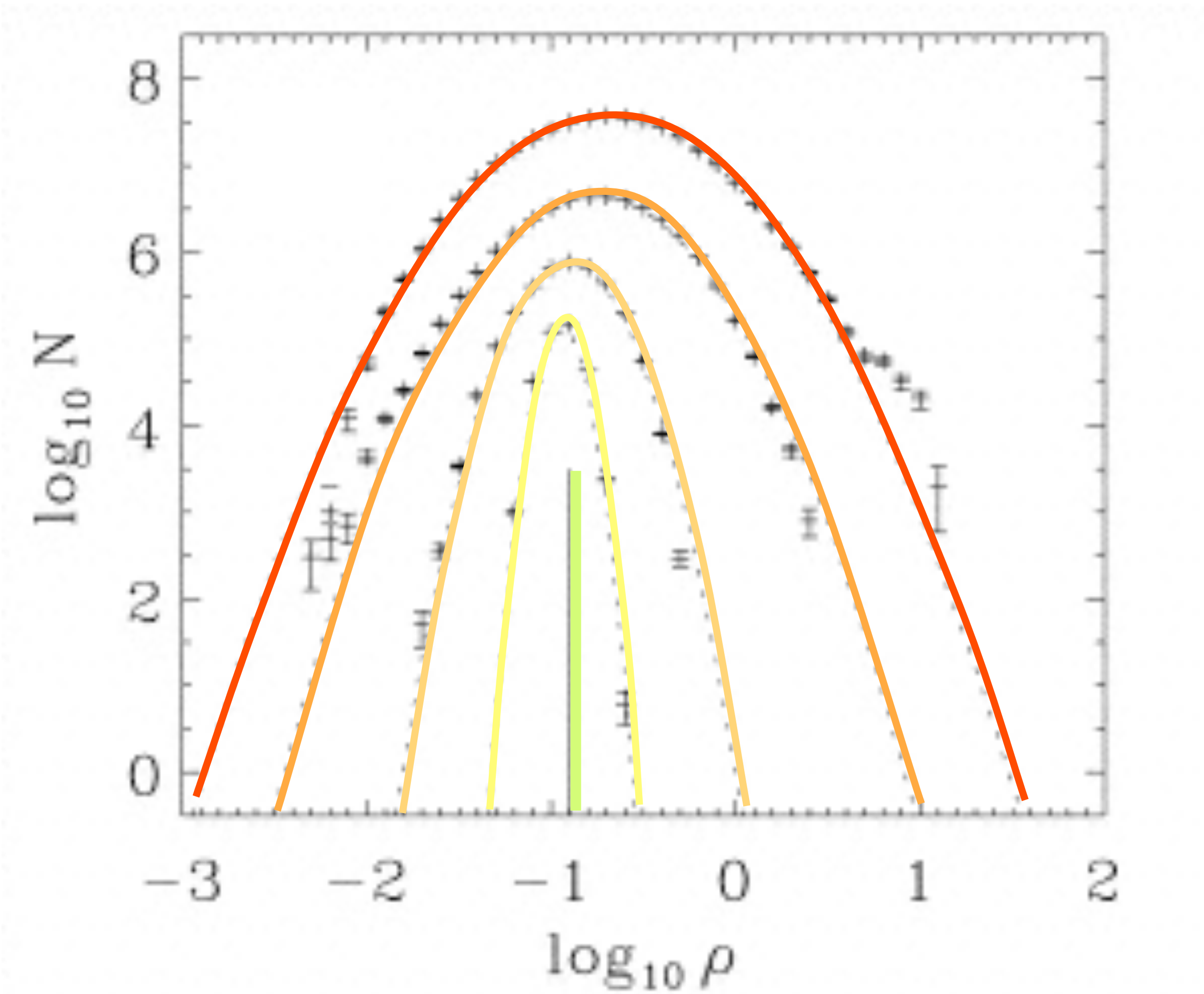

mass weighted ρ-pdf, each shifted by ΔlogN=1

(from Klessen, 2001; also Gazol et al. 2005, Mac Low et al. 2005)

probability distribution function of the density *(ρ-pdf)*

varying rms Mach numbers:

M1 > M2 > M3 > M4 > 0

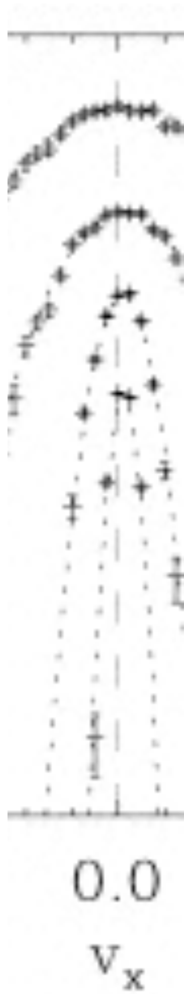

star formation on *global* scales

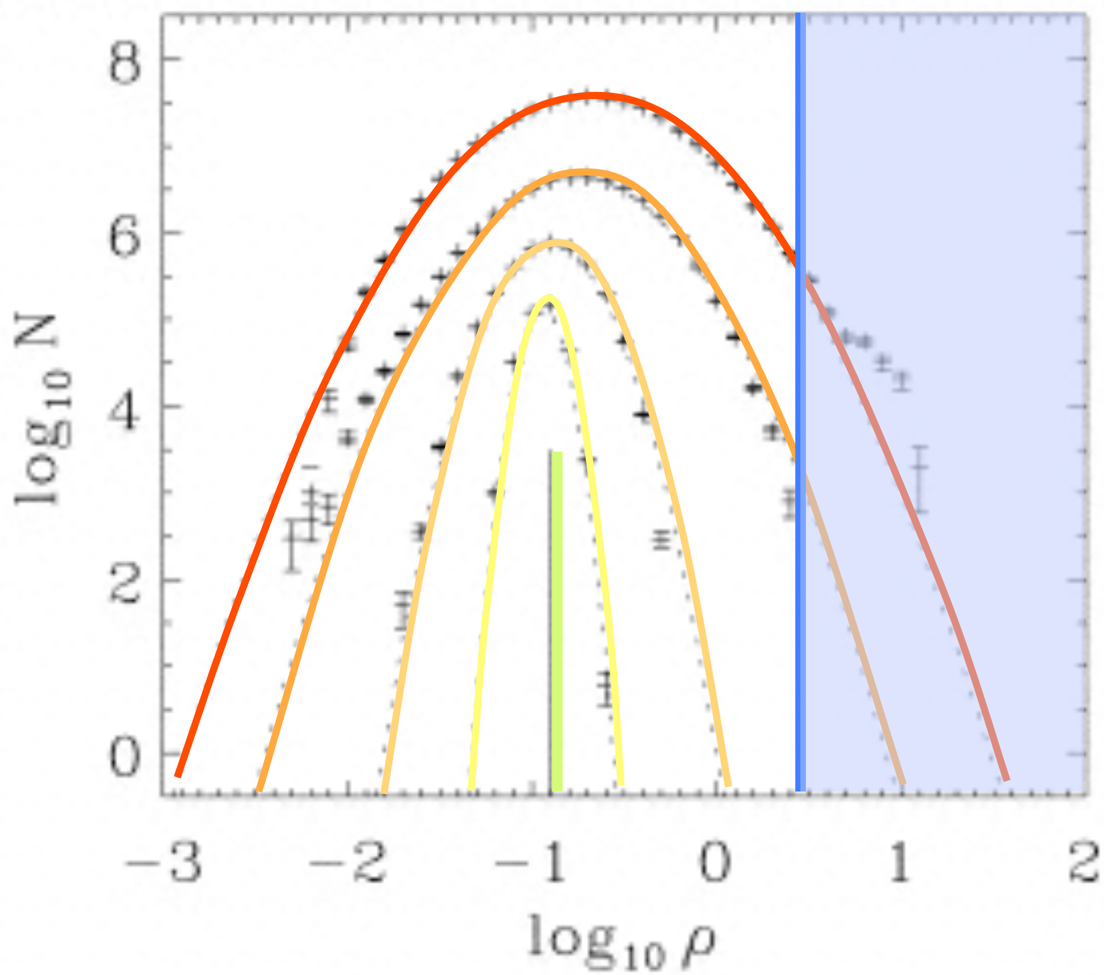

mass weighted ρ-pdf, each shifted by $\Delta \log N=1$

(rate from Hollenback, Werner, & Salpeter 1971)

H_2 formation rate:

$$\boxed{\tau_{H_2} \approx \frac{1.5\,\mathrm{Gyr}}{n_H / 1\mathrm{cm}^{-3}}}$$

for $n_H \geq 100\ \mathrm{cm}^{-3}$, H_2 forms within 10Myr, this is about the lifetime of typical MC's.

in turbulent gas, the H_2 fraction can become very high on short timescale

(for models with coupling between cloud dynamics and time-dependent chemistry, see Glover & Mac Low 2007a,b)

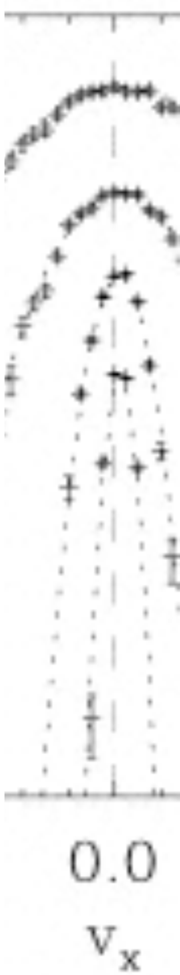

modeling galactic SF

SPH calculations of self-gravitating disks of stars and (isothermal) gas in dark-matter potential, sink particles measure local collapse --> star formation

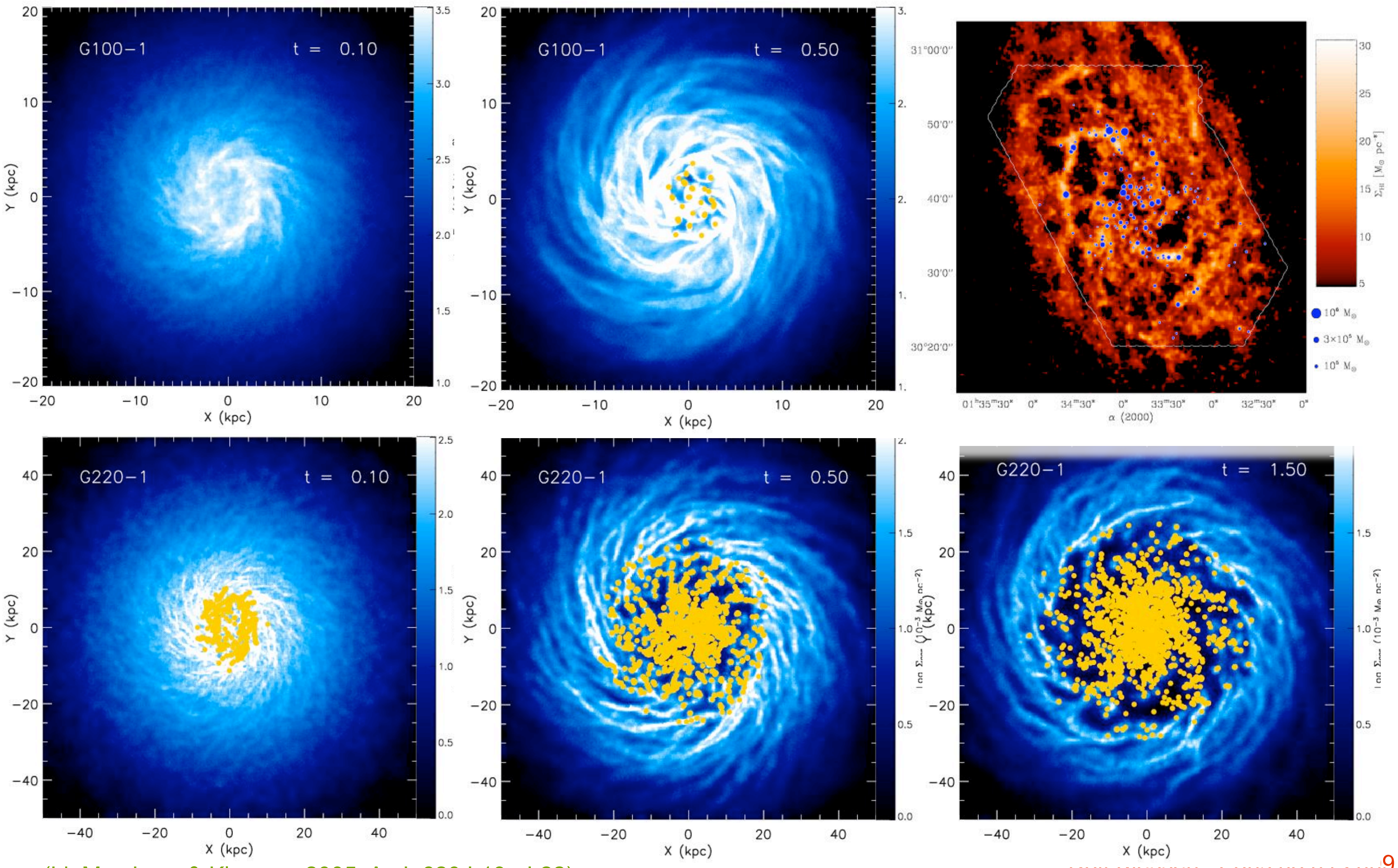

(Li, Mac Low, & Klessen, 2005, ApJ, 620,L19 - L22)

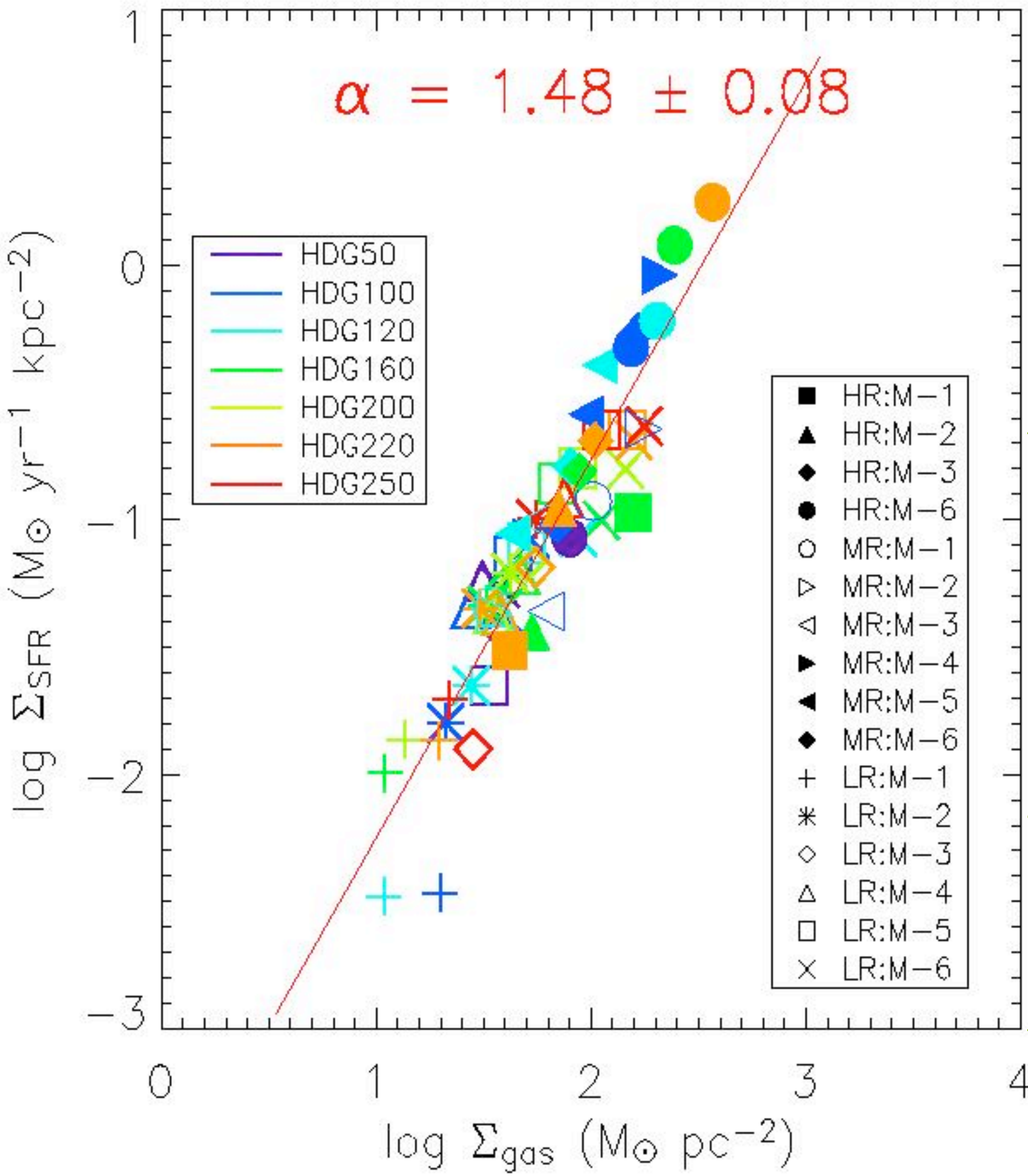

(Li, Mac Low, & Klessen, 2005, ApJ, 620, L19 - L22)

We find correlation between *star formation rate* and *gas surface density:*

$$\boxed{\Sigma_{SFR} \propto \Sigma_{gas}^{1.5}}$$

global Schmidt law

observed Schmidt law

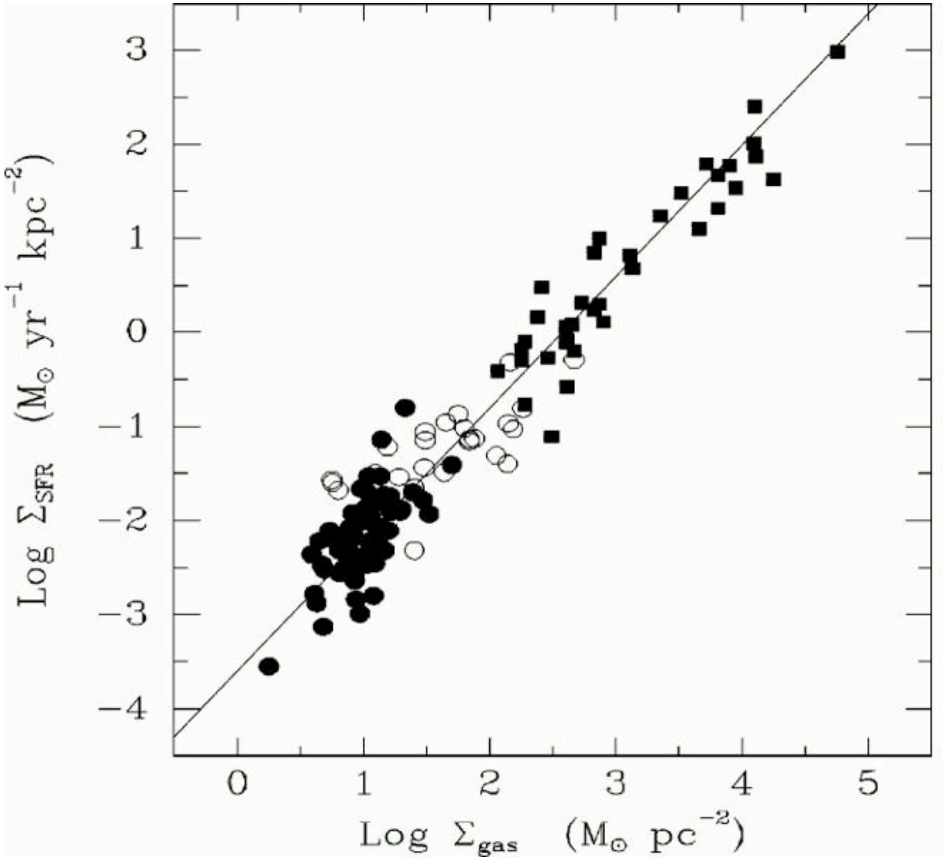

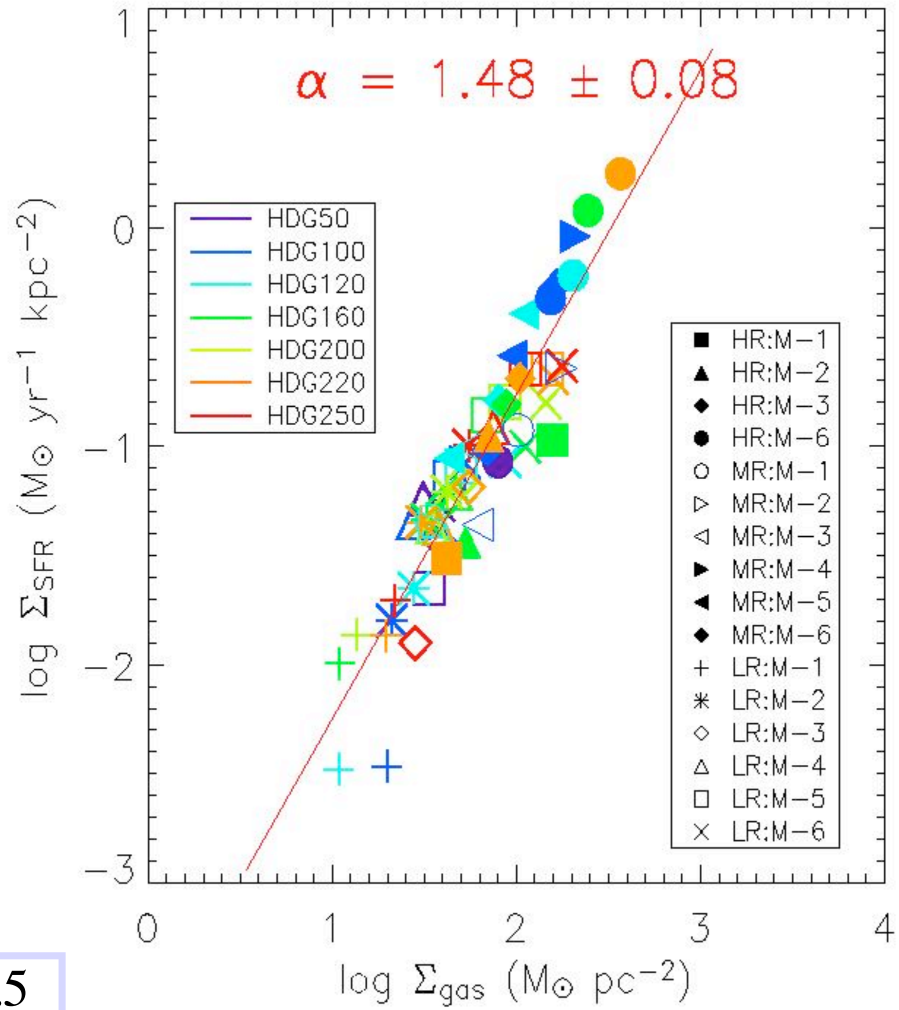

in both cases: $\boxed{\Sigma_{SFR} \propto \Sigma_{gas}^{1.5}}$

(from Kennicutt 1998)

molecular cloud formation

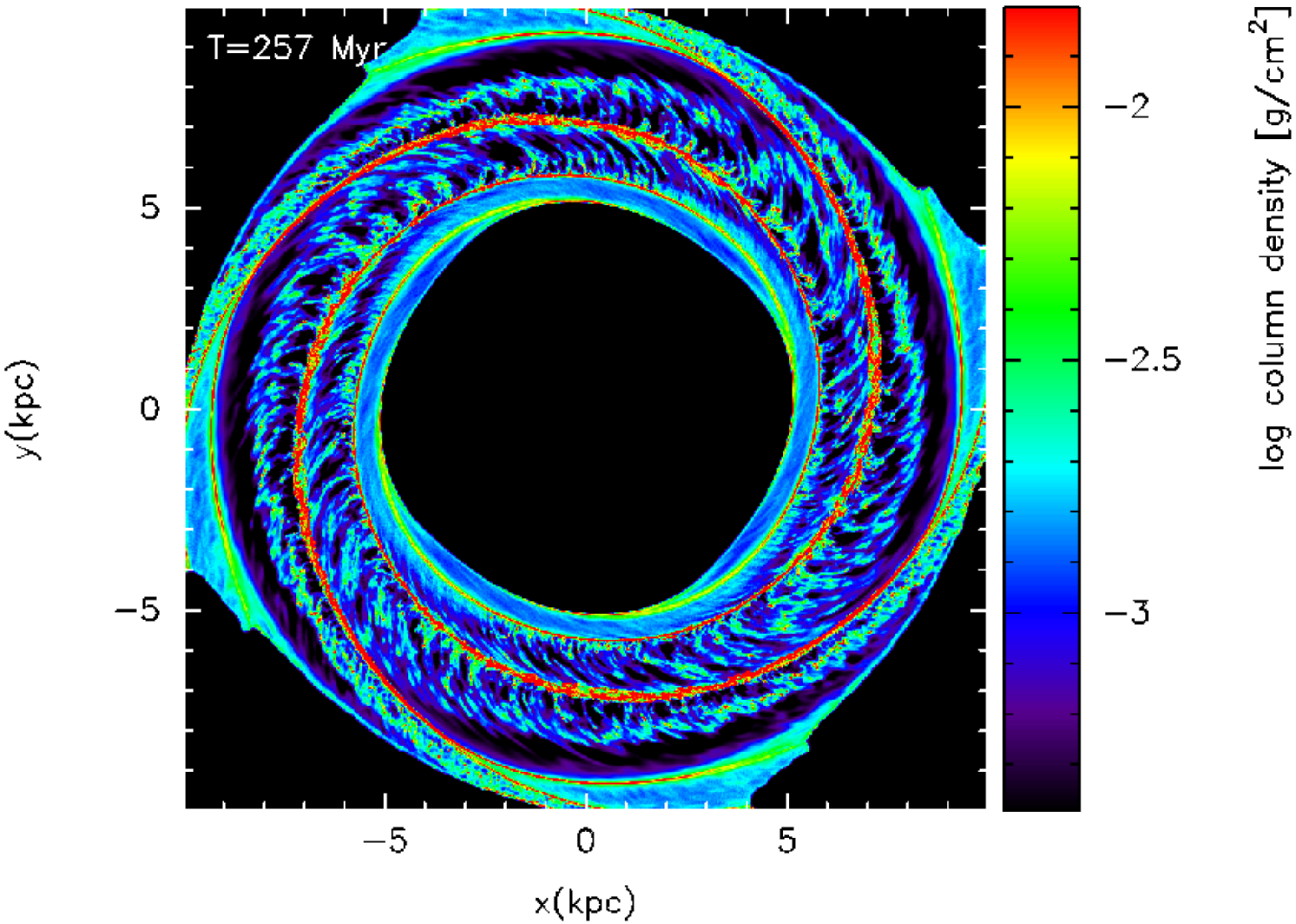

(from Dobbs, Glover, Clark, Klessen 2008)

molecular cloud formation

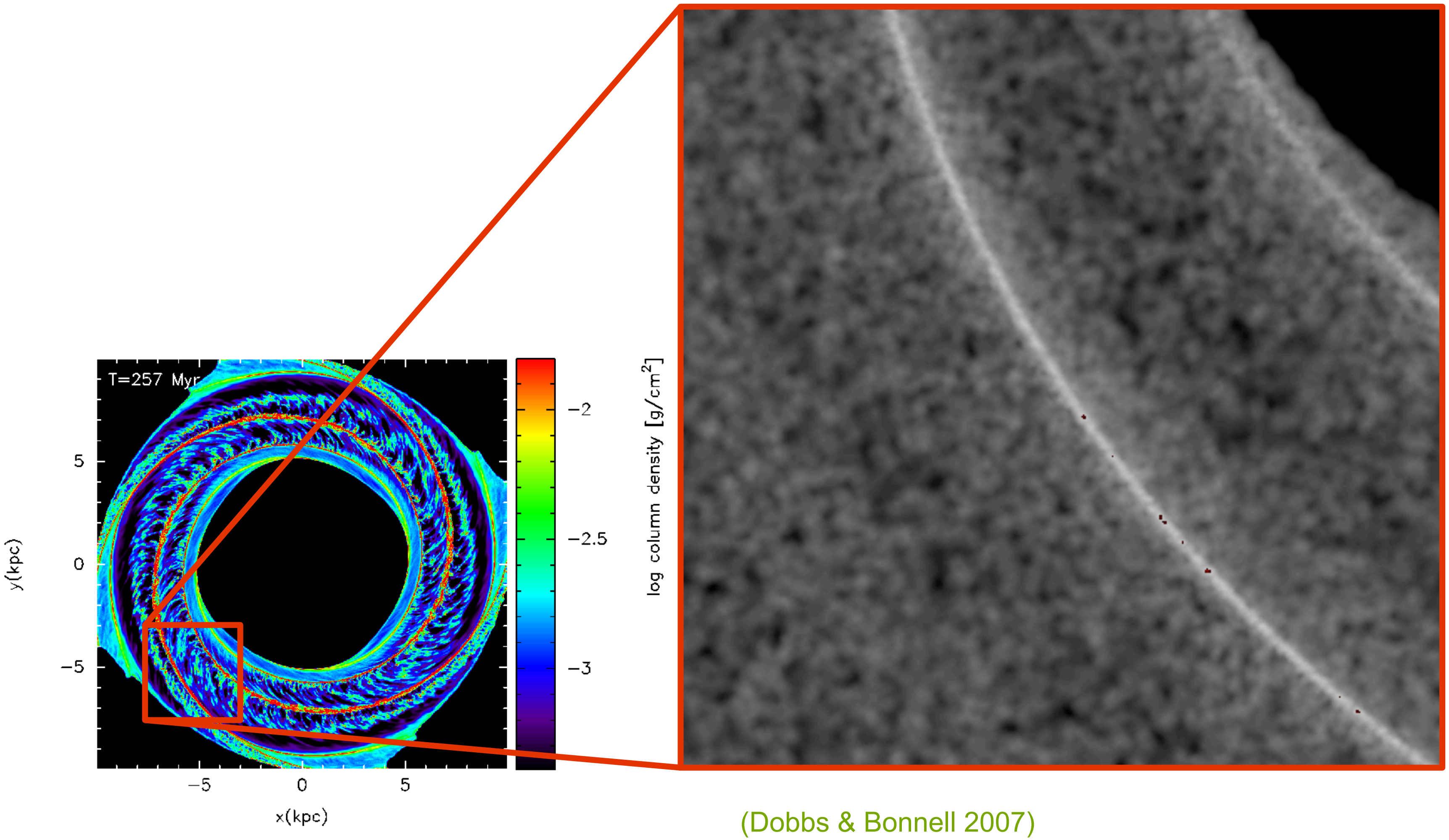

(Dobbs & Bonnell 2007)

molecular cloud formation

molecular gas fraction as function of time

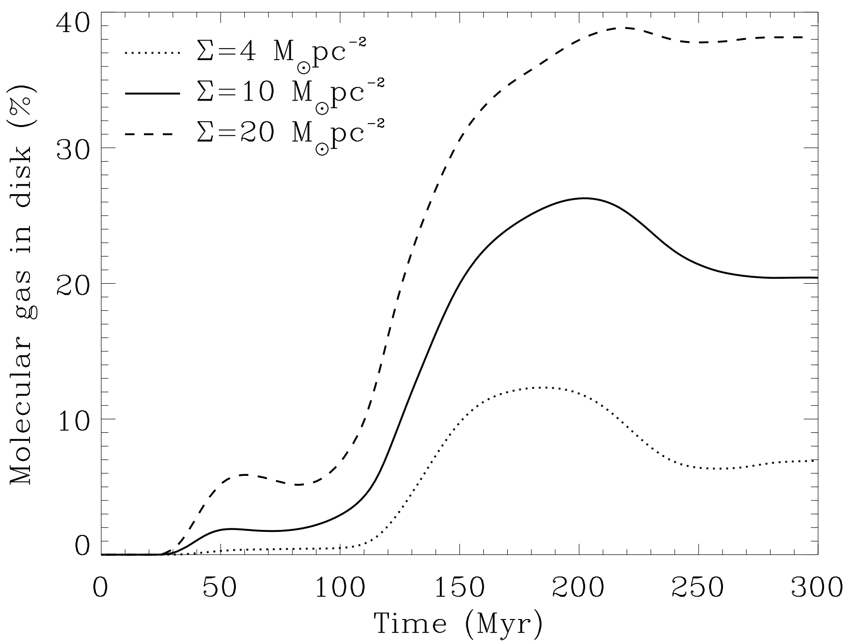

molecular gas fraction as function of density

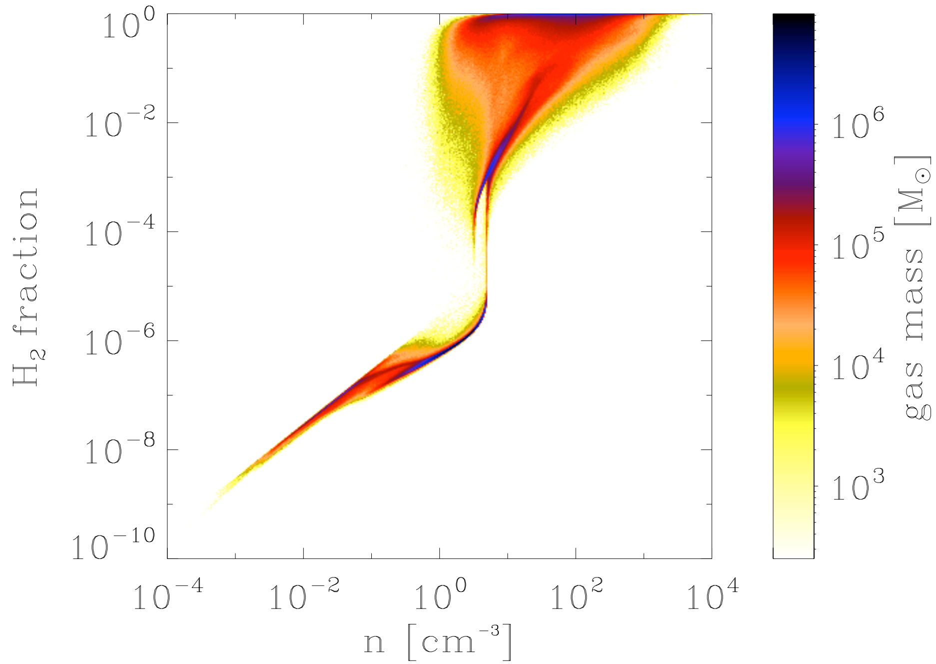

(Dobbs et al. 2008)

molecular cloud formation

molecular gas fraction of fluid element as function of time

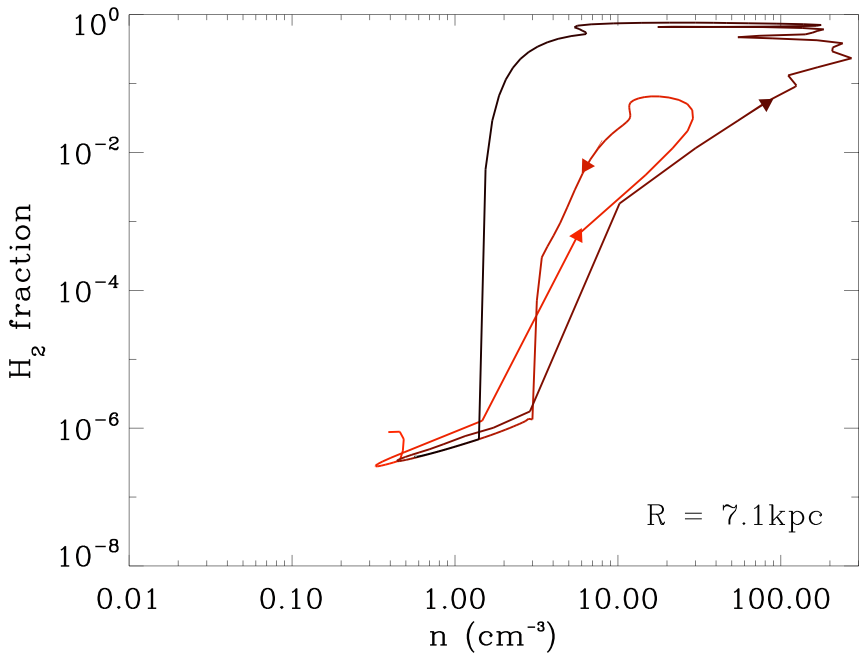

molecular gas fraction as function of density

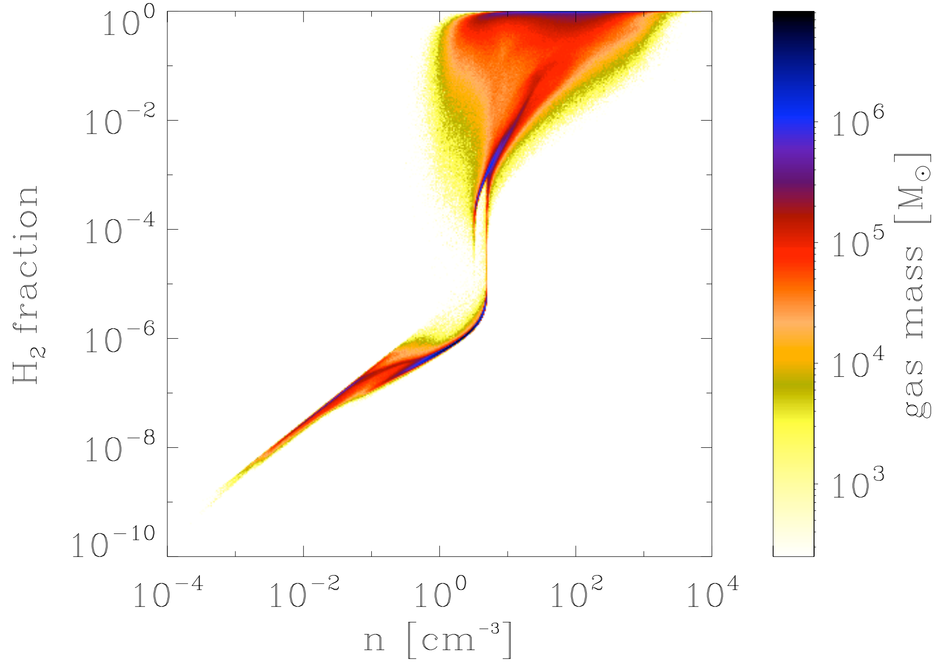

(Dobbs et al. 2008)

observed timescales

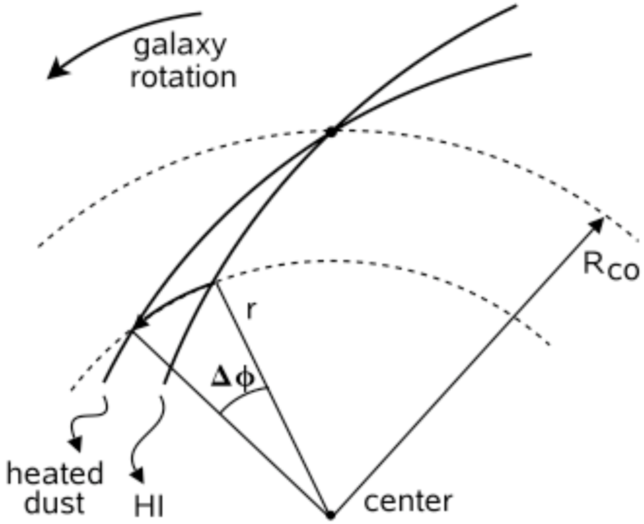

Tamburro et al. (2008)

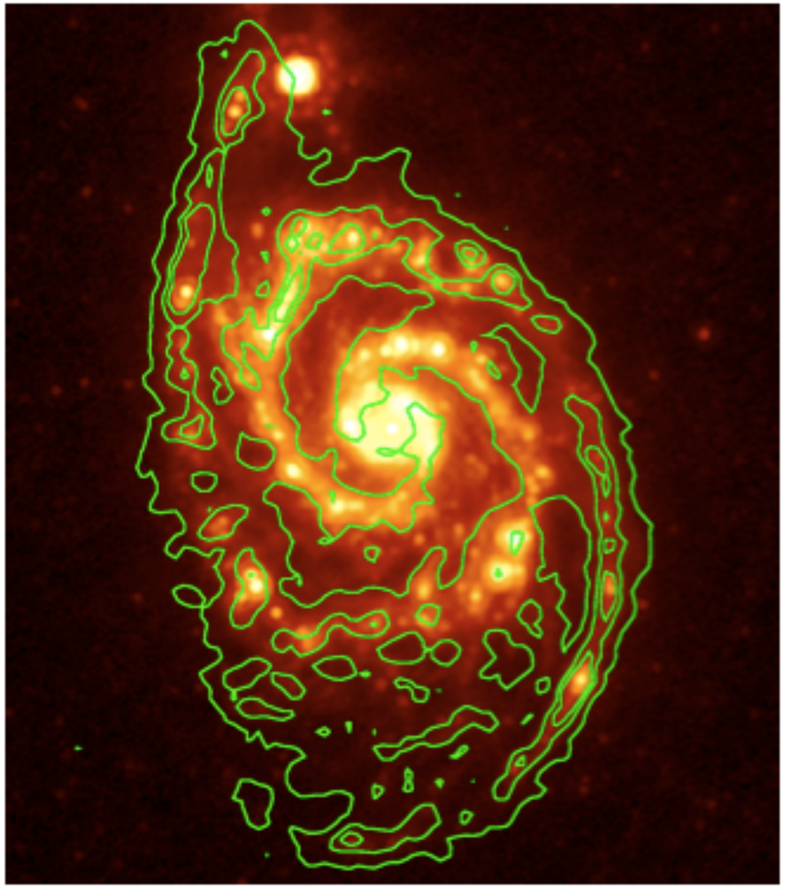

Fig. 1.— NGC 5194: the 24 μm band image is plotted in color scale; the H I emission map is overlayed with green contours.

observed timescales

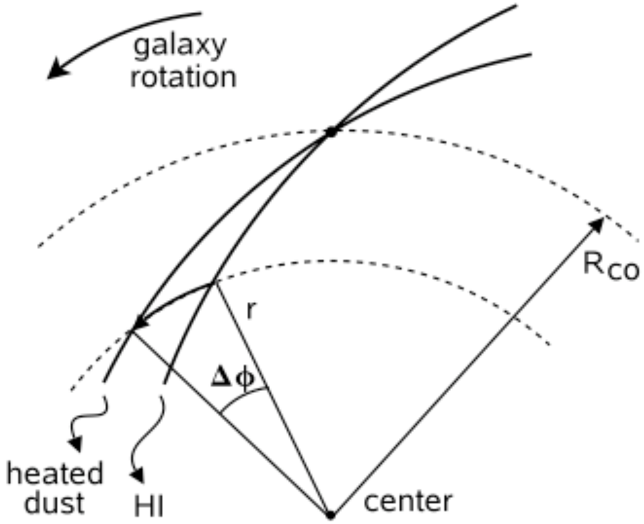

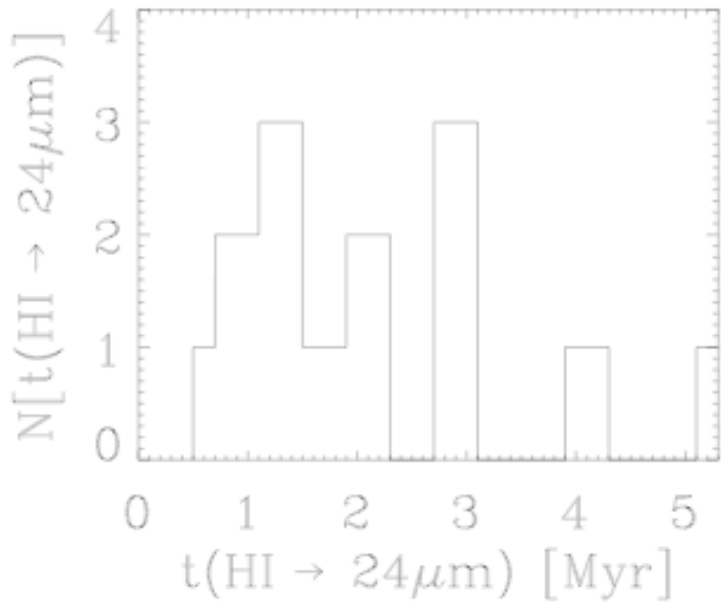

Fig. 5.— Histogram of the time scales $t_{HI \mapsto 24\,\mu m}$ derived from the fits in Figure 4 and listed in Table. 2 for the 14 sample galaxies listed in Table. 1. The timescales range between 1 and 4 Myr for almost all galaxies.

Tamburro et al. (2008)

models with B-fields

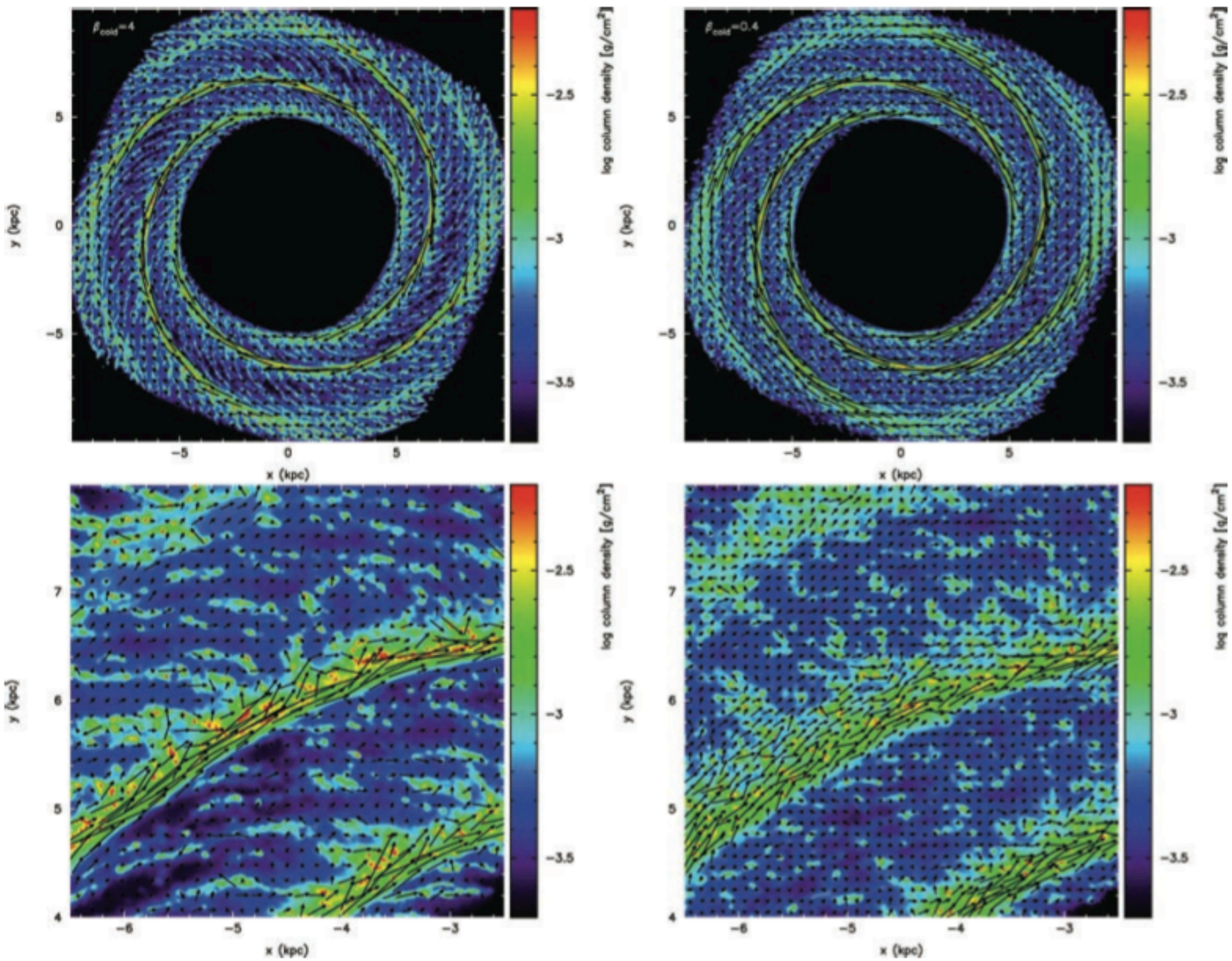

Figure 9. The column density is shown for the two-phase simulations after 250 Myr, for the whole disc (top panel) and a 4 × 4 kpc subsection (bottom panel). The left-hand panels show the case where $\beta_{cold} = 4$ and the right-hand panels where $\beta_{cold} = 0.4$. Both the cold and warm phases are shown in the plots, but we show them separately for the case where $\beta_{cold} = 4$ in Fig. 12. There is more structure in the cold gas when the magnetic field is weaker ($\beta_{cold} = 4$). The vectors show the magnetic field smoothed over a particular grid size. There is more detailed structure on smaller scales, particularly in the spiral arms which are better resolved.

Dobbs & Price (2008), Shetty & Ostriker (2007, 2008)

ISM: transition HI to H_2

consistent models of ISM dynamics require to go beyond the simple models!

- magnetohydrodynamics
  (account for large-scale dynamics
  + turbulence)
- time-dependent chemistry
  (reduced network, focus on few dominant species, e.g. H_2)
- radiation (currently simple assumptions)

H2 forms rapidly in shocks / transient density fluctuations / H2 gets destroyed slowly in low density regions / result: turbulence greatly enhances H2-formation rate

(Glover & Mac Low 2007ab:)

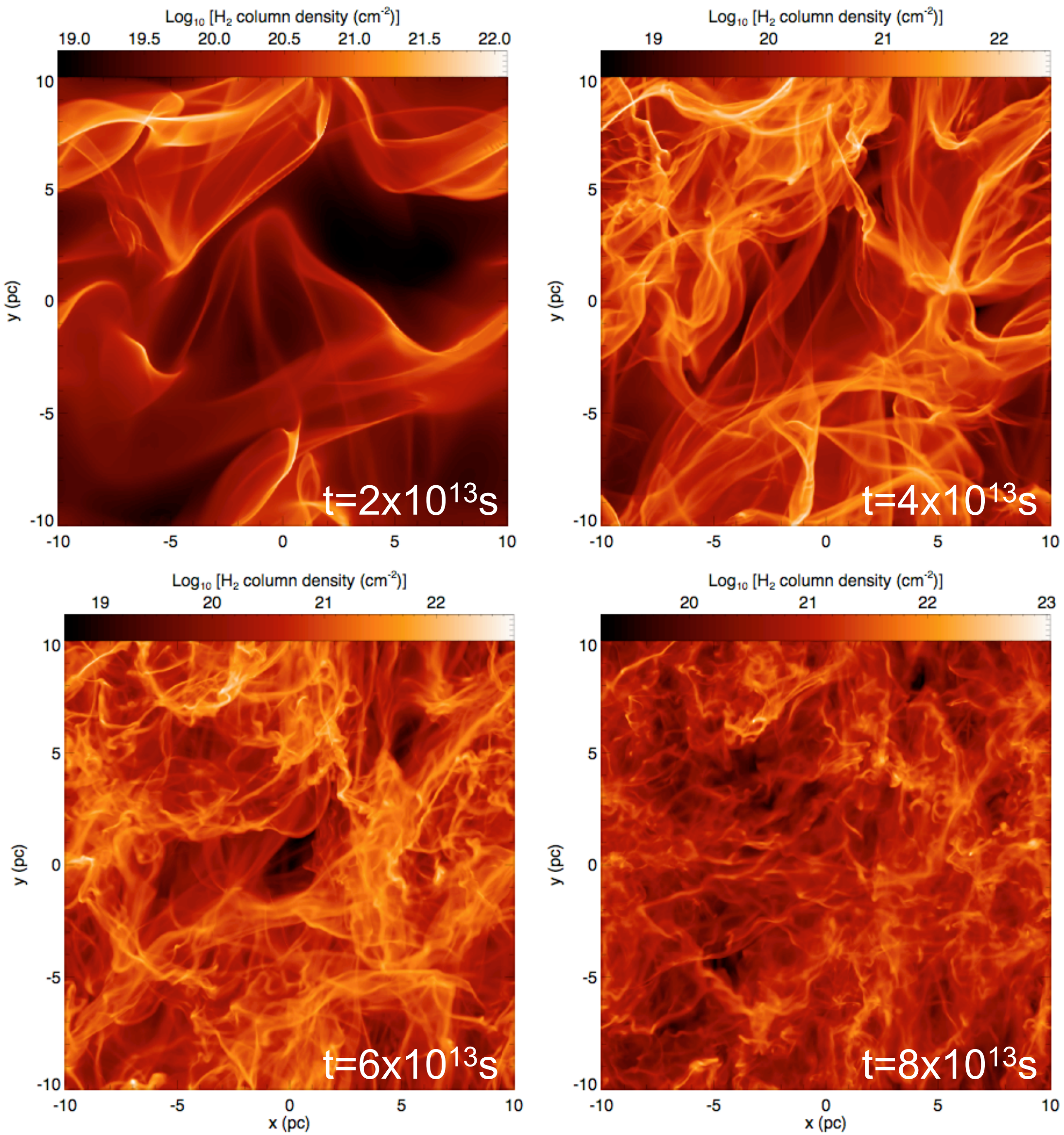

Reduced chemical network

Table 1. The set of chemical reactions that make up our model of non-equilibrium hydrogen chemistry.

Reaction	Reference
1. $H + H + grain \rightarrow H_2 + grain$	Hollenbach & McKee (1979)
2. $H_2 + H \rightarrow 3H$	Mac Low & Shull (1986) (low density), Lepp & Shull (1983) (high density)
3. $H_2 + H_2 \rightarrow 2H + H_2$	Martin, Keogh & Mandy (1998) (low densit; Shapiro & Kang (1987) (high density)
4. $H_2 + \gamma \rightarrow 2H$	See § 2.2.1
5. $H + c.r. \rightarrow H^+ + e$	Liszt (2003)
6. $H + e \rightarrow H^+ + 2e$	Abel *et al.* (1997)
7. $H^+ + e \rightarrow H + \gamma$	Ferland *et al.* (1992)
8. $H^+ + e + grain \rightarrow H + grain$	Weingartner & Draine (2001)

Table 2. Processes included in our thermal model.

Process	References
Cooling:	
C II fine structure lines	Atomic data – Silva & Viegas (2002)
	Collisional rates (H_2) – Flower & Launay (1977)
	Collisional rates (H, $T < 2000$ K) – Hollenbach & McKee (1989)
	Collisional rates (H, $T > 2000$ K) – Keenan *et al.* (1986)
	Collisional rates (e^-) – Wilson & Bell (2002)
O I fine structure lines	Atomic data – Silva & Viegas (2002)
	Collisional rates (H, H_2) – Flower, priv. comm.
	Collisional rates (e^-) – Bell, Berrington & Thomas (1998)
	Collisional rates (H^+) – Pequignot (1990, 1996)
Si II fine structure lines	Atomic data – Silva & Viegas (2002)
	Collisional rates (H) – Roueff (1990)
	Collisional rates (e^-) – Dufton & Kingston (1991)
H_2 rovibrational lines	Le Bourlot, Pineau des Forêts & Flower (1999)
Gas-grain energy transfer[1]	Hollenbach & McKee (1989)
Recombination on grains	Wolfire *et al.* (2003)
Atomic resonance lines	Sutherland & Dopita (1993)
H collisional ionization	Abel *et al.* (1997)
H_2 collisional dissociation	See Table 1
Heating:	
Photoelectric effect	Bakes & Tielens (1994); Wolfire *et al.* (2003)
H_2 photodissociation	Black & Dalgarno (1977)
UV pumping of H_2	Burton, Hollenbach & Tielens (1990)
H_2 formation on dust grains	Hollenbach & McKee (1989)
Cosmic ray ionization	Goldsmith & Langer (1978)

here: e^-, H^+, H, H_2

in primordial gas we do:

e^-, H^+, H, H^-, H_2^+, H_2, C, C^+, O, O^+

(Glover & Mac Low 2007ab)

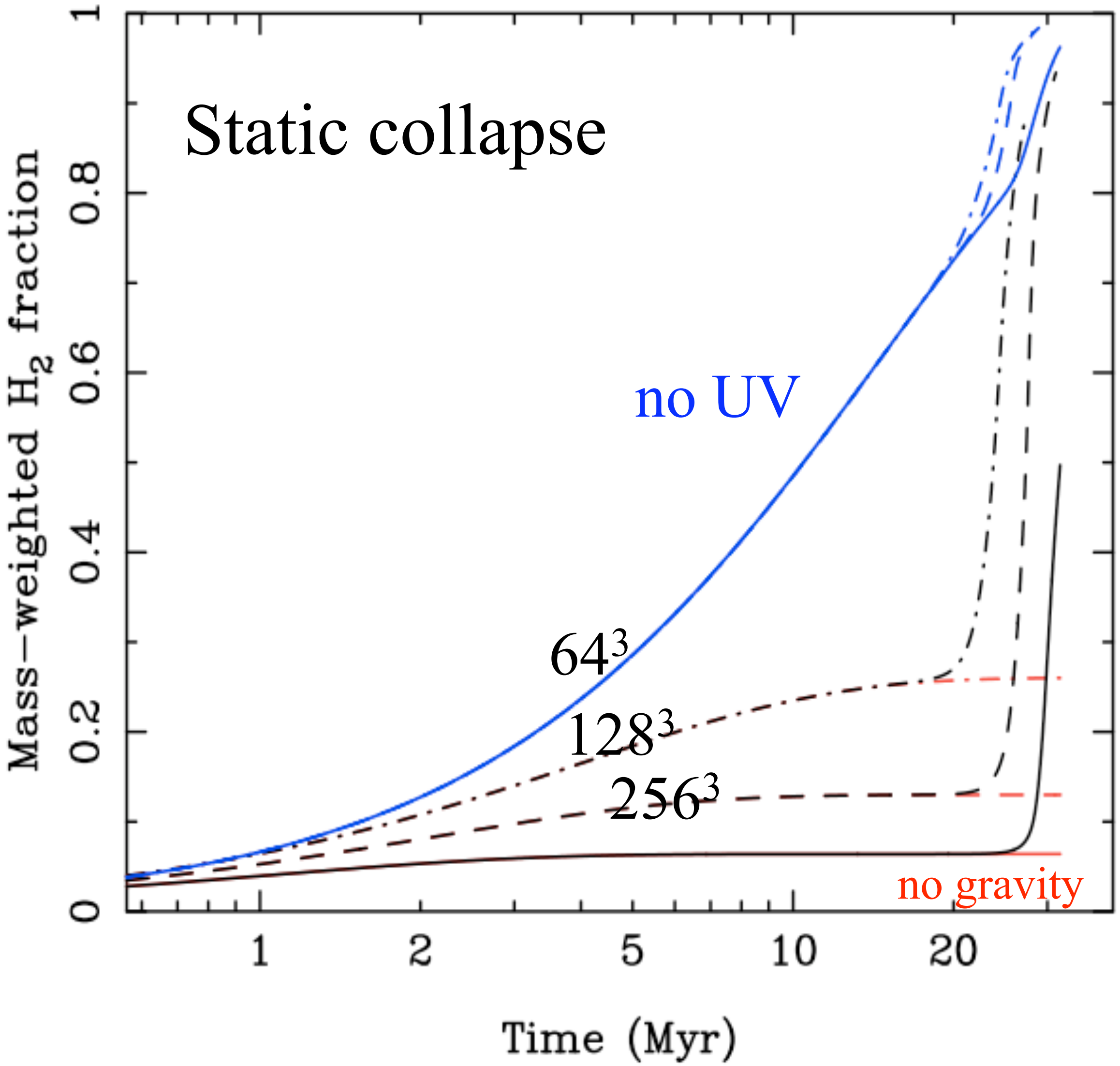

L = 40 pc, n_0 = 100 cm-3, B_0 = 5.85 mG, v_{rms} = 0.0

(Glover & Mac Low 2007a)

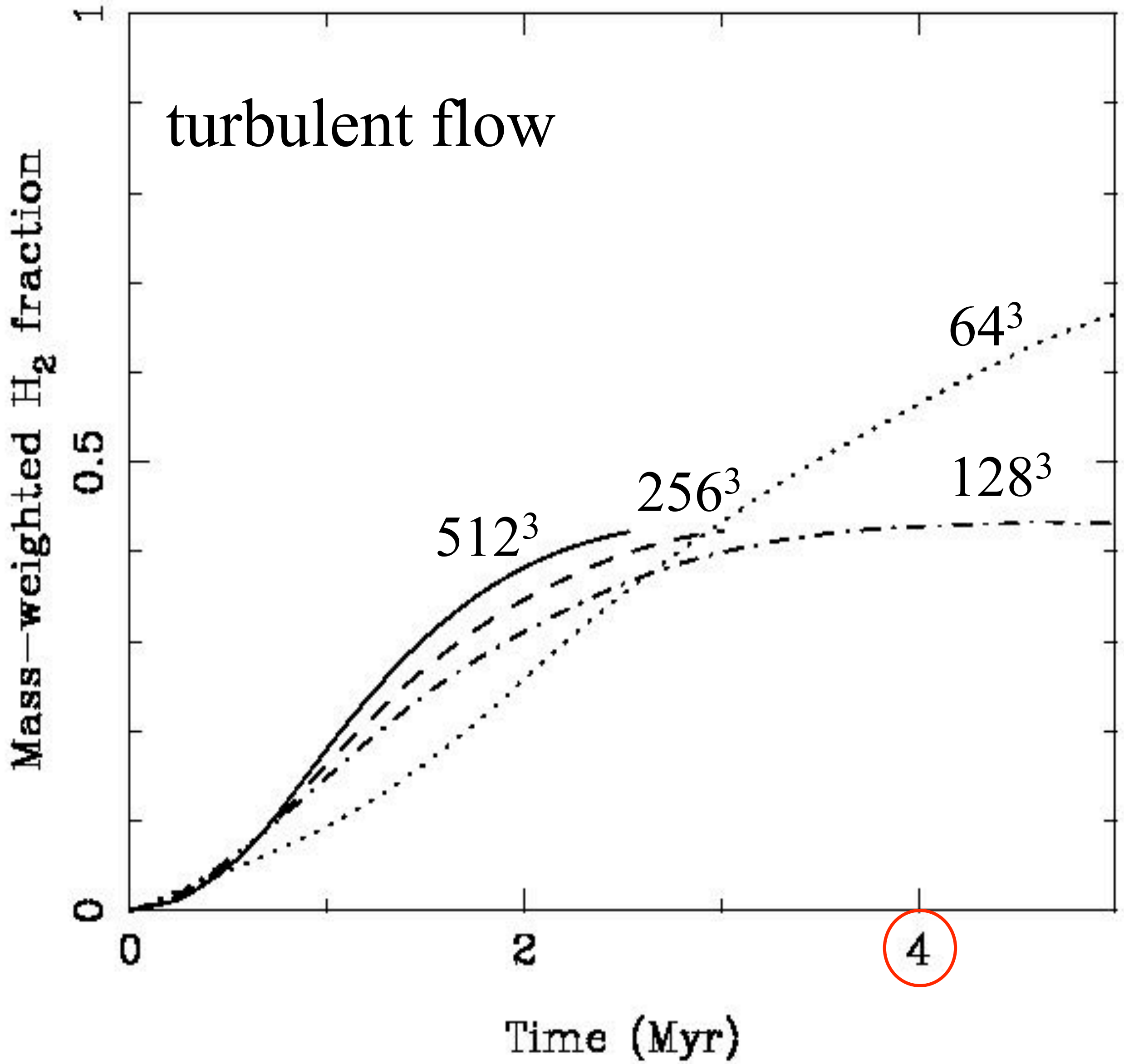

L = 20 pc, B_0 = 5.85 μG, v_{rms} = 10 km/s

(Glover & Mac Low 2007a)

molecular cloud scales

from atomic gas to molecular clouds

- hypothesis: *cold molecular clouds can form rapidly in high-density regions at stagnation points of convergent large-scale flows*
  - chemical phase transition: atomic → molecular
  - process is modulated by large-scale dynamics in galaxy
- questions
  - are molecular clouds truly "multi-phase" media?
  - turbulence? dynamical & morphological properties?
  - what is relation to initial & environmental conditions?
  - magnetic field structure?

Interstellar Matter: ISM

Abundances, scaled to 1.000.000 H atoms

element		atomic number	abundance
Wasserstoff	H	1	1.000.000
Deuterium	${}_1H^2$	1	16
Helium	He	2	68.000
Kohlenstoff	C	6	420
Stickstoff	N	7	90
Sauerstoff	O	8	700
Neon	Ne	10	100
Natrium	Na	11	2
Magnesium	Mg	12	40
Aluminium	Al	13	3
Silicium	Si	14	38
Schwefel	S	16	20
Calcium	Ca	20	2
Eisen	Fe	26	34
Nickel	Ni	28	2

Hydrogen is by far the most abundant element (more than 90% in number).

Phases of the ISM

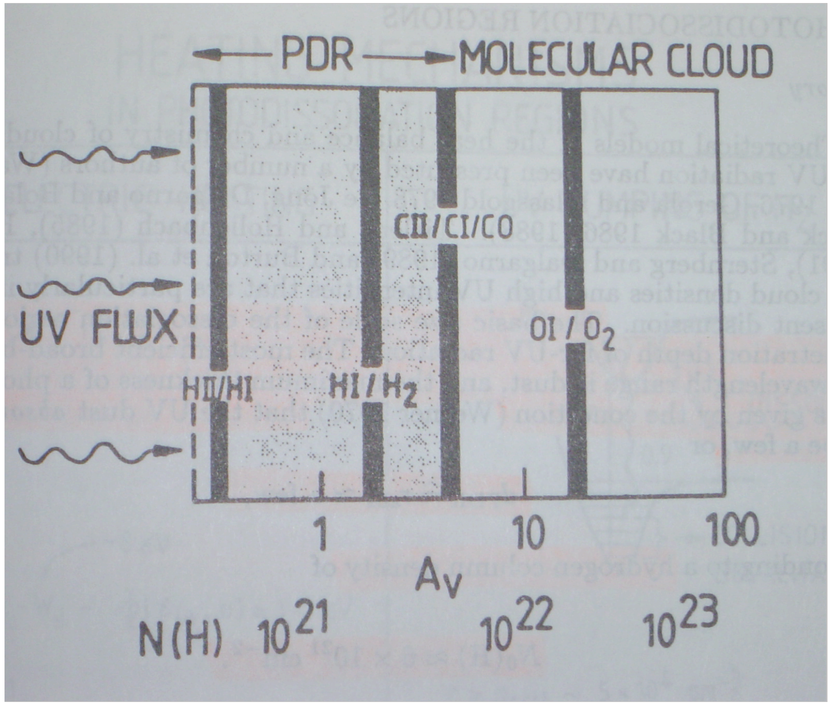

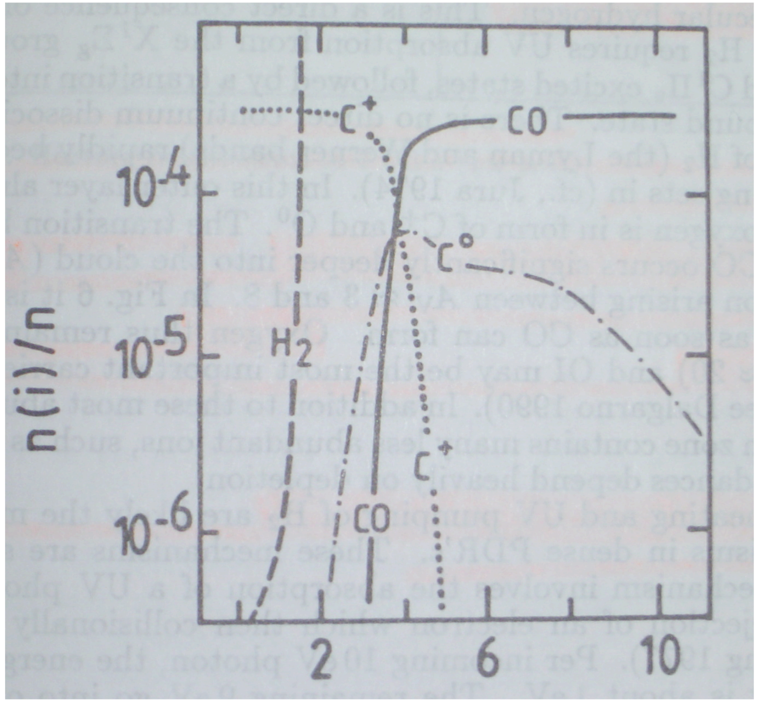

A_V

HII HI H_2

Dichte- / Säulendichte nimmt zu

A_V bezeichnet die Extinktion, dh. die Abschwächung der einfallenden Strahlung.

nearby clouds

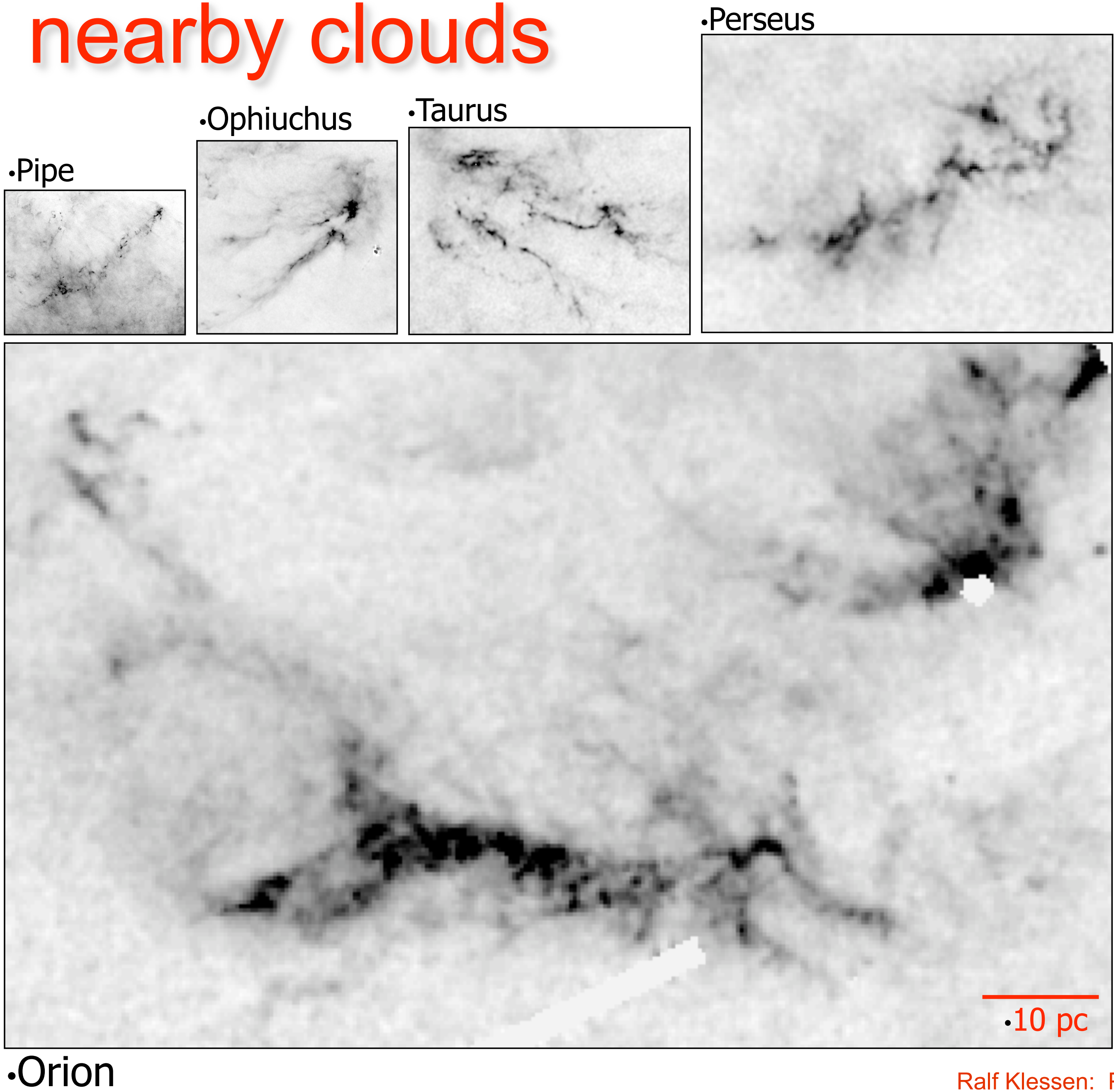

scales to same scale

(from A. Goodman)

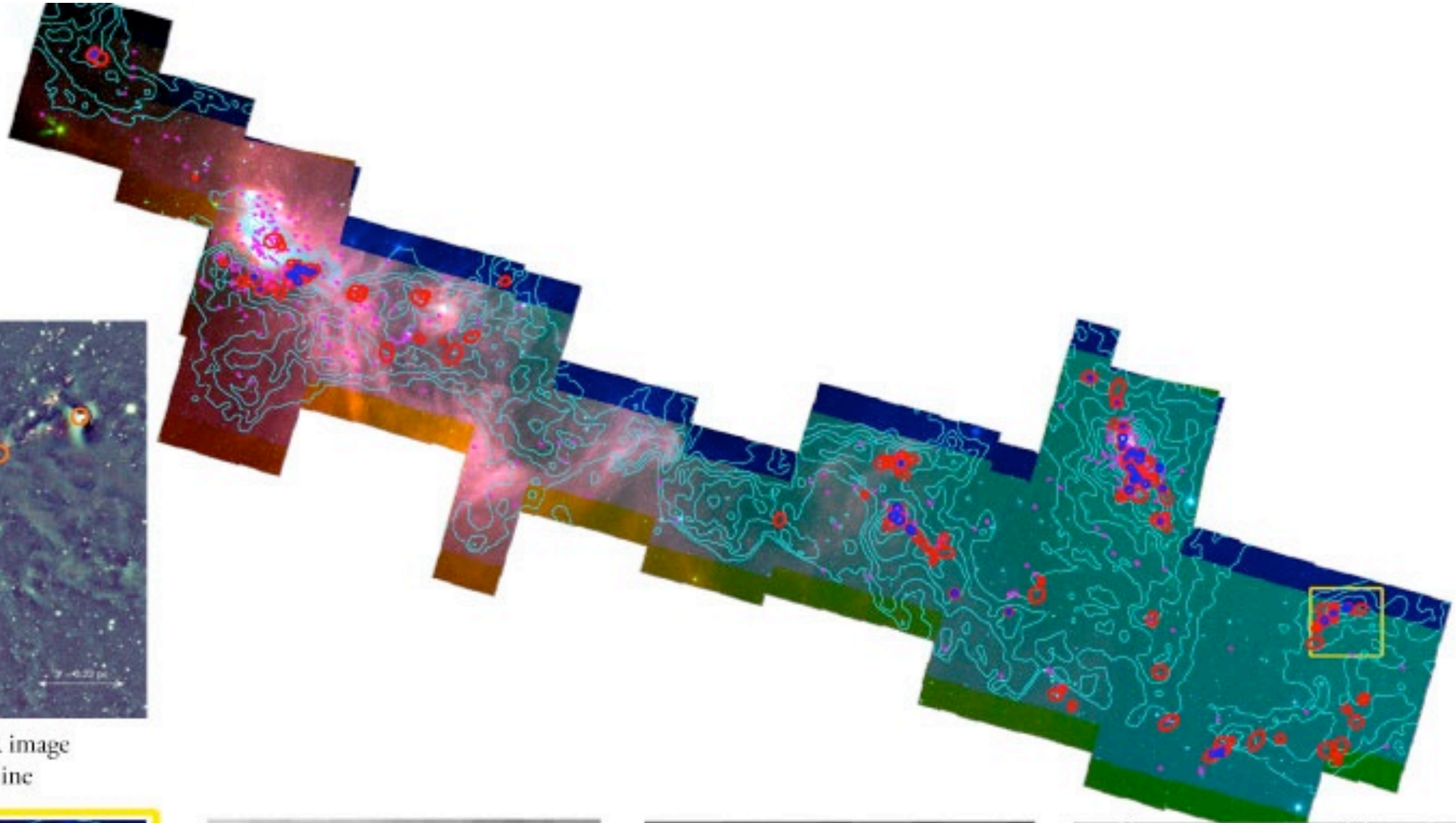

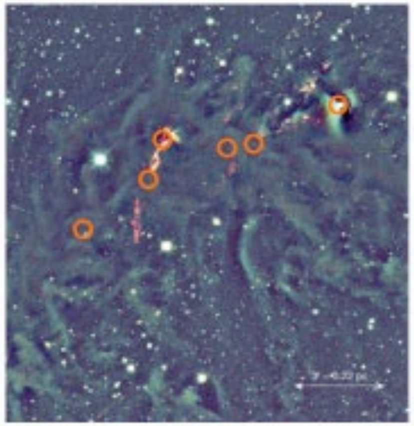

J,H,K Near-IR image
of Cloudshine

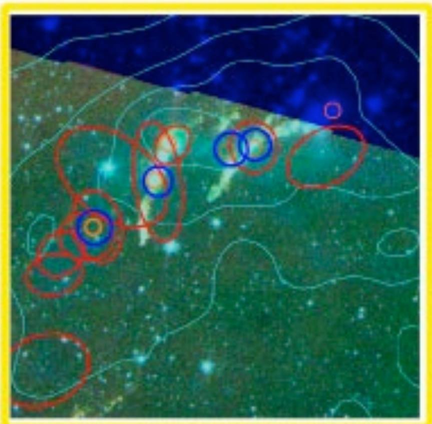

C 850 micron and 1.1 mm clumps on a c2d IRAC 3-color image

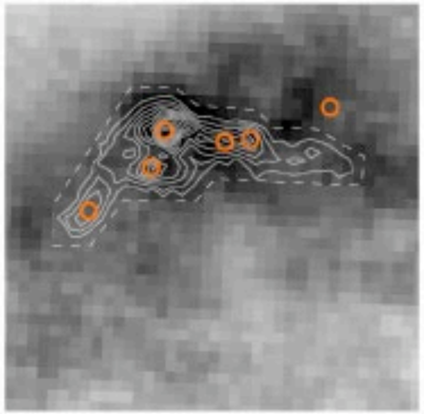

MPL N_2H^+ on ^{13}CO integrated intensity

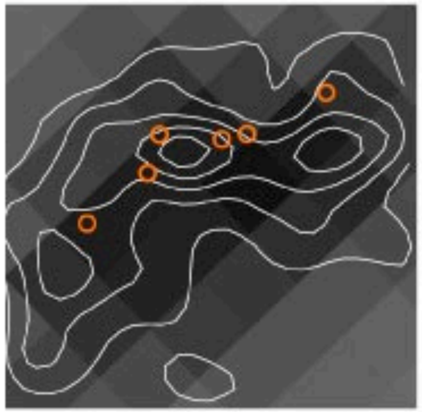

E Deep NIR Extinction on 2MASS Extinction

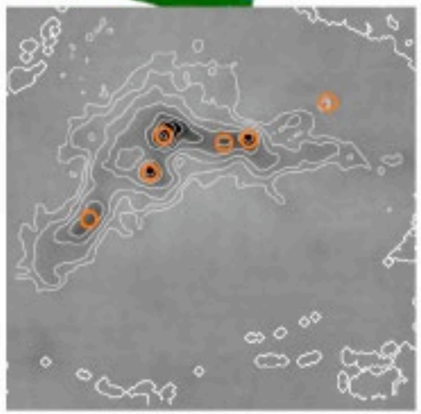

TE 1.2 mm (IRAM) on 850 micron (SCUBA) continuum

images from Alyssa Goodman

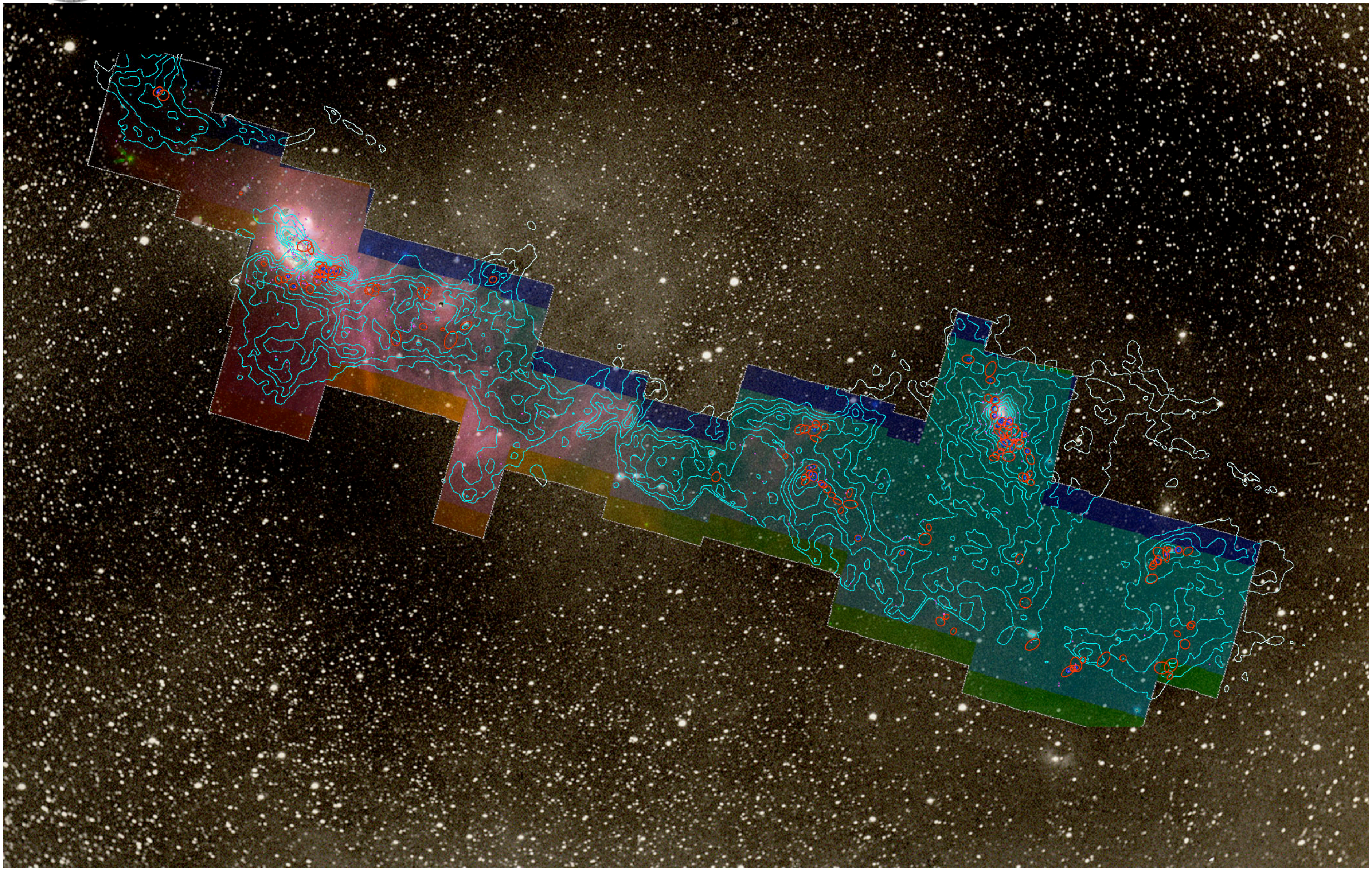

image from Alyssa Goodman: COMPLETE survey

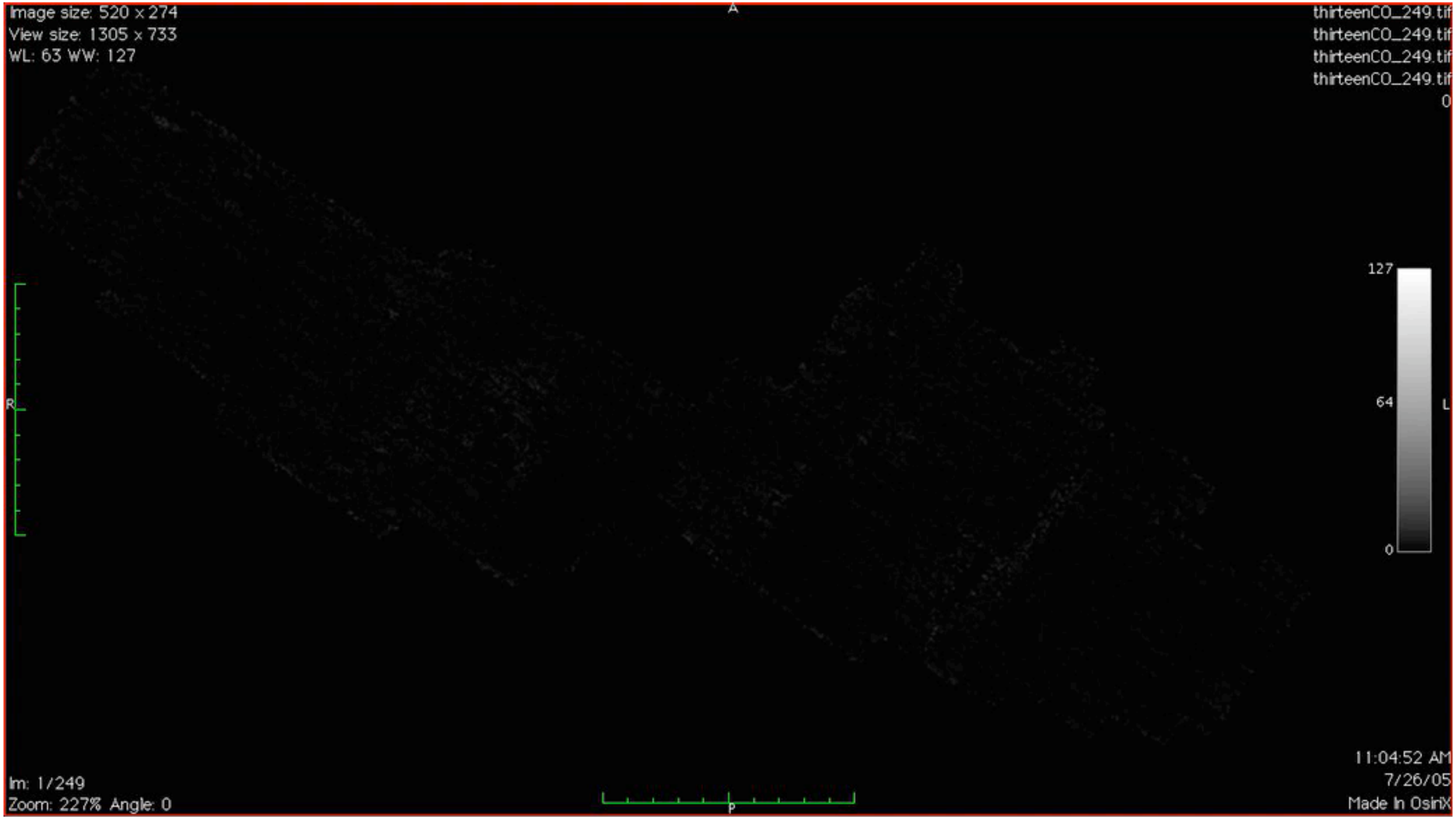

velocity distribution in Perseus

velocity cube from Alyssa Goodman: COMPLETE survey

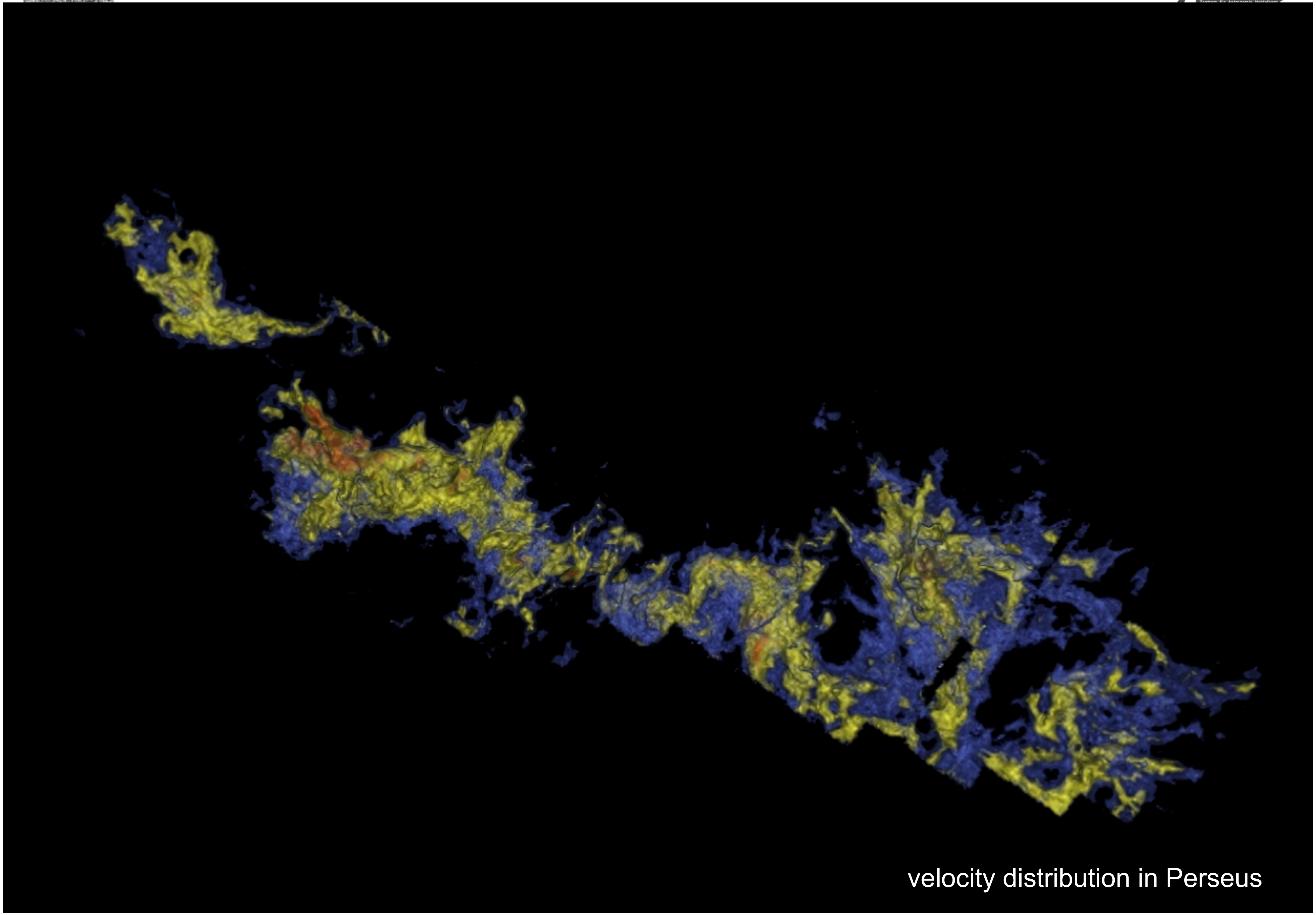

image from Alyssa Goodman: COMPLETE survey

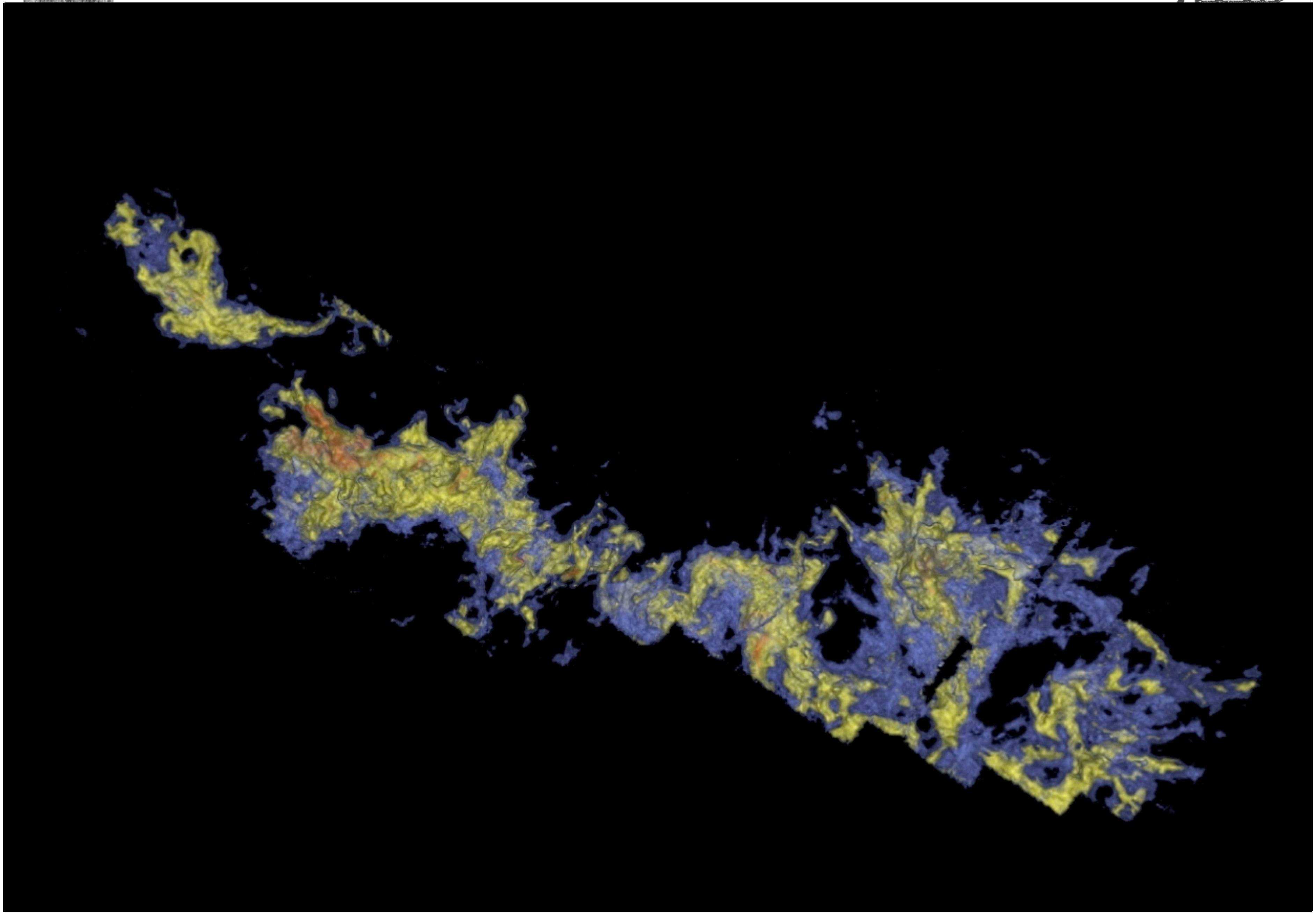

image from Alyssa Goodman: COMPLETE survey

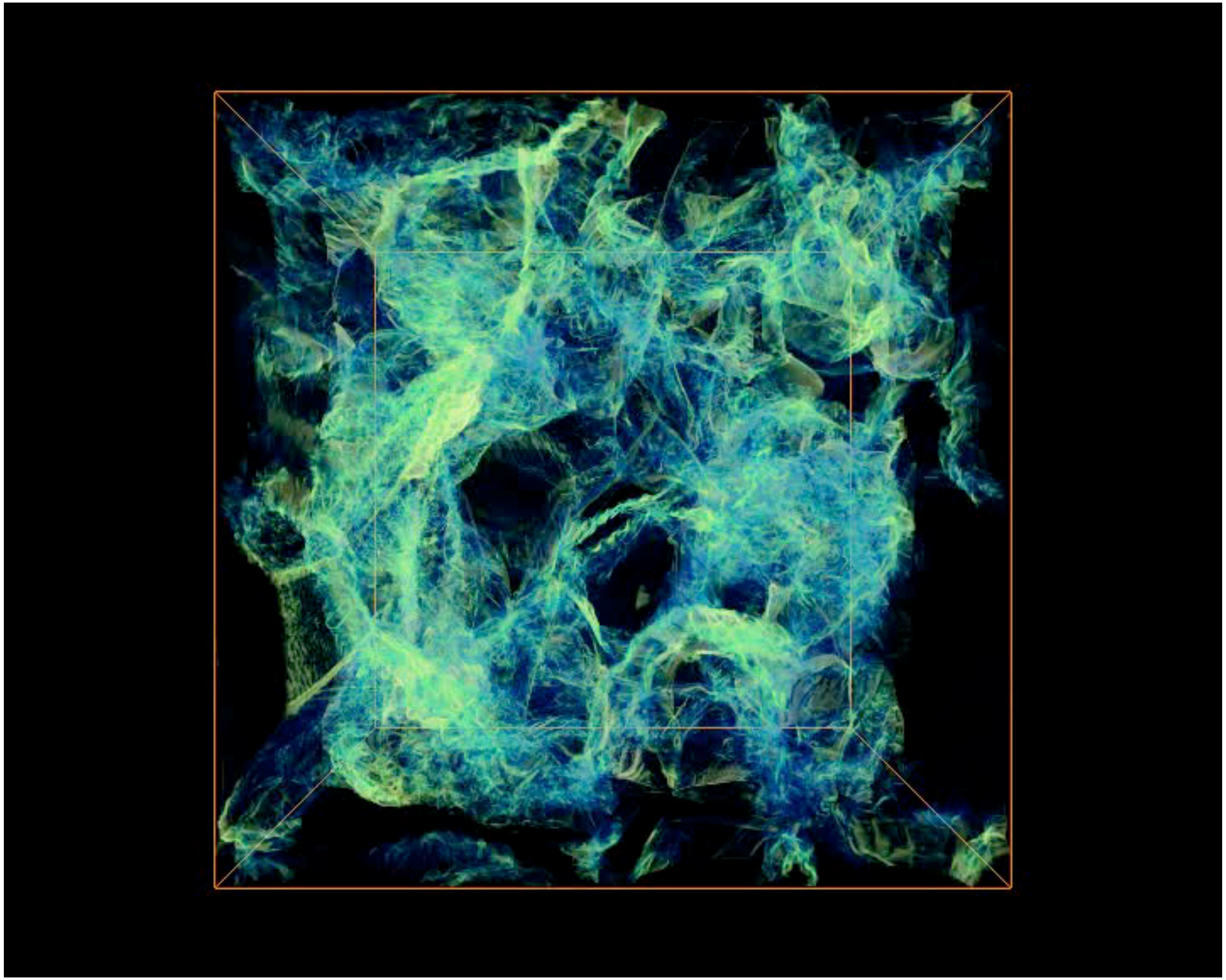

(movie from Christoph Federrath)

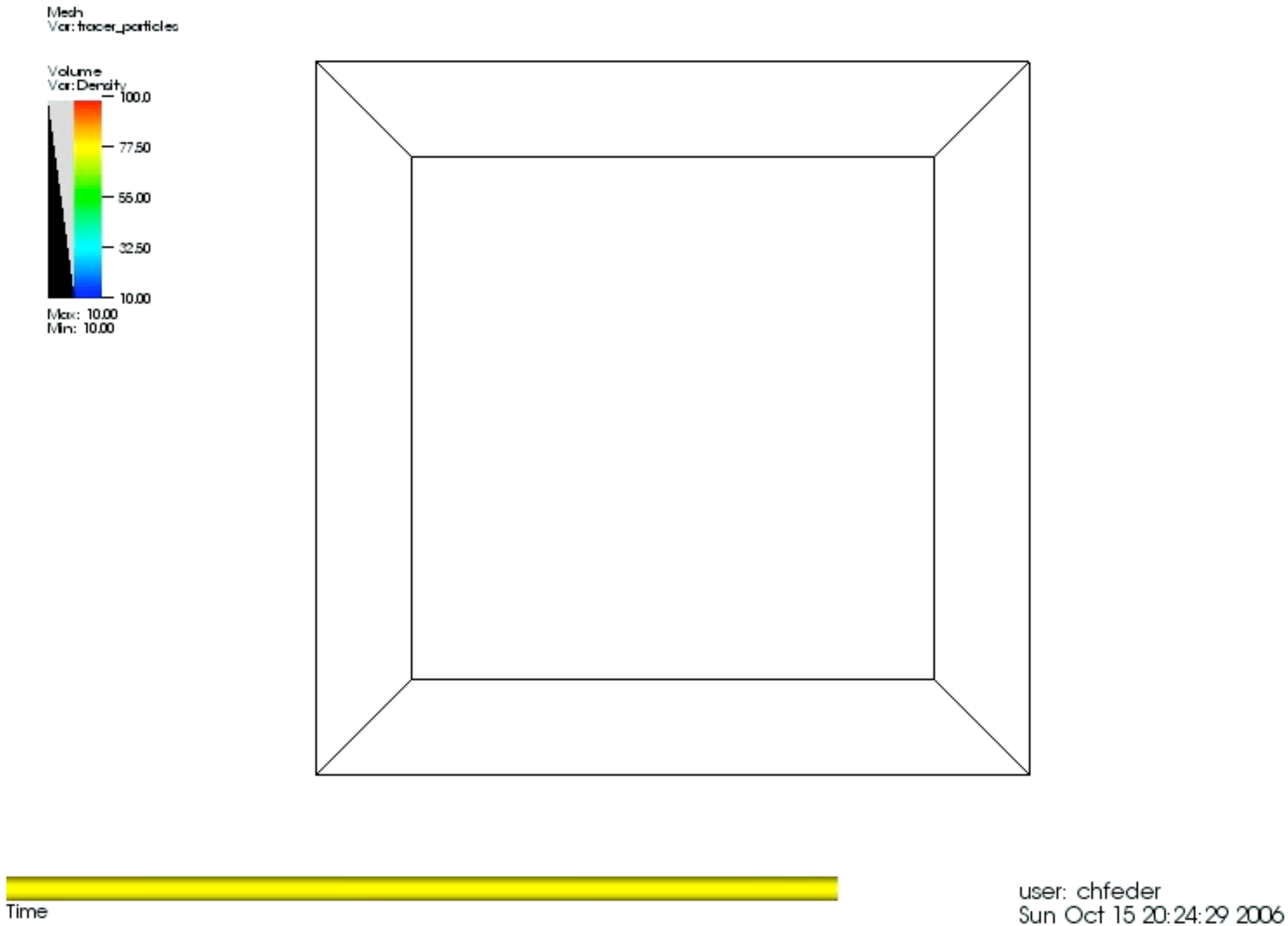
Mesh
Var: tracer_particles
Volume
Var: Density
100.0
77.50
55.00
32.50
10.00
Max: 10.00
Min: 10.00
Time
user: chfeder
Sun Oct 15 20:24:29 2006

ISM: transition HI to H_2

consistent models of ISM dynamics require to go beyond the simple models!

- magnetohydrodynamics
  (account for large-scale dynamics + turbulence)
- time-dependent chemistry
  (reduced network, focus on few dominant species, e.g. H_2)
- radiation (currently simple assumptions)

H2 forms rapidly in shocks / transient density fluctuations / H2 gets destroyed slowly in low density regions / result: turbulence greatly enhances H2-formation rate

(Glover & Mac Low 2007ab:)

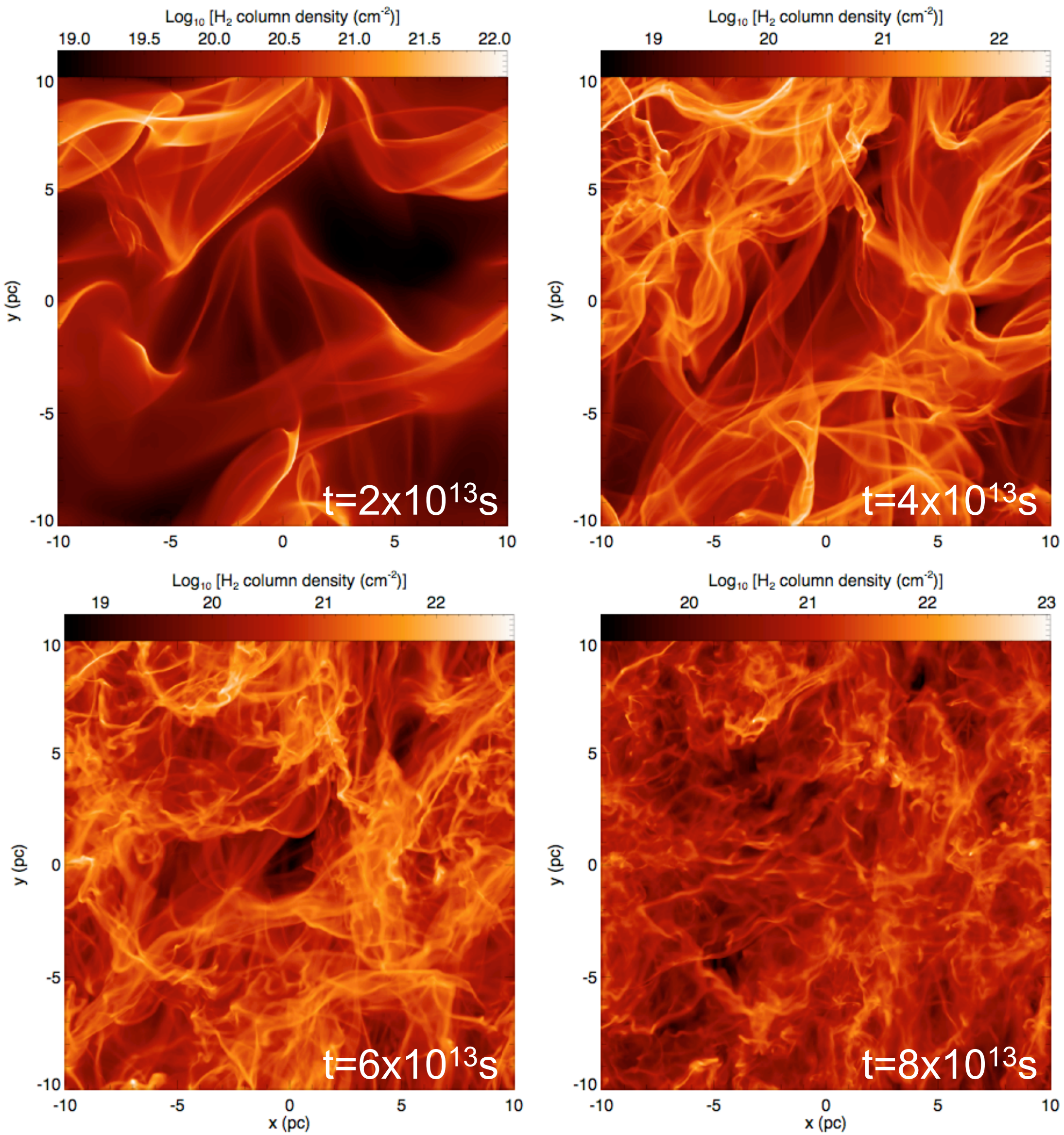

Reduced chemical network

Table 1. The set of chemical reactions that make up our model of non-equilibrium hydrogen chemistry.

Reaction	Reference
1. $H + H + grain \rightarrow H_2 + grain$	Hollenbach & McKee (1979)
2. $H_2 + H \rightarrow 3H$	Mac Low & Shull (1986) (low density), Lepp & Shull (1983) (high density)
3. $H_2 + H_2 \rightarrow 2H + H_2$	Martin, Keogh & Mandy (1998) (low densit Shapiro & Kang (1987) (high density)
4. $H_2 + \gamma \rightarrow 2H$	See § 2.2.1
5. $H + c.r. \rightarrow H^+ + e$	Liszt (2003)
6. $H + e \rightarrow H^+ + 2e$	Abel *et al.* (1997)
7. $H^+ + e \rightarrow H + \gamma$	Ferland *et al.* (1992)
8. $H^+ + e + grain \rightarrow H + grain$	Weingartner & Draine (2001)

here: e^-, H^+, H, H_2

in primordial gas we do:

e^-, H^+, H, H^-, H_2^+, H_2, C, C^+, O, O^+

Table 2. Processes included in our thermal model.

Process	References
Cooling:	
C II fine structure lines	Atomic data – Silva & Viegas (2002)
	Collisional rates (H_2) – Flower & Launay (1977)
	Collisional rates (H, $T < 2000$ K) – Hollenbach & McKee (1989)
	Collisional rates (H, $T > 2000$ K) – Keenan *et al.* (1986)
	Collisional rates (e^-) – Wilson & Bell (2002)
O I fine structure lines	Atomic data – Silva & Viegas (2002)
	Collisional rates (H, H_2) – Flower, priv. comm.
	Collisional rates (e^-) – Bell, Berrington & Thomas (1998)
	Collisional rates (H^+) – Pequignot (1990, 1996)
Si II fine structure lines	Atomic data – Silva & Viegas (2002)
	Collisional rates (H) – Roueff (1990)
	Collisional rates (e^-) – Dufton & Kingston (1991)
H_2 rovibrational lines	Le Bourlot, Pineau des Forêts & Flower (1999)
Gas-grain energy transfer[1]	Hollenbach & McKee (1989)
Recombination on grains	Wolfire *et al.* (2003)
Atomic resonance lines	Sutherland & Dopita (1993)
H collisional ionization	Abel *et al.* (1997)
H_2 collisional dissociation	See Table 1
Heating:	
Photoelectric effect	Bakes & Tielens (1994); Wolfire *et al.* (2003)
H_2 photodissociation	Black & Dalgarno (1977)
UV pumping of H_2	Burton, Hollenbach & Tielens (1990)
H_2 formation on dust grains	Hollenbach & McKee (1989)
Cosmic ray ionization	Goldsmith & Langer (1978)

(Glover & Mac Low 2007ab)

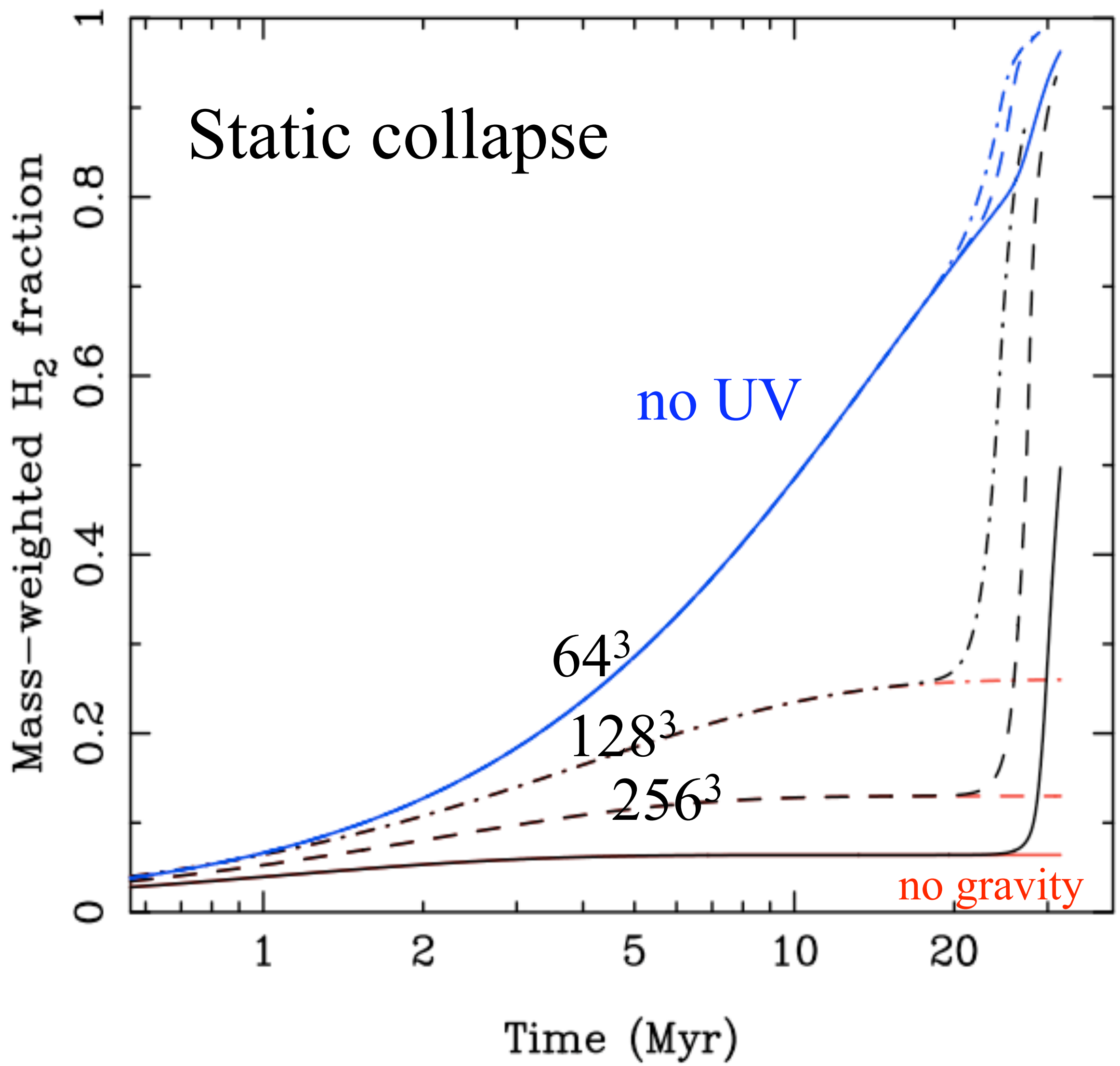

L = 40 pc, n_0 = 100 cm-3, B_0 = 5.85 mG, v_{rms} = 0.0

(Glover & Mac Low 2007a)

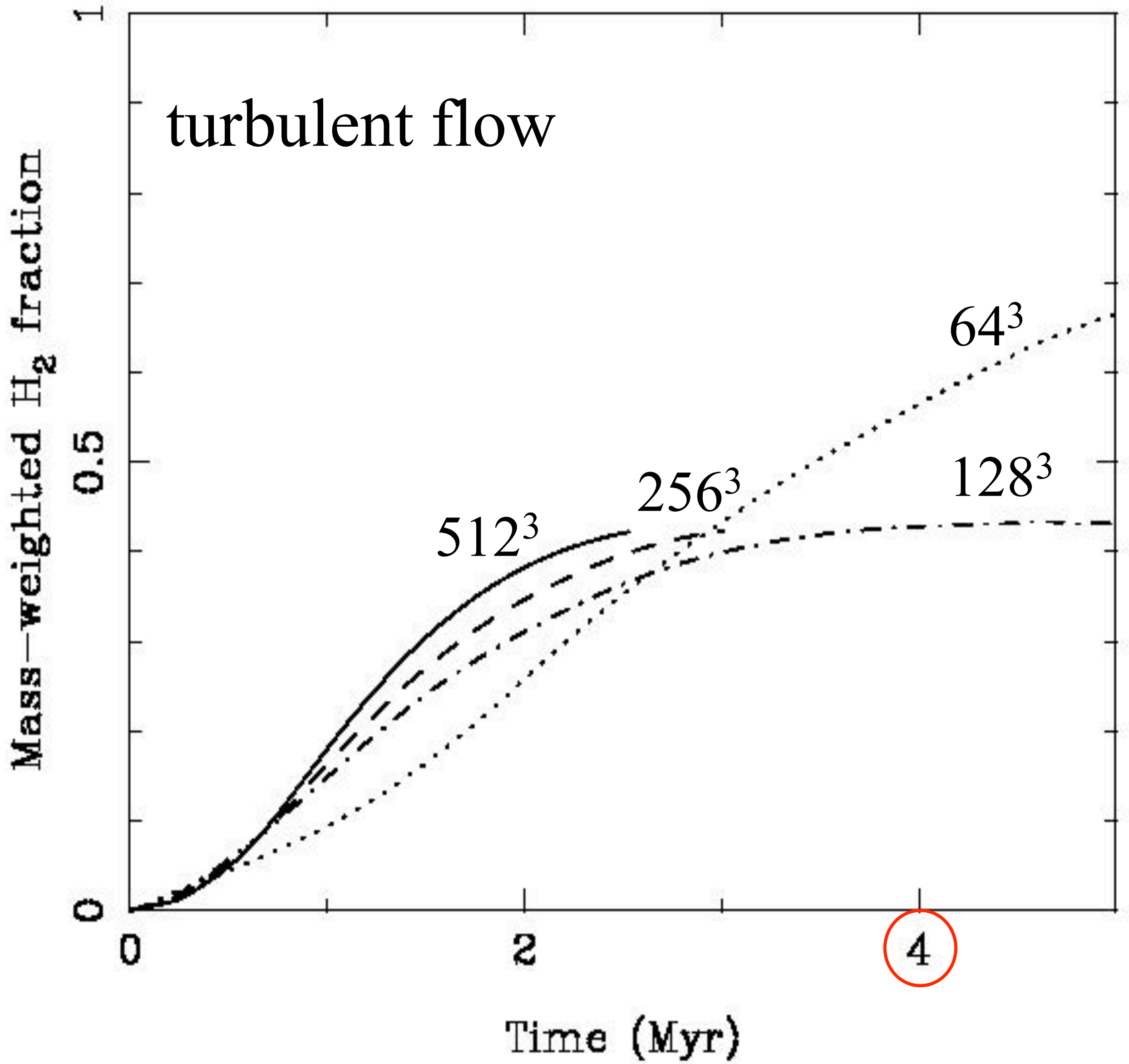

L = 20 pc, B_0 = 5.85 μG, v_{rms} = 10 km/s

(Glover & Mac Low 2007a)

effects of chemistry

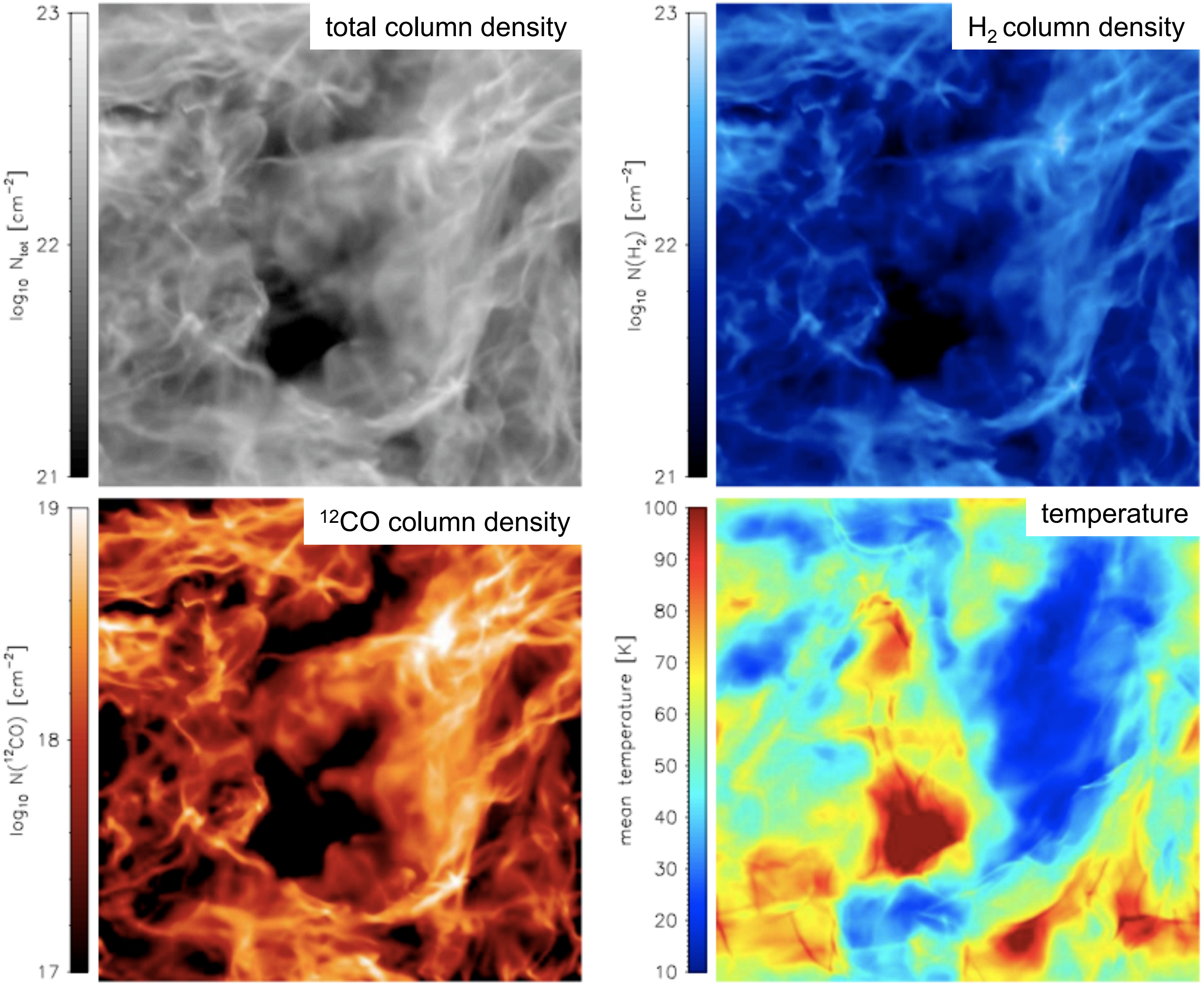

(Federrath, Glover et al.)

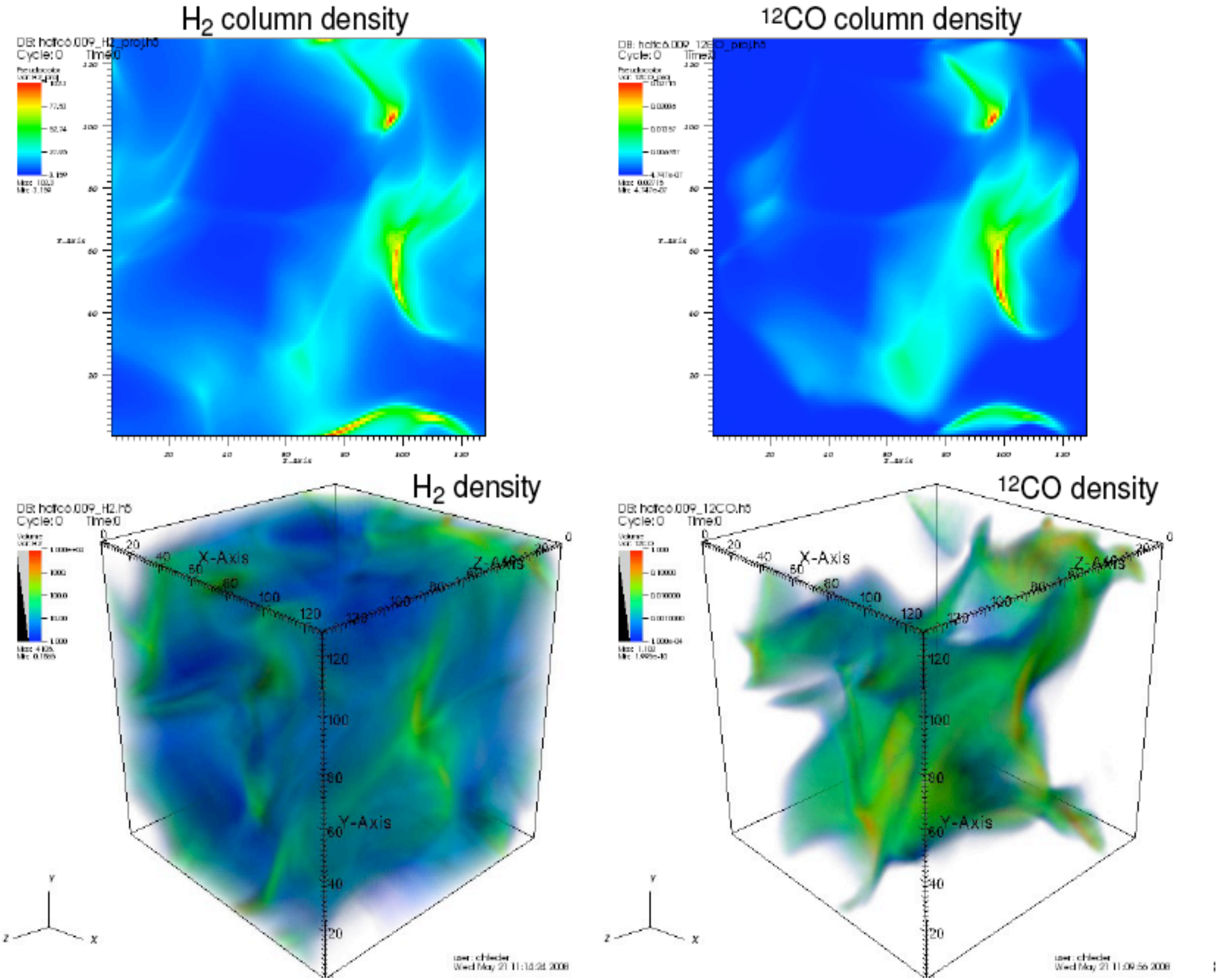

(Glover, Federrath, et al.)

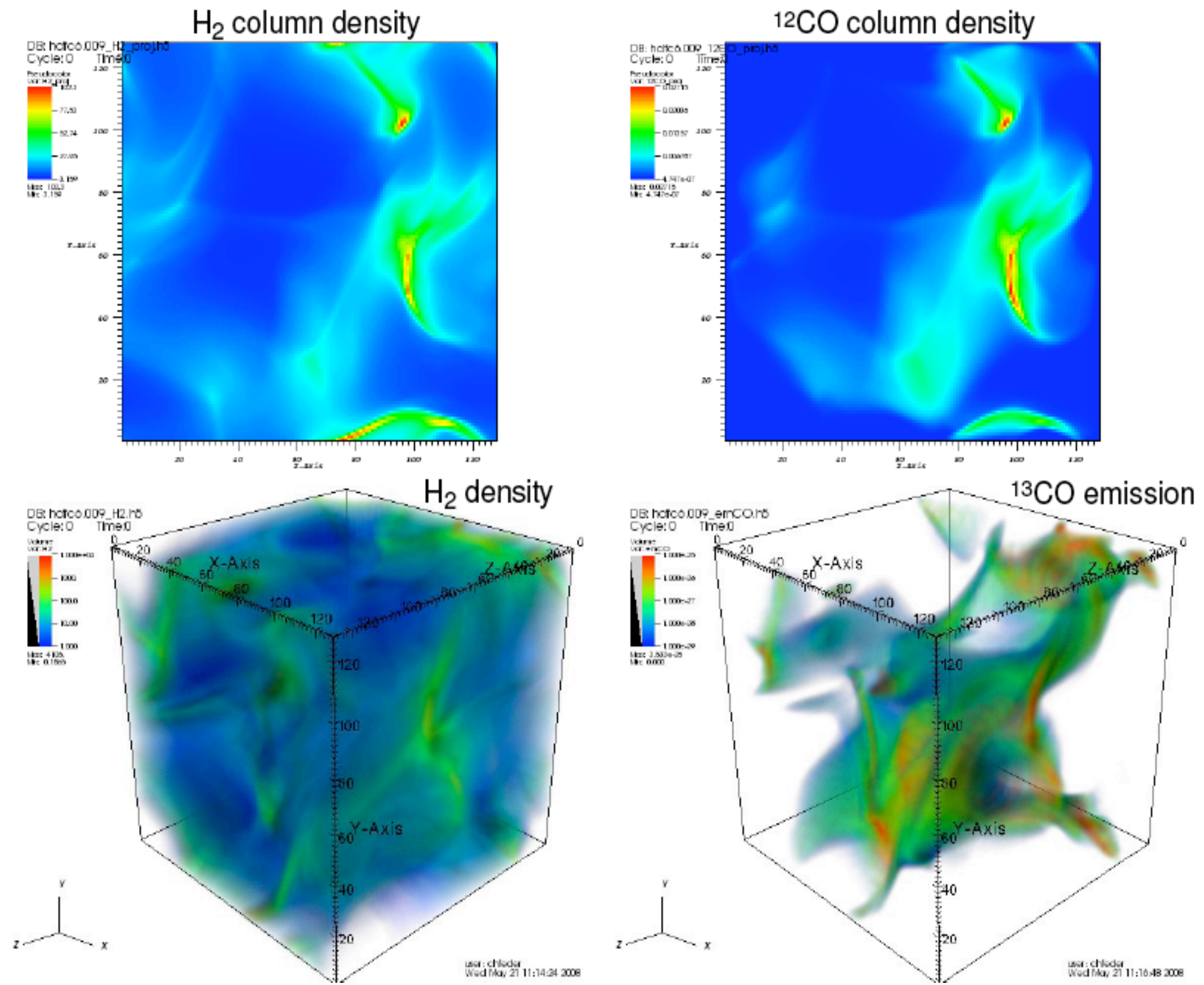

(Glover, Federrath, et al.)

turbulence

Properties of turbulence

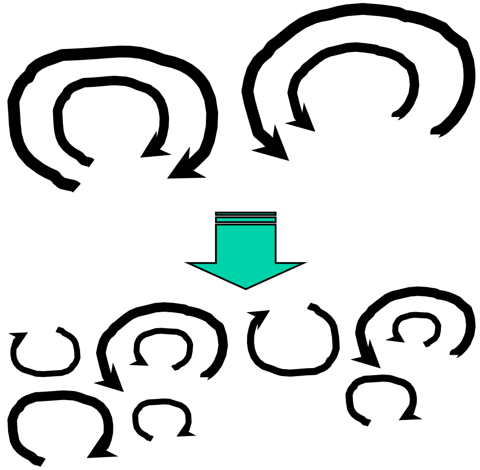

- laminar flows turn *turbulent* at *high* *Reynolds* numbers

$$\boxed{\mathrm{Re} = \frac{\text{advection}}{\text{dissipation}} = \frac{VL}{\nu}}$$

V= typical velocity on scale L, ν = viscosity, Re > 1000

- *vortex streching* --> turbulence is *intrinsically* *anisotropic* (only on large scales you *may* get homogeneity & isotropy in a statistical sense; see Landau & Lifschitz, Chandrasekhar, Taylor, etc.)

  (ISM turbulence: shocks & B-field cause additional inhomogeneity)

what drives turbulence?

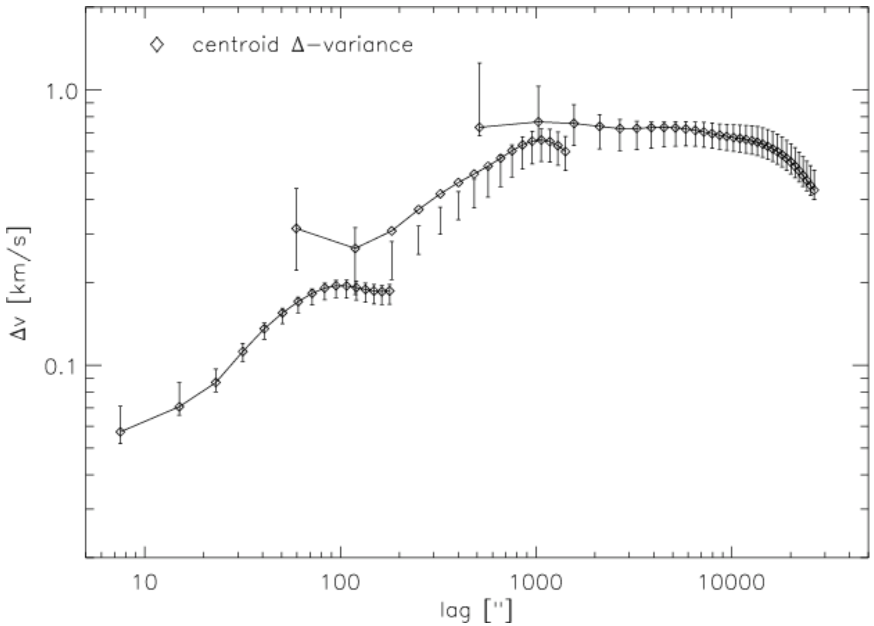

Polaris flare (from Ossenkopf & Mac Low 2002)

- turbulence characteristics
  - molecular cloud turbulence seems to be dominated by large-scale models
  - consistent with external driving
  - convergent flows?
    → the same process that creates the cloud supplies internal turbulence ...
  - alternative mechanisms:
    - gravity (spiral shocks), supernovae, HII regions?
    - internal sources: jets, outflows?

what drives turbulence?

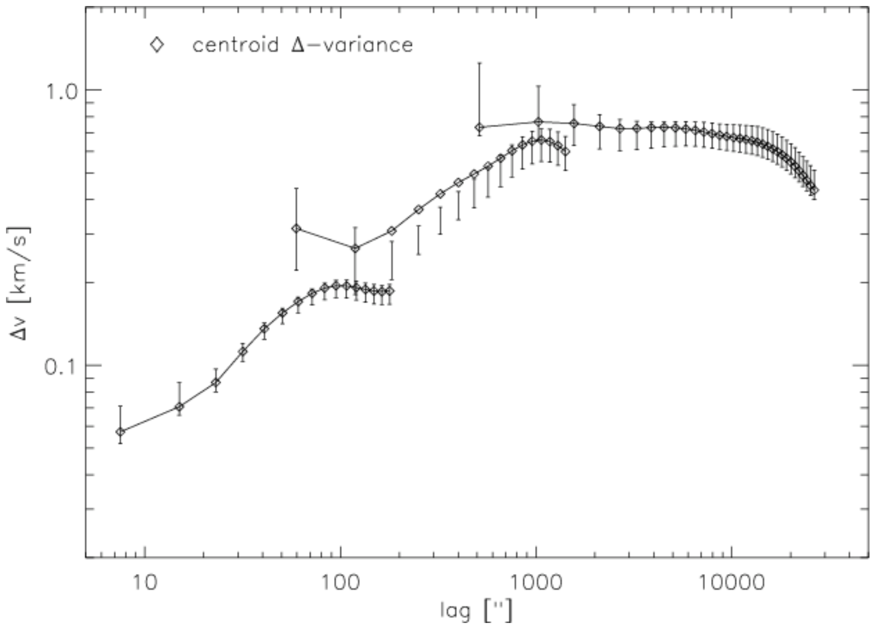

Polaris flare (from Ossenkopf & Mac Low 2002)

- turbulence characteristics
  - molecular cloud turbulence seems to be dominated by large-scale models
  - consistent with external driving
  - *convergent flows?*
    → the same process that creates the cloud supplies internal turbulence ..
    → caused by
    - *gravity (spiral shocks),* supernovae, HII regions?
  - alternative mechanisms:
    - internal sources: jets, outflows?

what drives turbulence?

- some words on internal sources
  - molecular cloud turbulence seems to be dominated by large-scale models
  - jets / outflow can only work after onset of star formation
    → what about turbulence in non-star forming parts of clouds, or during initial phases?
- there is debate on effectiveness of internal sources for driving supersonic turbulence
  (Li & Nakamura vs. Banerjee, Klessen, Fendt)

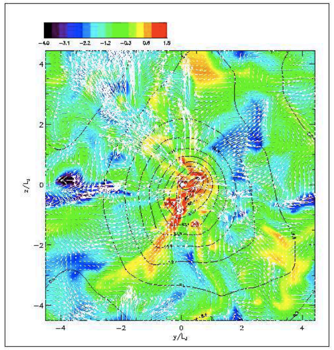

(Nakamura & Li 2007)

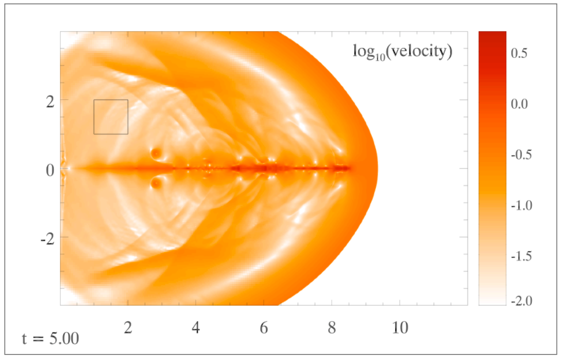

(Banerjee, Klessen, Fendt 2008)

local feedback

- individual jets cannot drive supersonic turbulence in a space-filling way → need additional physics

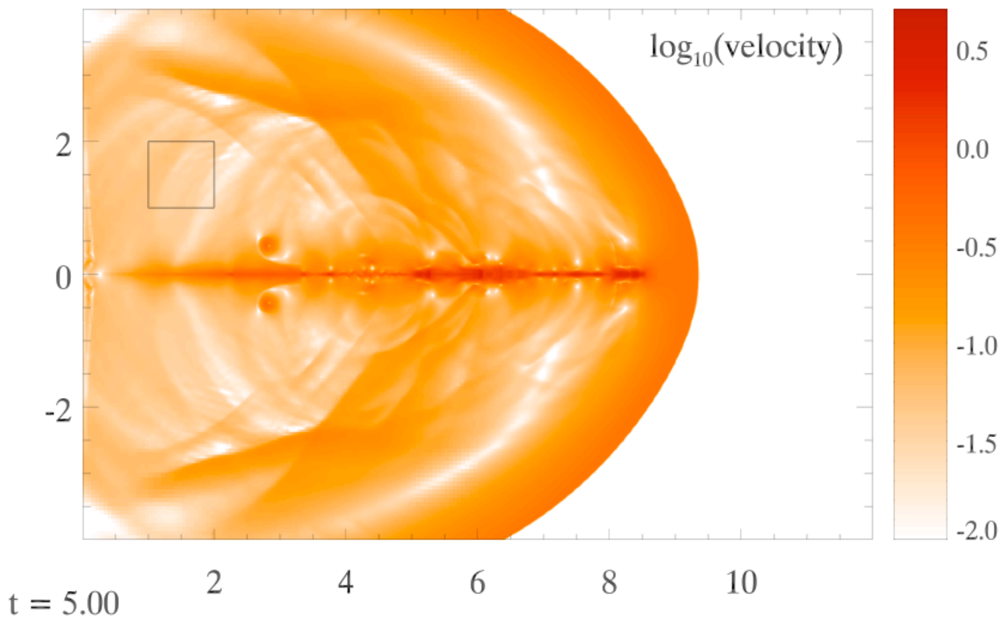

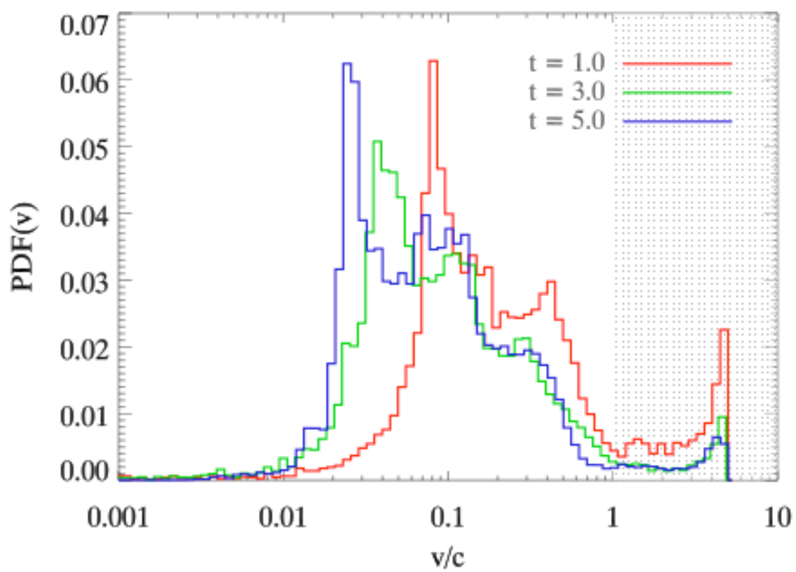

Banerjee, Klessen, & Fendt (2008)

cluster forming cloud with jets

- jets from cluster with self-gravity with AMR code FLASH

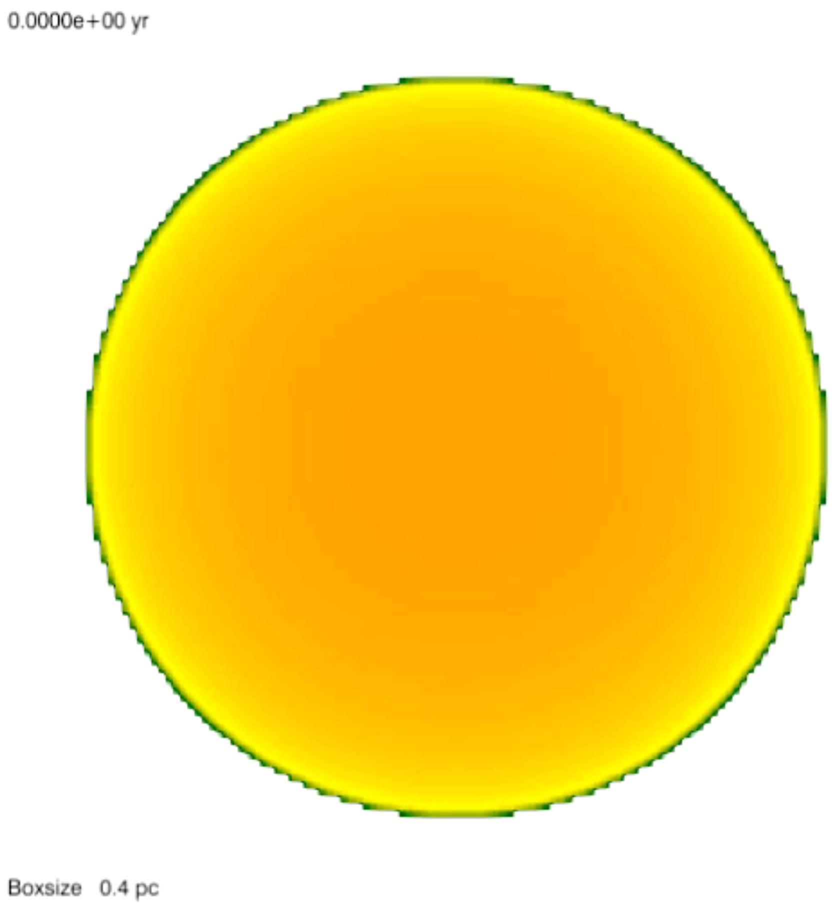

Banerjee et al. (very preliminary study)

Turbulent cascade

Kolmogorov (1941) theory
incompressible turbulence

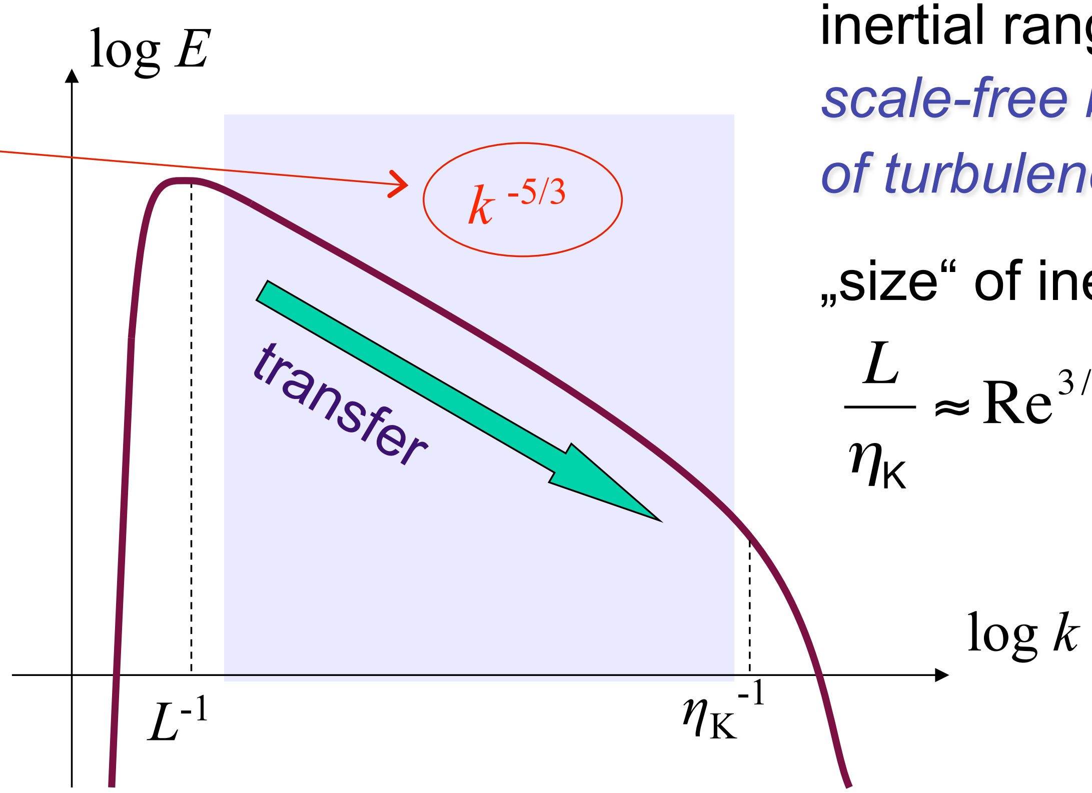

energy
input
scale

energy
dissipation
scale

inertial range:
scale-free behavior of turbulence

„size“ of inertial range:

$$\frac{L}{\eta_K} \approx \mathrm{Re}^{3/4}$$

Turbulent cascade

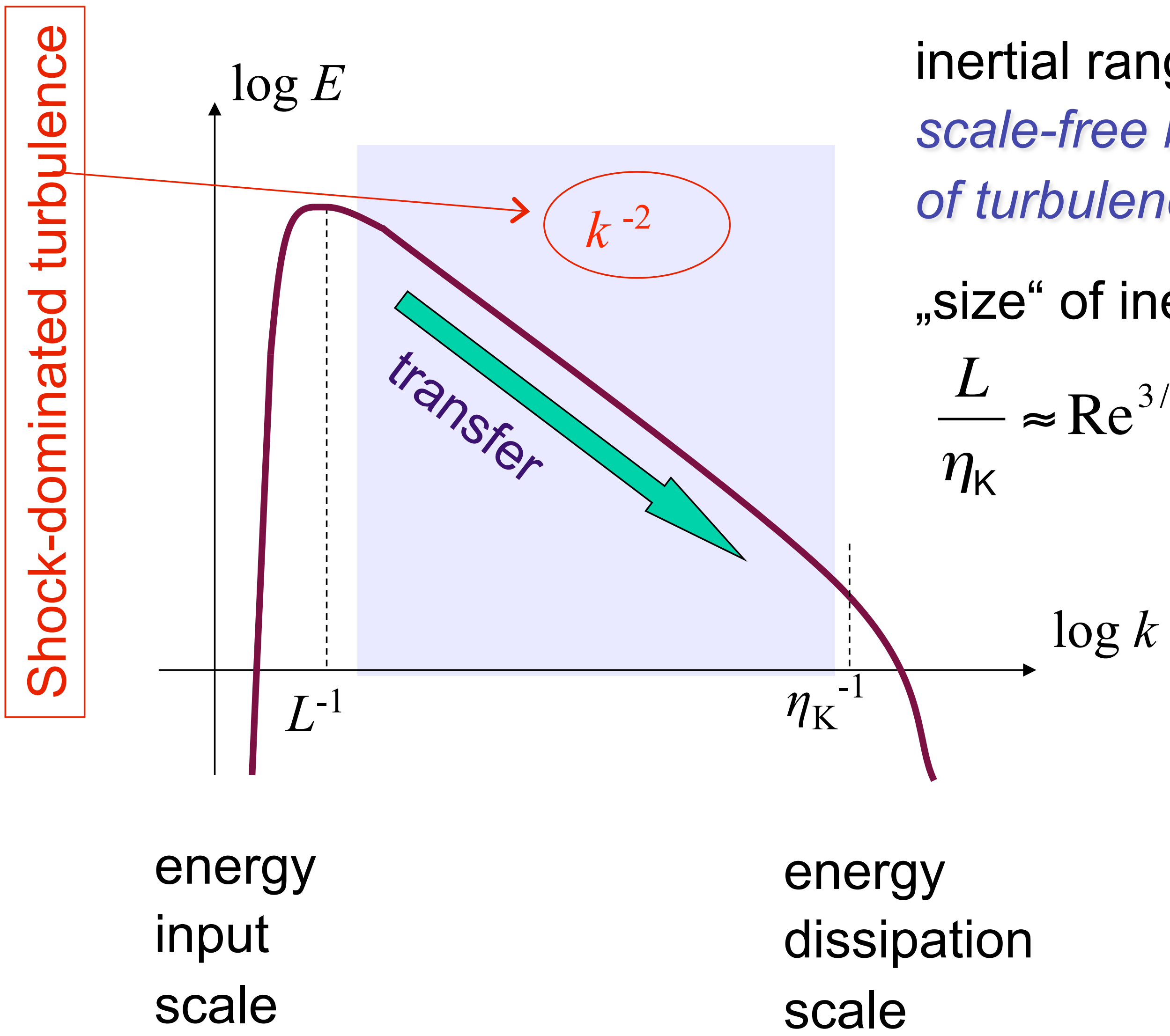

inertial range:

scale-free behavior of turbulence

„size“ of inertial range:

$$\frac{L}{\eta_K} \approx \mathrm{Re}^{3/4}$$

Turbulent cascade in ISM

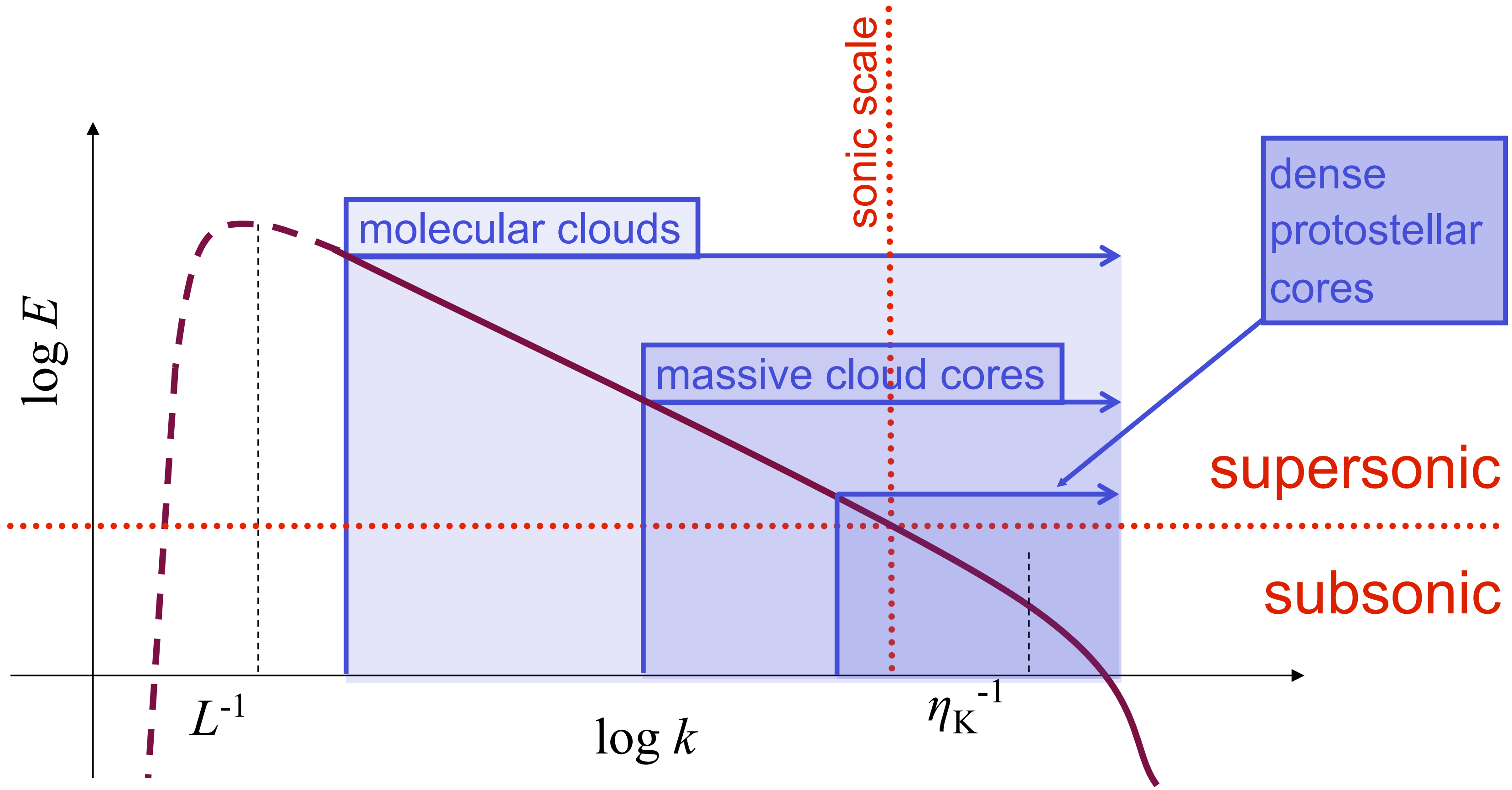

energy source & scale *NOT known* (supernovae, winds, spiral density waves?)

σ_{rms} << 1 km/s
$\mathcal{M}_{rms} \leq 1$
L ≈ 0.1 pc

dissipation scale not known (ambipolar diffusion, molecular diffusion?)

gravoturbulent fragmentation

- *turbulence* sets power-law distribution of clumps, *gravity* then selects for collapse

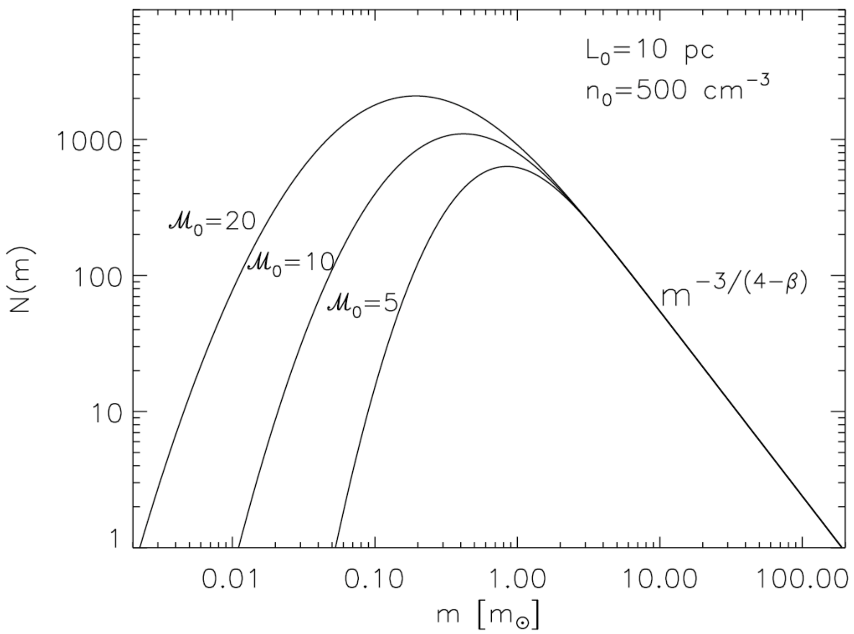

•Padoan & Nordlund (2002)

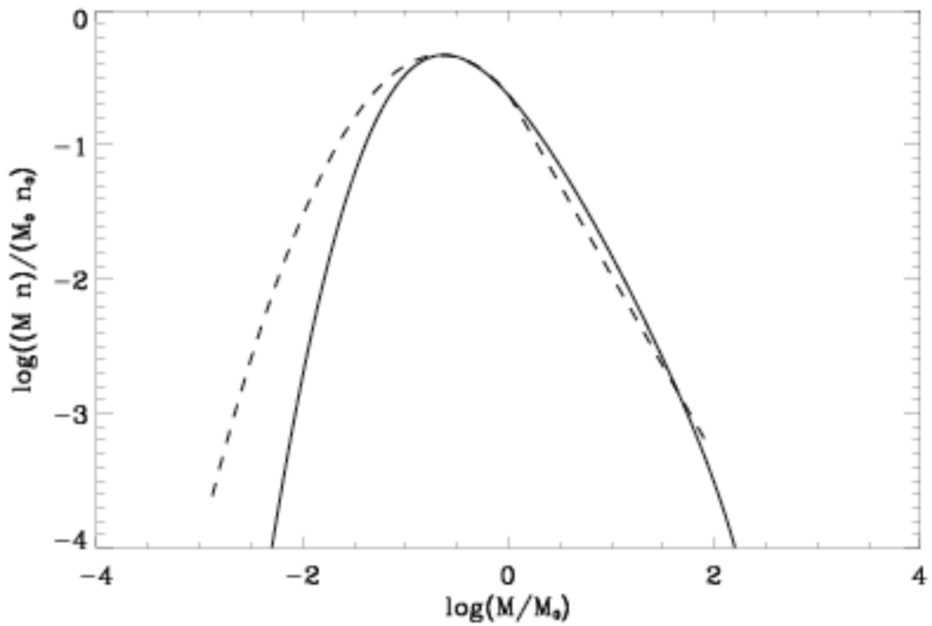

Hennebelle & Chabrier (2008)

Large-eddy simulations

- We use ***LES*** to model the large-scale dynamics
- Principal problem: only large scale flow properties
  - Reynolds number: Re = LV/ν ***(Re$_{nature}$ >> Re$_{model}$)***
  - dynamic range much smaller than true physical one
  - need *subgrid model* (in our case simple: only dissipation)
  - but what to do for more complex when processes on subgrid scale determine large-scale dynamics (chemical reactions, nuclear burning, etc)
  - Turbulence is "space filling" --> difficulty for AMR (don't know what criterion to use for refinement)
- How *large* a Reynolds number do we need to catch basic dynamics right?

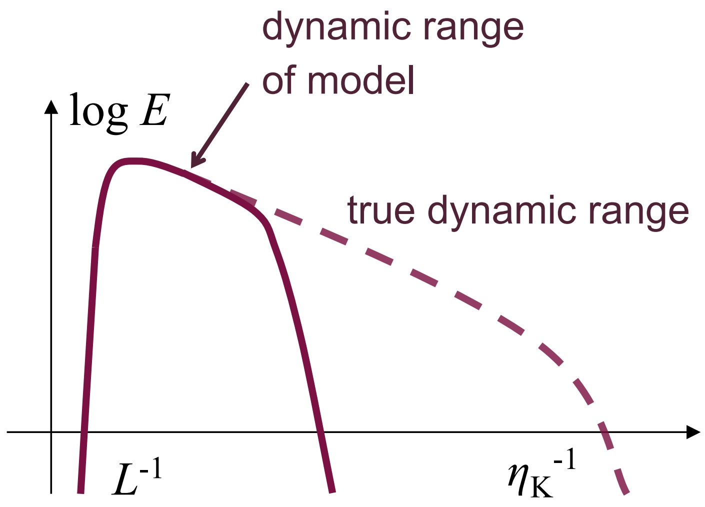

compressive vs. rotational driving

- statistical characteristics of turbulence depend strongly on „type“ of driving
- example: dilatational vs. solenoidal driving
- question: what drives ISM turbulence on different scales?

dilatational vs. solenoidal

density as function of time / cut through 1024^3 cube simulation (FLASH)

compressive
larger structures, higher ρ-contrast

rotational
smaller structures, small ρ-pdf

Federrath, Klessen, Schmidt (2008a,b)

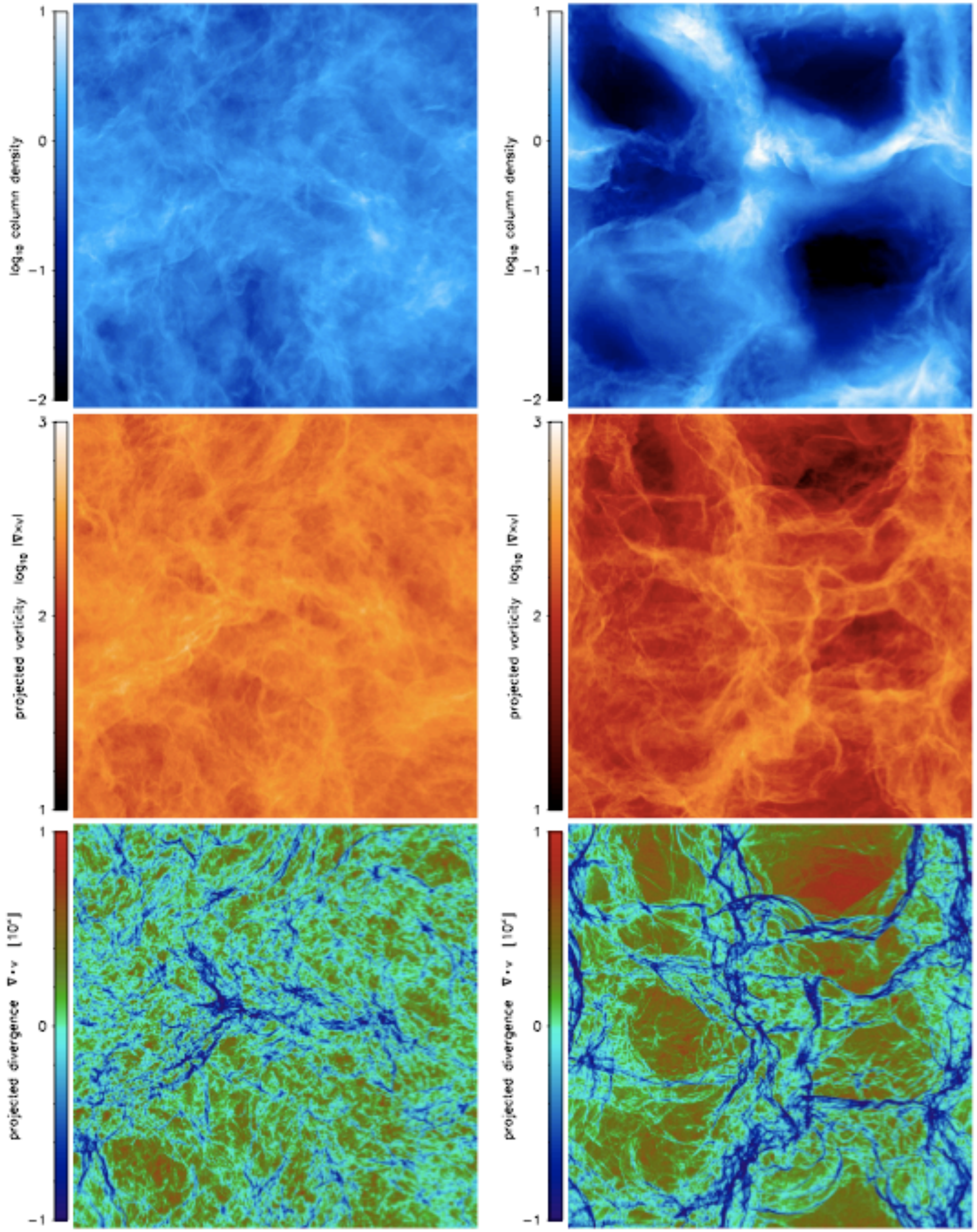

column density

projected vorticity

projected divergence

Fig. 1. Maps showing density, vorticity and divergence in projection along the z-axis at time $t = 2\,T$ as an example for the regime of statistically fully developed compressible turbulence for solenoidal forcing (*left*) and compressive forcing (*right*). *Top panels:* Column density fields in units of the mean column density. Both maps show three orders of magnitude in column density with the same scaling and magnitudes for direct comparison. *Middle panels:* Projections of the modulus of the vorticity $|\nabla \times v|$. Regions of intense vorticity appear to be elongated filamentary structures often coinciding with positions of intersecting shocks. *Bottom panels:* Projections of the divergence of the velocity field $\nabla \cdot v$ showing the positions of shocks. Negative divergence corresponds to compression, while positive divergence corresponds to rarefaction.

dilatational vs. solenoidal

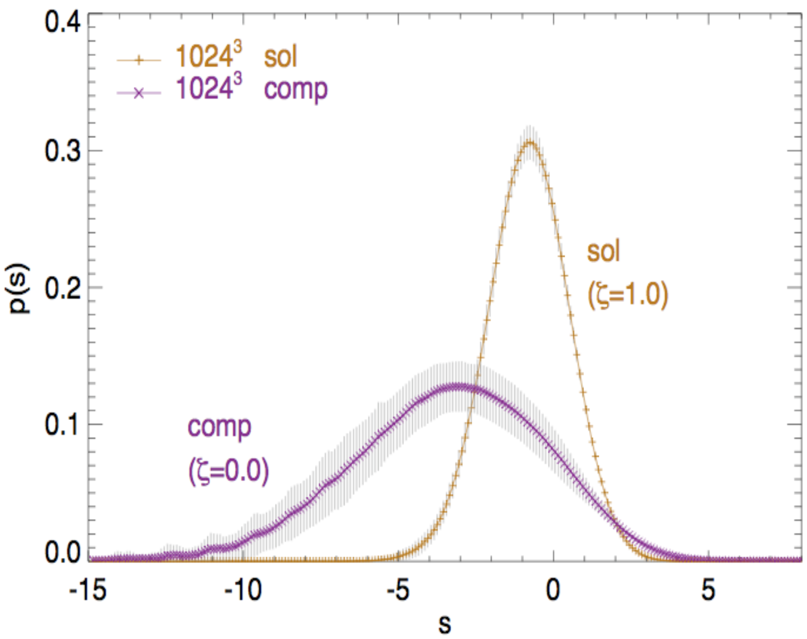

FIG. 2.— Volume-weighted density PDFs $p_s(s)$ in linear scaling where $s = \ln(\rho/\rho_0)$. The PDF obtained by compressive forcing (comp, $\zeta = 0.0$) is much broader compared to the solenoidal one (sol, $\zeta = 1.0$) at the same rms Mach number. The peak is shifted due to mass conservation (Vázquez-Semadeni 1994). Gray error bars indicate 1-sigma temporal fluctuations of the PDF. A sample of $\sim 10^{11}$ datapoints contribute to each PDF.

Federrath, Klessen, Schmidt (2008a)

- density pdf depends on "dimensionality" of driving
  - relation between width of pdf and Mach number

$$\boxed{\sigma_\rho/\rho_0 = b\mathcal{M}}$$

  - with b depending on ζ via

$$b = 1 + \left[\frac{1}{D} - 1\right]\zeta = \begin{cases} 1 - \frac{2}{3}\zeta & \text{, for } D = 3 \\ 1 - \frac{1}{2}\zeta & \text{, for } D = 2 \\ 1 & \text{, for } D = 1 \end{cases}$$

  - with ζ being the ratio of dilatational vs. solenoidal modes:

$$\mathcal{P}_{ij}^{\zeta} = \zeta \mathcal{P}_{ij}^{\perp} + (1-\zeta)\mathcal{P}_{ij}^{\parallel} = \zeta\delta_{ij} + (1-2\zeta)\frac{k_i k_j}{|k|^2}$$

dilatational vs. solenoidal

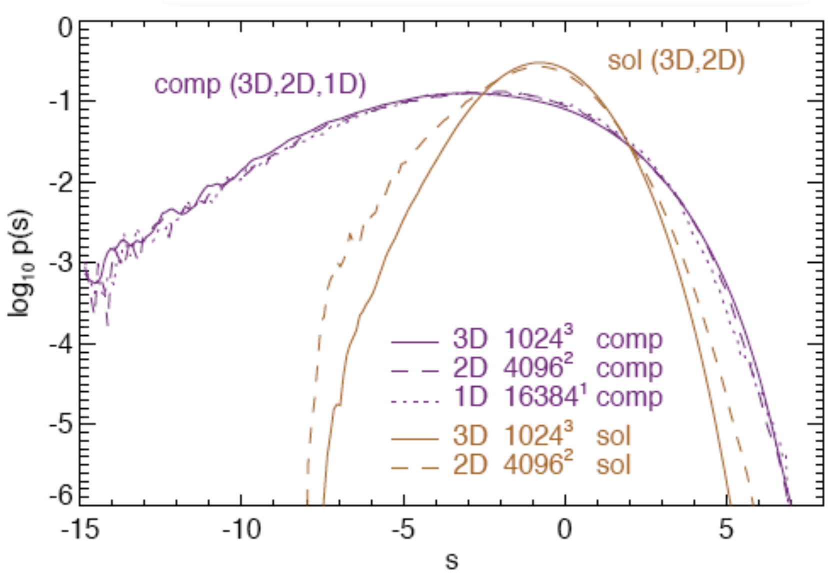

FIG. 3.— Volume-weighted density PDFs $p(s)$ obtained from 3D, 2D and 1D simulations with compressive forcing and from 3D and 2D simulations using solenoidal forcing. Note that in 1D, only compressive forcing is possible as in the study by Passot & Vázquez-Semadeni (1998). As suggested by eq. (5), compressive forcing yields almost identical density PDFs in 1D, 2D and 3D with $b\sim 1$, whereas solenoidal forcing leads to a density PDF with $b\sim 1/2$ in 2D and with $b\sim 1/3$ in 3D.

Federrath, Klessen, Schmidt (2008a)

- density pdf depends on "dimensionality" of driving
  - relation between width of pdf and Mach number

$$\boxed{\sigma_\rho/\rho_0 = b\mathcal{M}}$$

  - with b depending on ζ via

$$\boxed{b = 1 + \left[\frac{1}{D} - 1\right]\zeta = \begin{cases} 1 - \frac{2}{3}\zeta & \text{, for } D = 3 \\ 1 - \frac{1}{2}\zeta & \text{, for } D = 2 \\ 1 & \text{, for } D = 1 \end{cases}}$$

  - with ζ being the ratio of dilatational vs. solenoidal modes:

$$\mathcal{P}_{ij}^{\zeta} = \zeta\mathcal{P}_{ij}^{\perp} + (1-\zeta)\mathcal{P}_{ij}^{\parallel} = \zeta\delta_{ij} + (1-2\zeta)\frac{k_i k_j}{|k|^2}$$

dilatational vs. solenoidal

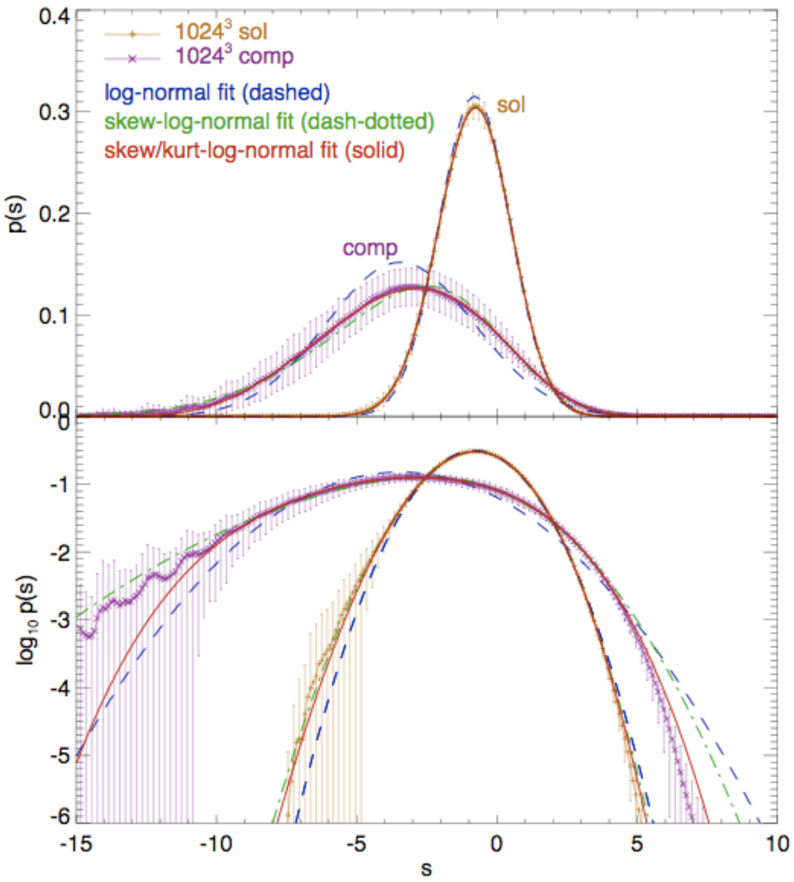

good fit needs 3rd and 4th moment of distribution!

Federrath, Klessen, Schmidt (2008b)

- density pdf depends on "dimensionality" of driving
  → is that a problem for the Krumholz & McKee model of the SF efficiency?
- density pdf of compressive driving is *NOT log-normal*
  → is that a problem for the Padoan & Nordlund IMF model?
- most "physical" sources should be *compressive* (convergent flows from spiral shocks or SN)

dilatational vs. solenoidal

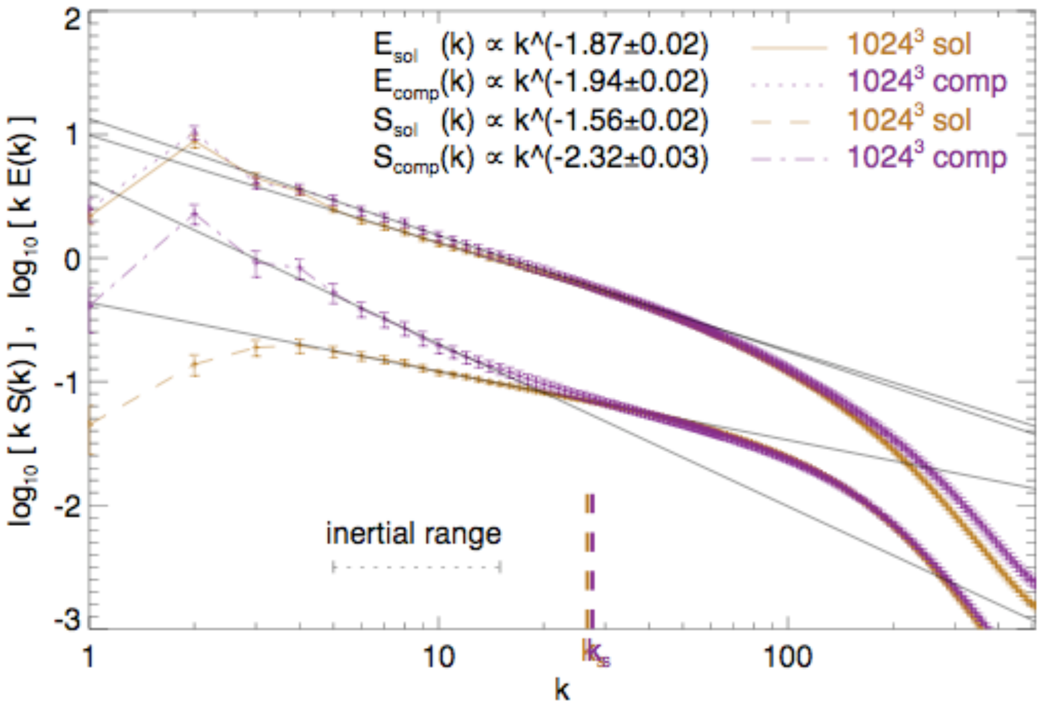

compensated density spectrum kS(k) shows clear break at sonic scale. below that shock compression no longer is important in shaping the power spectrum ...

- density power spectrum differs between dilatational and solenoidal driving!

  → dilatational driving leads to break at sonic scale!

- can we use that to determine driving sources from observations ?

Federrath, Klessen, Schmidt (2008b)

dilatational vs. solenoidal

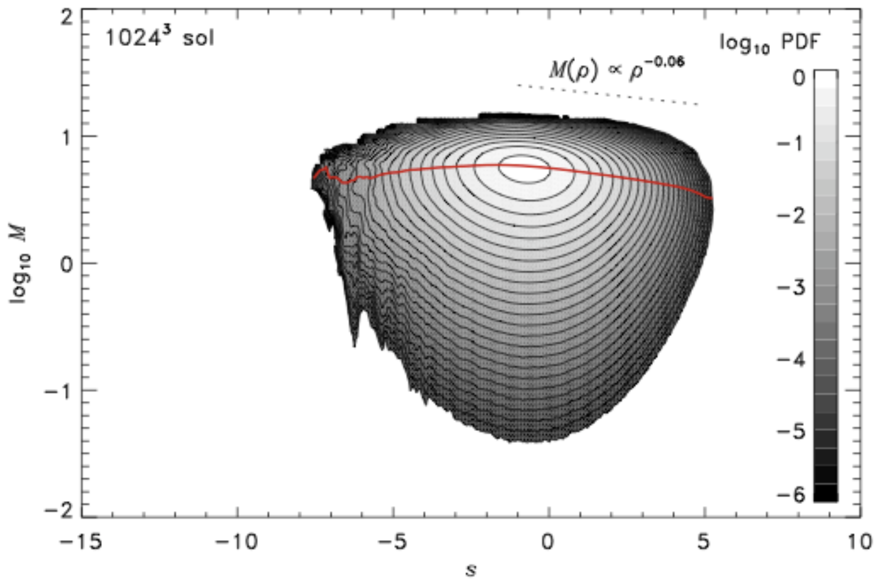

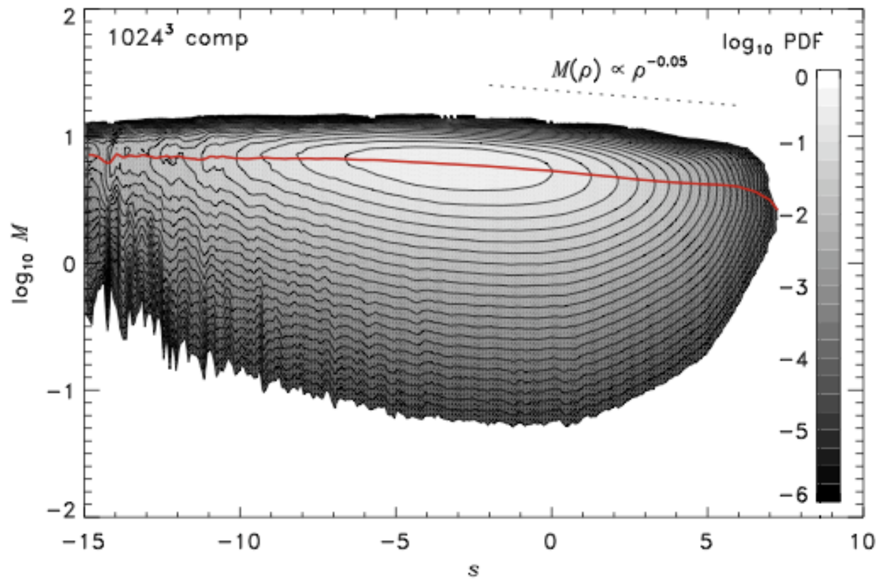

there is a weak *log density – log Mach number* relation ...

Federrath, et al. (2009)

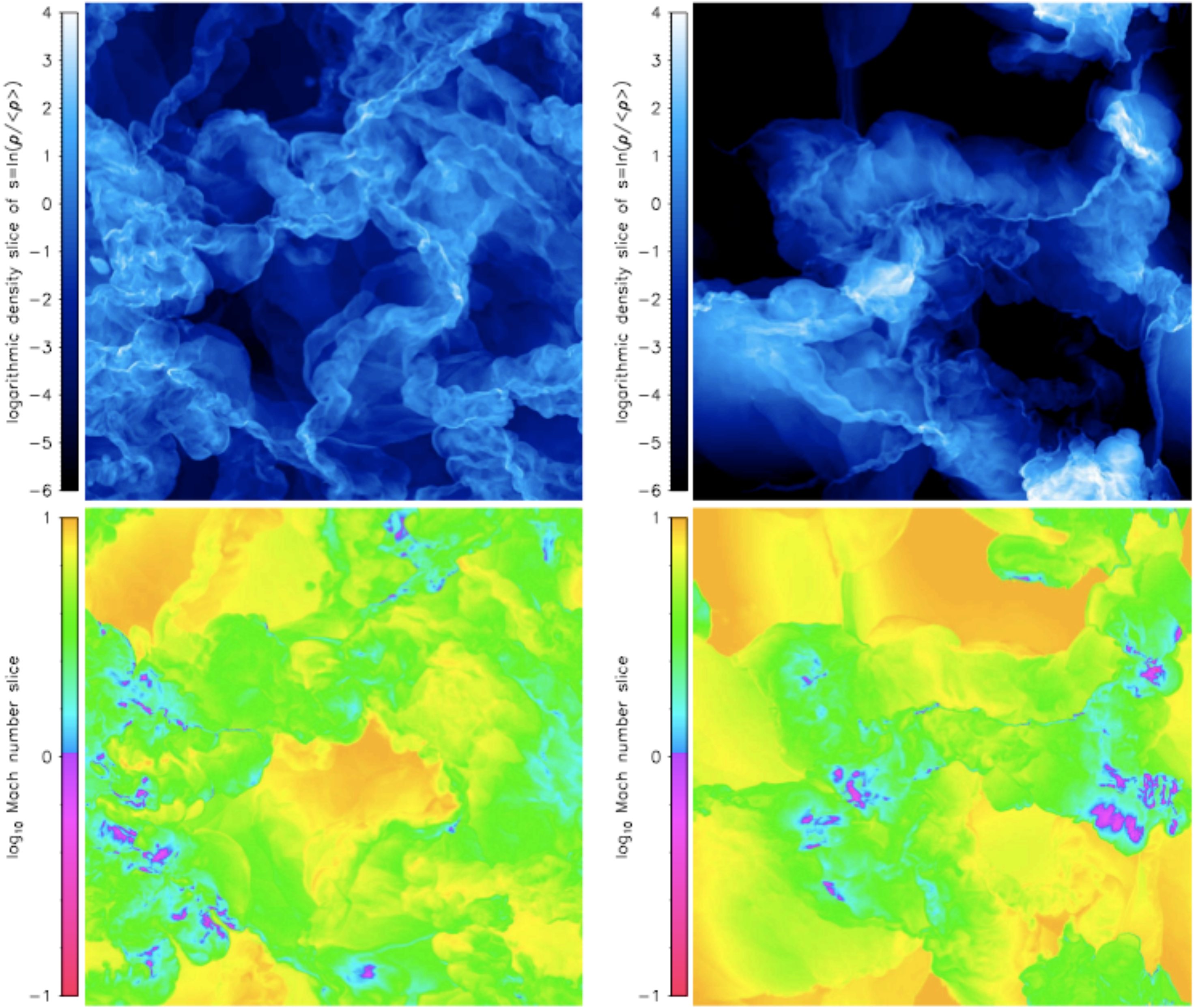

Fig. 14. z-slices through the local density (*top panels*) and Mach number fields (*bottom panels*) at $z = 0$ and $t = 2\,T$ for solenoidal forcing (*left*), and compressive forcing (*right*). Regions with subsonic velocity dispersions (Mach < 1) are distinguished from regions with supersonic velocity dispersions (Mach > 1) in the colour scheme used. The correlation between density and Mach number is quite weak. However, as shown in Fig. 4, high-density regions exhibit smaller Mach numbers on average.

dilatational vs. solenoidal

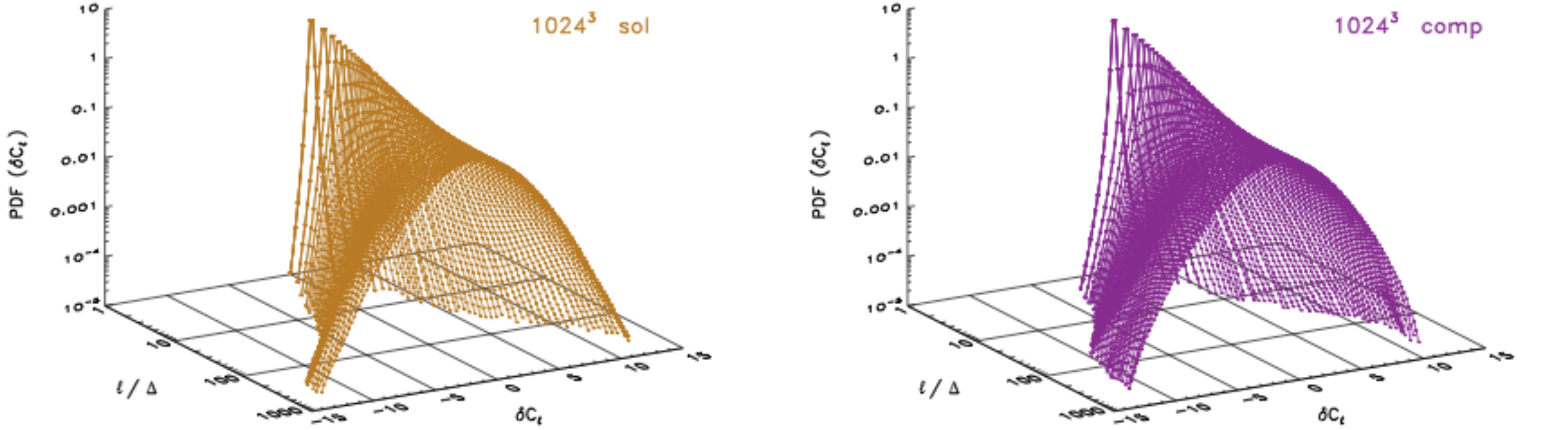

Fig. 7. PDFs of centroid velocity increments computed using equations (18) and (19) are shown as a function of the lag ℓ in units of grid cells $\Delta = L/1024$ for solenoidal forcing (*left*) and compressive forcing (*right*). The PDFs are very close to Gaussian distributions for large lags ℓ, whereas for small lags, they develop exponential tails, which is a manifestation of intermittency (e.g., Hily-Blant et al. 2008).

Federrath, et al. (2009)

dilatational vs. solenoidal

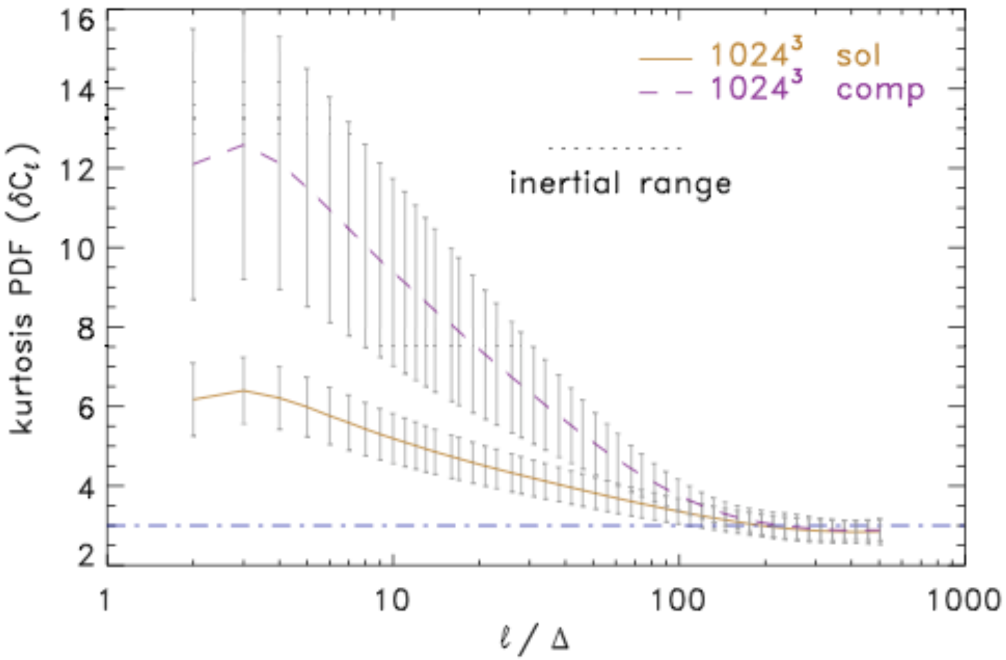

Fig. 8. Kurtosis $\mathcal{K}$ of the PDFs of centroid velocity increments shown in Fig. 7 as a function of the lag ℓ in units of grid cells $\Delta = L/1024$ for solenoidal and compressive forcing. Note that a kurtosis value of 3 (horizontal dot-dashed line) corresponds to the value for a Gaussian distribution. Non-Gaussian values of the kurtosis are obtained for $\ell \lesssim 100\Delta$. The error bars contain both snapshot-to-snapshot variations as well as the variations between centroid velocity increments computed by integration along the x, y and z axes. This figure can be compared to observations of the Polaris Flare and Taurus MC (see Fig. 7 of Hily-Blant et al. 2008).

Federrath, et al. (2009)

dilatational vs. solenoidal

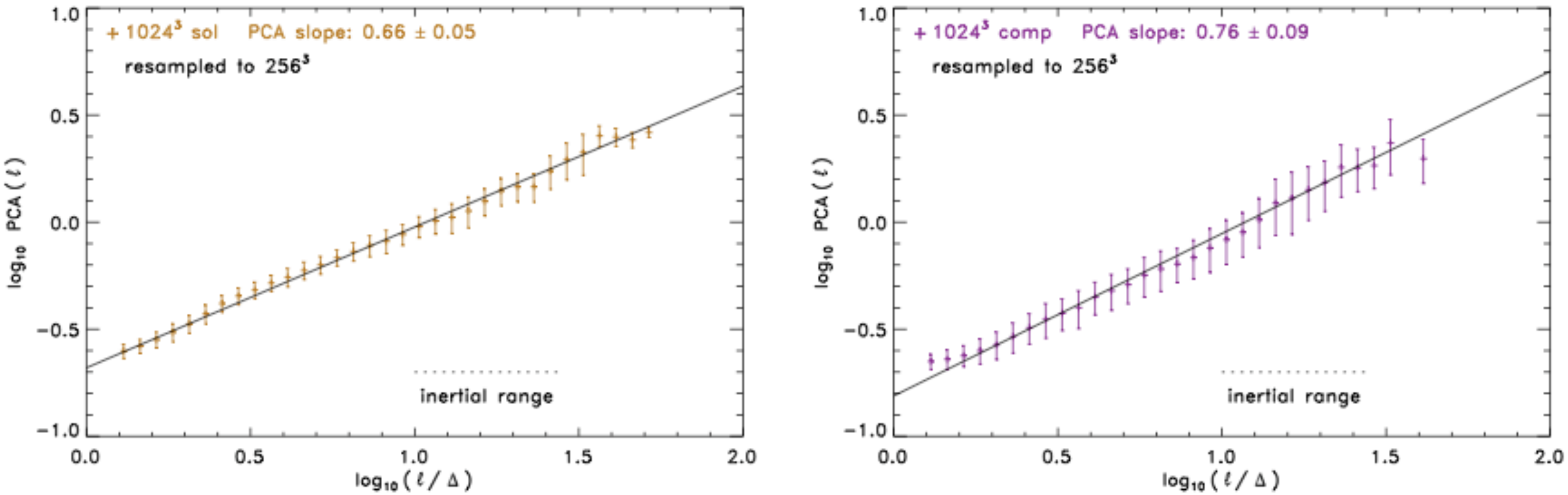

Fig. 11. Principal component analysis (PCA) for solenoidal (*left*) and compressive forcing (*right*). The PCA slopes obtained for solenoidal and compressive forcings are summarised and compared with observations by Heyer et al. (2006) in Table 4. The error bars contain the contribution from temporal variations and from three different projections along the x, y and z-axes. The data were resampled from 1024^3 to 256^3 grid points prior to PCA. The resampling speeds up the PCA and has virtually no effect on the inertial range scaling (see e.g., Padoan et al. 2006; Federrath et al. 2009).

Federrath, et al. (2009)

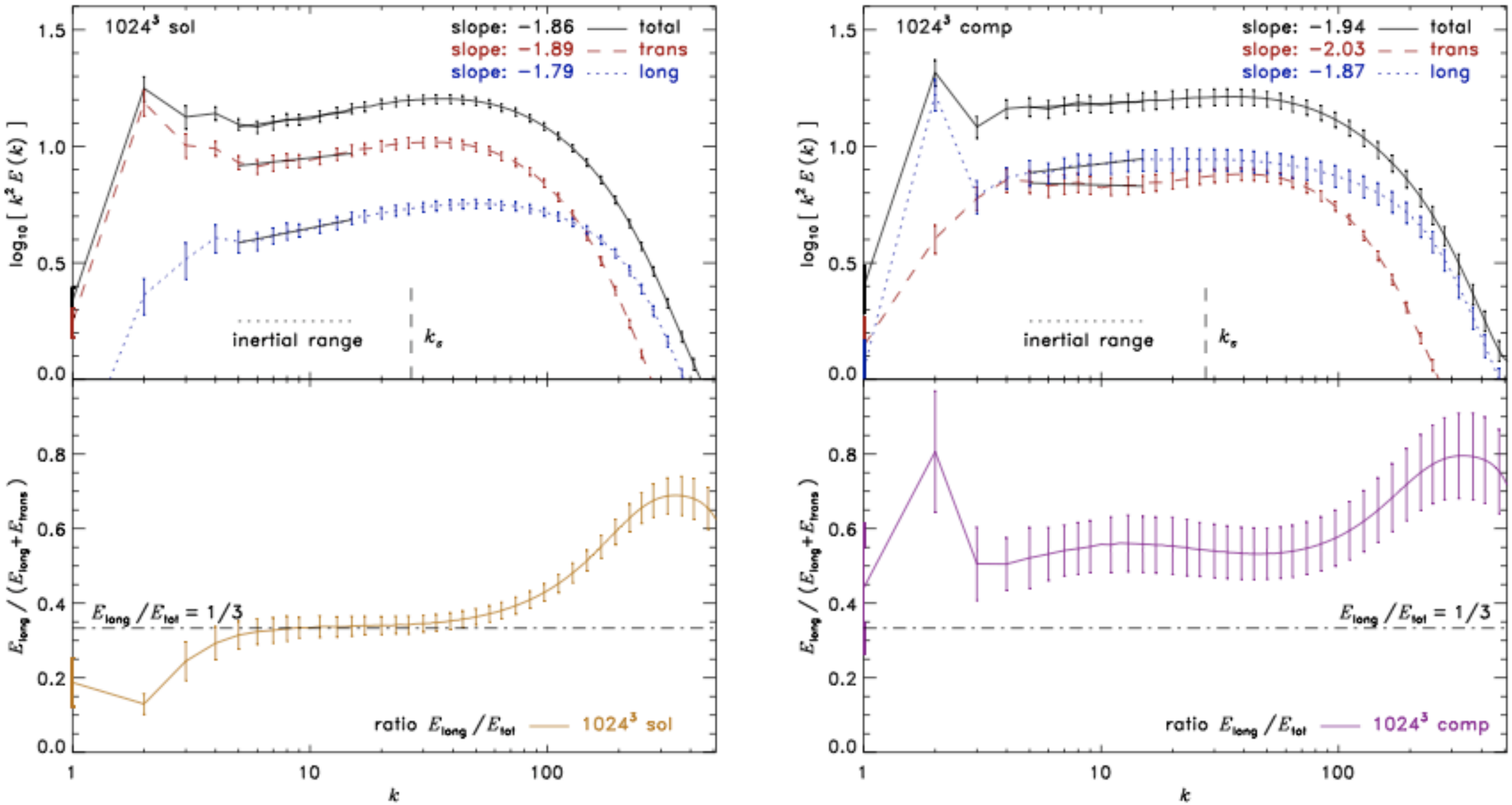

Fig. 12. *Top panels:* Total, transverse (rotational) and longitudinal (compressible) velocity Fourier spectra $E(k)$ defined in equation (25) and compensated by k^2 for solenoidal (*left*) and compressive forcing (*right*). Error bars indicate temporal variations, which account for an uncertainty of roughly ±0.05 of all scaling slopes reported for the inertial range $5 \lesssim k \lesssim 15$. The inferred inertial range scaling exponents for both solenoidal and compressive forcing are consistent with independent numerical simulations and with observations of the size–linewidth relation (see text). *Bottom panels:* Ratio of the energy in longitudinal velocity modes E_{long} to the total energy in velocity modes $E_{tot} = E_{trans} + E_{long}$. For solenoidal forcing, we obtain $E_{long}/E_{tot} \approx 1/3$ in the inertial range (horizontal dash-dotted line), because compression can only occur in one of the three spatial dimensions on average (Elmegreen & Scalo 2004; Federrath et al. 2008b). For compressive forcing, this ratio is roughly 1/2, which corresponds to an equipartition of longitudinal and transverse velocity modes. Note however that compressive forcing can compress the gas in all three spatial dimensions *directly*, whereas solenoidal forcing can only induce compression *indirectly* through the velocity field (Federrath et al. 2008b). The excess of longitudinal modes at high wavenumbers $k \gtrsim 40$ stems from numerical dissipation, which is more effectively dissipating transverse than longitudinal modes on small scales due to the discretisation onto a grid. This suggests that roughly 30 grid cells are needed to accurately resolve a vortex, while a shock is typically resolved with roughly 3 grid cells using the piecewise parabolic method (Colella & Woodward 1984). However, for a numerical resolution of 1024^3 grid cells, we find that wavenumbers $k \lesssim 40$ are almost unaffected by the discretisation and by the parameters of the numerical scheme (see Appendix C).

Federrath et al. (2009)

summary

Summary I

- interstellar gas is highly *inhomogeneous*
  - *thermal instability*
  - *gravitational instability*
  - *turbulent compression* (in shocks $\delta\rho/\rho \propto \mathcal{M}^2$; in atomic gas: $\mathcal{M} \approx 1...3$)

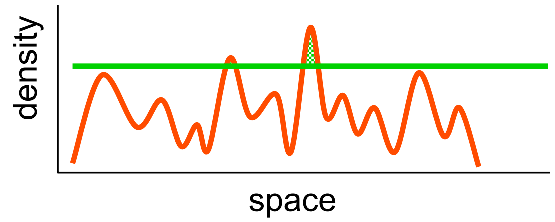

- cold *molecular clouds* can form rapidly in high-density regions at *stagnation points* of *convergent large-scale flows*
  - chemical *phase transition*: atomic → molecular
  - process is *modulated* by large-scale *dynamics* in the galaxy
- inside *cold clouds:* turbulence is highly supersonic ($\mathcal{M} \approx 1...20$)
  → *turbulence* creates density contrast, *gravity* selects for collapse

→ ***GRAVOTUBULENT FRAGMENTATION***

- *turbulent cascade:* local compression *within* a cloud provokes collapse → formation of individual *stars* and *star clusters*
- *star cluster:* gravity dominates in large region (--> competitive accretion)

(e.g. Mac Low & Klessen, 2004, Ballesteros-Paredes et al. 2006, McKee & Ostriker 2007)

Summary II

- *thermodynamic response* (EOS) determines fragmentation behavior
  - characteristic stellar mass from fundamental atomic and molecular parameters
    --> explanation for quasi-universal IMF?

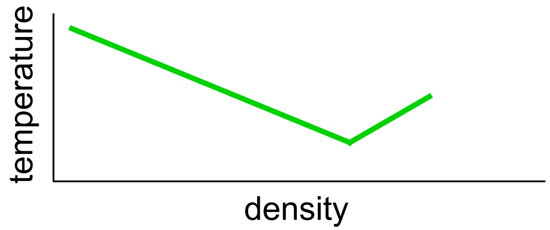

- *stellar feedback* is important
  - accretion heating may reduce degree of fragmentation
  - ionizing radiation will set efficiency of star formation
- *CAVEATS:*
  - star formation is *multi-scale, multi-physics* problem --> VERY difficult to model
  - in simulations: very small turbulent inertial range (Re < 1000)
  - can we use EOS to describe thermodynamics of gas, or do we need time-dependent chemical network and radiative transport?
  - stellar feedback requires (at least approximative) radiative transport, most numerical calculations so far have neglected that aspect

(e.g. Mac Low & Klessen, 2004, Ballesteros-Paredes et al. 2006, McKee & Ostriker 2007)